

Road surface noise research
Porous asphalt variability study – final report



Prepared for
NZ Transport Agency

Victoria Arcade
50 Victoria Street
Wellington 6141

Date: 24 January 2020
Ref: 18-103/R11/B

Prepared for (the Client):
NZ Transport Agency

Prepared by (the Consultant):
Altissimo Consulting Ltd (NZBN 9429046516350)

Project: Road surface noise
Report: Porous asphalt thickness and variability study
Reference: 18-103/R11/B

Prepared by:

John Bull
Acoustics Engineer

Version history:

Version	Date	Comment
A	30/06/2019	Preliminary results
B	24/01/2020	Add core sample results, roller data, permeability testing, dielectric constant to air void content relationship.

Executive Summary

This report presents results of the 2018-2019 study into the effects of porous asphalt thickness on noise generation, and potential causes of variability of noise generation along a 'uniform' section of road (longitudinal variability).

Data collected

The below table summarises the data that forms the basis of this study.

Property	Parameter	Measured by	Spatial resolution	Comments
Tyre/road noise	LCPX (80 km/h)	CPX trailer	1 metre 20 metre	Raw audio data processed into 1 and 20 metre road segments.
Macrotexture	Mean profile depth ("MPD")	WDM*	1 metre 10 metre	The standardised MPD parameter captures texture wavelength between 0.5 and 50 mm. Tyre/road noise generation is affected by a narrower range of texture wavelengths.

Property	Parameter	Measured by	Spatial resolution	Comments
Void content	Dielectric constant	Ground penetrating radar	0.25 metre	Averaged over 1 and 20 metre segments.
	<i>direct</i>	Core samples	100 mm diameter cores	Cores taken at 9 locations (3 cores per location).
Thickness	<i>direct</i>	Lidar	0.25 metre	Averaged over 1 metre road segments.
		Ground penetrating radar	0.25 metre	Averaged over 1 metre road segments.
		Tracesheet	Varies (20-50 metres)	
		Core samples	100 mm diameter cores	Cores taken at 9 locations (3 cores per location).
Roughness	NAASRA count	WDM*	20 metre	Not usually associated with tyre/road noise. Included for material transfer vehicle ("MTV") and construction property investigations.
Paving temperature	<i>direct</i>	Infrared sensor	2 seconds (~0.2 metre)	GPS accuracy 3-5 metres. Averaged over 20 metre road segments.
Paving speed, stops	<i>direct</i>	GPS		
Rolling temperature	<i>direct</i>	Infrared sensor		
Rolling passes	<i>direct</i>	GPS		
Permeability	<i>direct</i>	Constant head water column		

* WDM high-speed data collection truck

Thickness study

Sections of differing asphalt thickness (30 mm, 40 mm and 50 mm) were constructed as part of the Western Belfast Bypass project ("WBB") in Christchurch in November 2018. The average thickness effect was found to be a noise reduction of 2.2 dB $L_{CPX,P1:80}$ per 10 mm increase in thickness, which represents a significant acoustic effect. This relationship was verified by taking core samples from nine locations (3 cores per location).

Differences in L_{CPX} (80 km/h) of up to 1.4 dB were seen between the lanes for sections with the same nominal thickness; however, the lane differences are not consistent between each thickness section or between the two test tyres. The previous high-void trials at Sawyers to Groynes (2017) contained left-right lane mean profile depth differences that correlated with $L_{CPX,P1:80}$. No significant variations in mean profile depth exist between the lanes at the WBB thickness trial sections indicating that macrotexture is not the main driver of the L_{CPX} lane differences.

There is a relationship between the one-third octave band shape and surface thickness. A visual review of the left and right lane spectra does not suggest a difference in thickness between the lanes.

Longitudinal variability study

Thickness as a source of tyre/road noise variability

It was not possible to reliably measure the as-built asphalt thickness across the full project; however, the core samples showed differences of up to 15 mm between the target and as-built thicknesses which represents a noise effect of 3.3 dB $L_{CPX,P1,80}$. It is therefore hypothesised that the variations in tyre/road noise over the main WBB project are primarily due to deviations of the as-built thickness from the target thickness.

Effect of material transfer vehicle

A material transfer vehicle ("MTV") was used on the majority of the WBB project to investigate its effect on longitudinal variability. While consistency of macrotexture, void content (measured through surface dielectric constant) and paving temperature were increased with the MTV, no significant differences in average $L_{CPX,P1,80}$ and acoustic variability were directly measured. This indicates that use of the MTV has no effect on tyre/road noise.

Effect of surface and construction properties on tyre/road noise

The lack of a comprehensive as-built thickness dataset limited the ability to investigate other (less significant) sources of variability. The effect of local surface and construction properties on tyre/road noise was investigated by simply plotting the 20 metre road segment data for each property against the tyre/road noise. Apart from a weak correlation between the surface dielectric constant and tyre/road noise, no clear relationships were observed. This supports the hypothesis that the thickness effect is the dominant source of tyre/road noise variability in porous asphalt surfaces.

No clear relationship was observed between surface dielectric constant and laboratory air void content for core samples at the nine coring locations, and it was not possible to perform a reliable calibration of the dielectric constant measurement.

Permeability testing

Field permeability measurements showed a general trend of shorter drain times (high permeability) in thicker sections of asphalt and longer drain times (low permeability) in thinner sections of asphalt.

Executive Summary.....	ii
1 Introduction.....	1
1.1 Background	1
1.2 Aim.....	2
1.3 Previous trials.....	2
1.4 Current trials.....	4
1.5 Report structure.....	4
2 Project details	4
2.1 Project area.....	4
2.2 Surface design details.....	5
2.3 Construction methodology and scheduling.....	6
3 Methodology	8
3.1 Surface thickness.....	8
3.2 Material transfer vehicle effects.....	8
3.3 Longitudinal variability.....	8
3.4 Data collection, storage and pre-processing	10
4 Thickness trial results.....	17
4.1 Thickness relationship using target thickness.....	17
4.2 Thickness relationship from core samples	18
4.3 Left-right lane differences in L_{CPX}	19
5 Longitudinal variability trial results	22
5.1 Heatmaps	22
5.2 $L_{CPX:P1,80}$, surface properties and construction properties with and without MTV	31
5.3 Effect of surface and construction properties on $L_{CPX:P1,80}$	41
5.4 Thickness as determined by $L_{CPX:P1,80}$	48
5.5 Field permeability.....	49
6 Conclusions.....	51
7 Further work	53
Acknowledgements	53
References	54
Appendix A Summary of previous porous asphalt trials.....	56
Appendix B Porous asphalt trial results	60
Appendix C Construction observations	72
Appendix D Ground Penetrating Radar.....	81
Appendix E Temperature and position loggers.....	92
Appendix F 3D Lidar Scan Data.....	99
Appendix G 1 metre Mean Profile Depth Data.....	101
Appendix H Permeability Testing.....	103

1 Introduction

1.1 Background

The NZ Transport Agency has an ongoing research programme to reduce road surface noise. Work in this programme conducted between 2016 and June 2018, together with a summary of previous work, is set-out in Transport Agency report "Road surface noise research 2016-2018" [1]. Further to that report, the 2018/2019 financial year research programme included four main investigations being undertaken by WSP and Altissimo Consulting. This report sets out the current findings of one of those investigations relating to porous asphalt surfaces and a trial conducted during the surfacing of the Western Belfast Bypass ("WBB") project in Christchurch. This report summarises the aspects of previous work that led to the trial. Other road surface noise investigations in 2018/2019 are reported separately (Table 1).

For context, Table 1 provides a summary of the road-surface noise research programme since 2017, which is when the Transport Agency began use and development of a close-proximity ("CPX") road-surface noise measurement trailer. The CPX trailer measures sound levels with microphones mounted adjacent to the moving test wheel.

Table 1 Road surface noise research activities (following delivery of CPX trailer)

Date	Activity	Documentation
2017-2019	On-going development and improvement to CPX trailer (John Bull).	2016-2018 report [1] CPX trailer guide [2]
Feb 2017	High-void and texture trial sections constructed at Sawyers to Groynes, Christchurch.	2016-2018 report [1]
Mar 2017	CPX testing of Sawyers to Groynes trial sections (John Bull).	2016-2018 report [1]
Jun-Oct 2017	CPX testing of new North Island expressway sections and chipseal in Tairua (John Bull).	2016-2018 report [1] M2PP report [3] Tairua report [4]
Nov 2017	Small chip (EPA7) trial section constructed at Clearwater to Groynes (Christchurch).	2016-2018 report [1]
Jan-Feb 2018	Biennial certification of CPX trailer (John Bull).	2016-2018 report [1] CPX trailer guide [2]
Mar 2018	Small chip (EPA7) trial section constructed at Memorial Ave bridge (Christchurch).	2016-2018 report [1]
Mar 2018	CPX testing of small chip (EPA7) trial sections at Clearwater and Memorial Ave bridge (John Bull).	2016-2018 report [1]
Jul-Dec 2018	Way-side and tyre investigation using CPX and SPB methods (Richard Jackett).	WSP report [5]
Sep-Oct 2018	CPX testing of North Island motorway asphalt surfaces (Robin Wareing).	Altissimo report [6]
Nov 2018 – Jan 2020	Western Belfast Bypass porous asphalt variability study.	This report
Feb-Jun 2019	Chipseal investigation using CPX and SPB methods (Richard Jackett).	WSP report [7]
Jun 2019	CPX testing of Auckland Motorways (Robin Wareing).	Altissimo report [8]

1.2 Aim

Existing data in New Zealand and internationally has shown significant variations in road surface noise from porous asphalt surfaces, both along the same section of road and between different sections of road having nominally the same surface [3] [6].

Since acquiring the CPX trailer in 2017, the Transport Agency has had two main goals for porous asphalt research:

1. To understand how bulk changes to the physical properties of a road surface (through mix design) affects the road surface noise of porous asphalt surfaces, in the interest of finding an improved low-noise porous asphalt mix design.
2. To investigate causes of longitudinal variability in porous asphalt surface noise and identify methods to reduce variability.

A number of the noise generating and amplification mechanisms associated with porous asphalt road surfaces are affected by surface macrotexture, void content and thickness [9]. These three surface properties often form the basis of international research into road surface noise [10] [11] [12]. The surface macrotexture, void content and thickness are in direct control of the surfacing engineer (through mix design) and the construction contractor (through construction methodology and quality control).

This report details the latest research activities undertaken in 2018/2019 to address the above two goals. Central to this work has been trials conducted on the WBB.

1.3 Previous trials

High-void and texture trials

A set of trial sections involving epoxy-modified porous asphalt (EPA) were commissioned by the Transport Agency in late 2016 to investigate the influence of void content on road surface noise (see Appendix A for details). Originally four porous asphalt mix designs were planned, however, one mix failed to pass the pre-construction lay-down trial resulting in that mix being excluded from the field trials. The final mix designs are described in Table 2 below.

Table 2 Details of the high-void and texture trial sections

Surface	Details
EPA10 (30 mm)	Epoxy-modified porous asphalt with 10 mm chip and 30 mm nominal surface thickness.
EPA10HV (30 mm)	Epoxy-modified porous asphalt with 10 mm chip, a lower ratio of fine aggregate to achieve a more open mix and 30 mm nominal surface thickness.
EPA14 (30 mm)	Epoxy-modified porous asphalt with a 14 mm chip and 30 mm nominal surface thickness.

The three trial sections were constructed by Downer New Zealand in February 2017 on both lanes of the northbound carriageway at the Sawyers to Groynes section of Johns Road (SH1) in Christchurch. CPX and macrotexture (mean profile depth) testing followed in March 2017 and the results revealed a linear relationship between mean profile depth and $L_{CPX:P1,80}$ (Figure 1). The graph has a separate data point for each lane for each trial surface.

Due to the differing macrotexture properties of the EPA10 and EPA10HV trial sections, the effect of the increased void content in the EPA10HV section could not be isolated from

macrotexture and no improvement due to the increased void content could be seen. Statistical pass-by (“SPB”) testing was performed by WSP in July 2018 to check for noise reduction effects at the way-side that may not be detectable using the CPX method; no additional way-side noise reduction was observed [5].

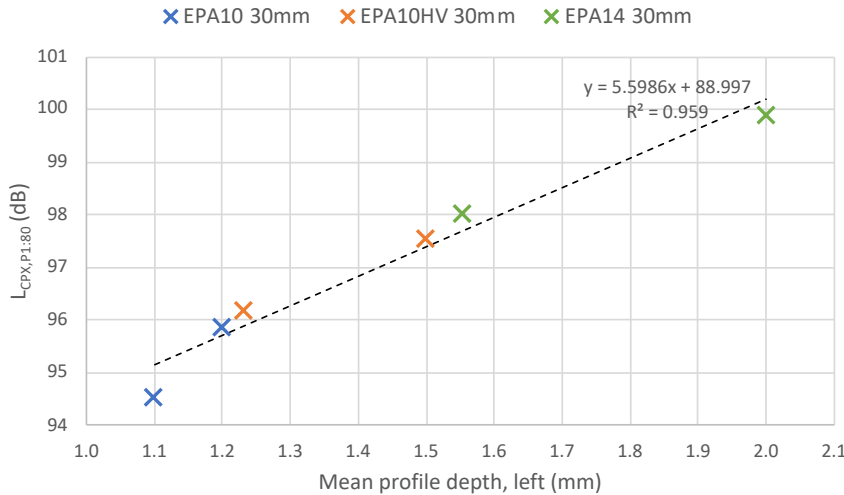


Figure 1 Macrottexture (mean profile depth) vs L_{CPX:P1,80} at the high-void trial sections

The results of the Sawyers to Groyne trail demonstrated how macrotexture is a strong driver of differences in tyre/road noise between different porous asphalt mixes. It also showed how an increase in void content results in an increase in macrotexture, and that any noise reduction due to increased void content appears to be insufficient to make up for the increase in noise due to macrotexture. These surfaces are subject to ongoing monitoring to identify any differences with wearing/aging, such as through voids clogging.

Small chip trials

To reduce the macrotexture of porous asphalt surfaces smaller chip mixes were trialed at two locations on SH1 in Christchurch (Table 3) (see Appendix A for details). Both trial sections of EPA7 used aggregate from the same source (Fulton Hogan quarry).

CPX testing on the Clearwater EPA7 surface (40 mm thick) showed a 2-3 dB improvement in L_{CPX:P1,80} over the previous EPA10 trial surface, although the EPA7 surface was 10 mm thicker than the EPA10 surface and part of the noise reduction is likely associated with the increased thickness.

The second EPA7 trial section on the Memorial Ave bridge showed a L_{CPX:P1,80} improvement of 0.5-1.5 dB over the previous EPA10 trial surface and represents a more reliable comparison given the common thicknesses of the two surfaces.

The small chip trials showed an improvement in L_{CPX} when moving from the EPA10 to the EPA7 mix.

Table 3 Small chip porous asphalt trial sections

Surface	Location	Details
EPA7 (40 mm)	Clearwater to Groynes trial (October 2017, Fulton Hogan)	Epoxy-modified porous asphalt with 7 mm chip and 40 mm nominal surface thickness.
EPA7 (30 mm)	Memorial Ave bridge trial (April 2018, Downer)	Epoxy-modified porous asphalt with 7 mm chip and 30 mm nominal surface thickness.

1.4 Current trials

On the basis of the above trials the main surfacing works for WBB have been used to investigate changes to surface thickness and causes of longitudinal tyre/road noise variability.

From the previous work, an EPA7 mix was selected for the main WBB surfacing, with a 40 mm nominal surface thickness. Within the works, trial sections of lesser (30 mm) and greater (50 mm) surface thickness were introduced. The surfacing process was closely scrutinised with various parameters measured during and after the works to investigate root causes of variability.

1.5 Report structure

A description of the project area, surface mix design, construction equipment and construction methodology are detailed in Section 2. The research methodology and surface and construction parameters being considered are outlined in Section 3. The results and discussion of results are presented together in Section 4. Where appropriate additional information has been included in the appendices.

2 Project details

2.1 Project area

The Western Belfast Bypass project forms a new part of SH1 in the northwest of Christchurch. Fulton Hogan was responsible for the construction of the WBB project.

The thickness trial sections were constructed on a section of the northbound carriageway (in both lanes) (see Figure 2). The thickness trial sections are short sections of road, approximately 260 metre in length. These sections form a continuous part of the rest of the WBB project, with thickness modification happening during a continuous paving run including gradual ramps (10 mm over 20-30 metres) between sections of differing thickness. The longitudinal variability study includes the whole of the WBB project area.

Details of the project area are provided in Table 4 below. In addition to the sections listed below, there were three bridge decks paved with a SMA surface (at an earlier date) and several EPA7 ramp sections before, after and between the thickness trial sections. All SMA and EPA7 ramp sections have been excluded from the analysis.

Table 4 Project area (all on State highway 01S)

Study	Carriageway	Lane	Thickness	Start	End	Length
Thickness trial sections	Northbound	Both	30 mm	0327/04.864	0327/05.126	262 m
			40 mm	0327/04.585	0327/04.845	260 m
			50 mm	0327/04.292	0327/04.566	274 m
Longitudinal variability	Northbound ⁺	Left	40 mm	0327/02.400	0333/0.316	2,500 m
		Right		0327/02.400	0333/0.316	2,500 m
	Southbound ⁺	Left	40 mm	0327/02.472	0333/0.507	3,600 m
		Right		0327/02.472	0333/0.510	3,600 m

† 30mm and 50mm thickness trial sections and joining ramps excluded.

+ SMA bridge decks excluded.

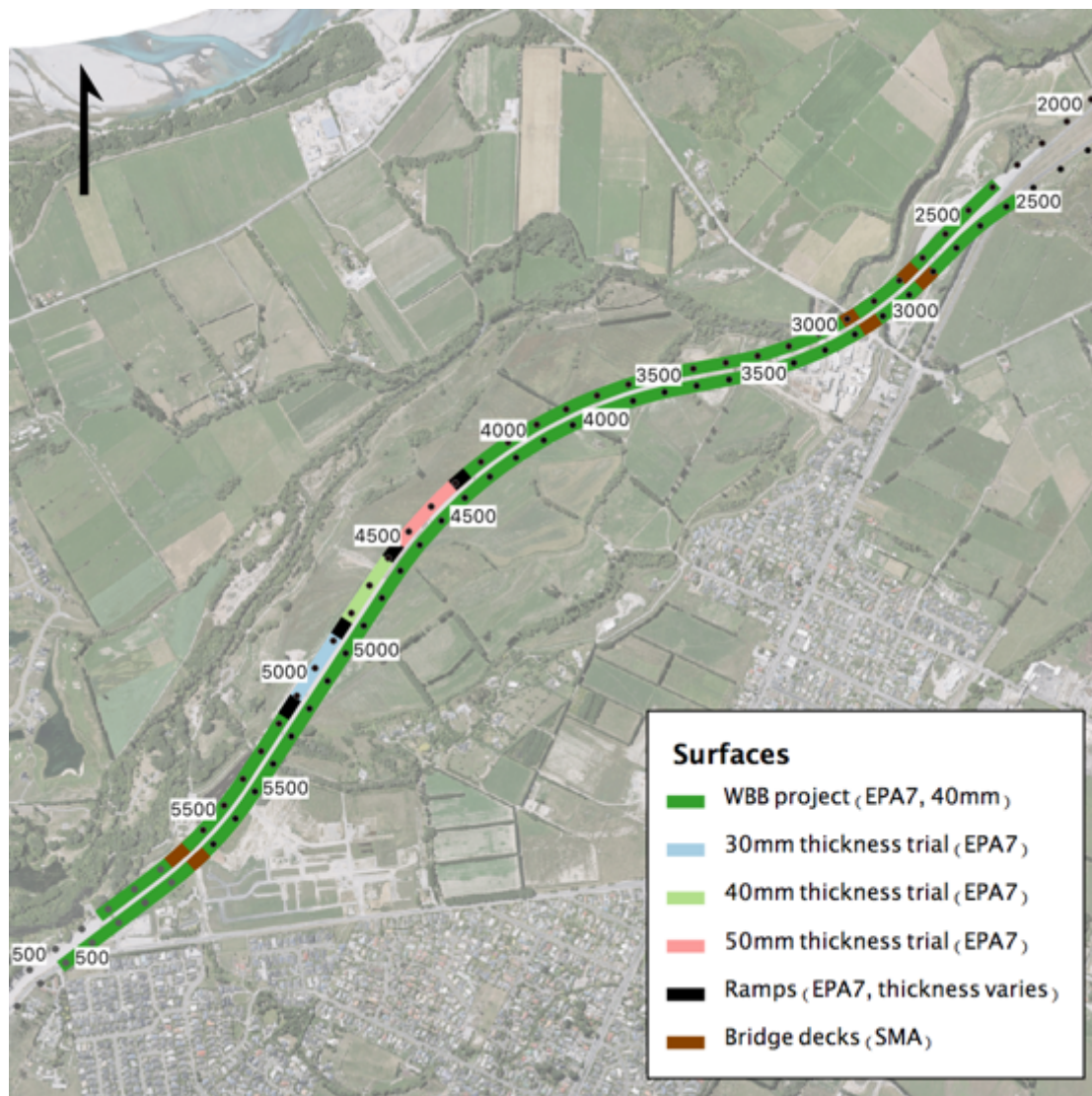


Figure 2 Project area and trial sections

2.2 Surface design details

The porous asphalt mix used on the entire WBB project was an epoxy modified porous asphalt with a nominal chip size of 7 mm. Specific details are provided in Table 5 below.

Table 5 Surface mix details

Property	Target
Asphalt plant temperature	120°C
Air void content	20%
Binder content	5.3 – 6.3%
Bitumen grade	80/100
Binder epoxy content	25%
Aggregate (sieve size)	% passing
13.2 mm	100 – 100
9.5 mm	95 – 100
6.7 mm	91 – 100
4.75 mm	45 – 55
2.36 mm	13 – 19
75 µm	1 – 5

2.3 Construction methodology and scheduling

A material transfer vehicle (MTV) was used on all but one construction shift to investigate whether it reduced variations in asphalt temperature and whether it would avoid artefacts caused as trucks offload into the paver. Normal practice in most of New Zealand does not include use of a MTV.

A list of construction equipment used by the paving contractor is provided in Table 6. The paver worked at a nominal speed of 5 metres/minute although at times was operated at other speeds. Once the surface temperature had dropped below 90°C the breakdown roller performed one pass (both forward and reverse directions), with one of the directions being under vibration. The secondary roller then performed one pass (both forward and reverse directions) after the surface temperature had dropped below 50°C. The temperature was measured by the contractor QC staff using a hand-held infrared temperature probe.

Specific notes on the construction activities and temporary traffic management for each shift are provided in Appendix C. The construction schedule is provided in Table 7 below. Figure 3 shows the extents of each paving shift.

Table 6 Construction equipment

Category	Make/model	Details
Paver	Vogele 1803-3	Wheeled paver, capable of 8 metre wide runs.
Material transfer vehicle (MTV)	Roadtec SB-1500-C	Material transfer only (no on-board reheating).
Breakdown roller	Bomag BW 151 AD-4	9.2t, 1.68 metre wide drum, tandem vibratory.
Secondary roller	HAMM HD75	8t, 1.68 metre wide drum, tandem vibratory.

Table 7 Construction schedule

Shift no.	Date	Direction and lane	Start	End	Length*	Notes
1	Tue, 23/10/18	SB right lane	0327/2.472	0327/4.400	1,798 m	No MTV
2	Wed, 24/10/18	SB left lane	0327/2.472	0327/4.439	1,836 m	
3	Fri, 26/10/18	SB right lane	0327/4.400	0333/0.510	1,802 m	
4	Sun, 28/10/18	SB left lane	0327/4.439	0333/0.507	1,763 m	
5	Sun, 4/11/18	NB right lane	0333/0.310	0327/2.998	2,898 m	
6	Mon, 5/11/18	NB left lane	0333/0.310	0327/3.624	2,274 m	
7	Tue, 6/11/18	NB left lane	0327/3.624	0327/2.386	1,116 m	
8	Wed, 7/11/18	NB right lane	0327/2.945	0327/2.387	494 m	

* Excludes SMA bridge decks.



Figure 3 Extent of paving shifts. The displacement values are the Rp in metres from Rs 01S-0327 (black marks) and Rs 01S-0333 (grey marks).

3 Methodology

3.1 Surface thickness

CPX measurements were taken over the thickness trial sections using two test tyres (P1 and H1) and on two measurement dates (December 2018 and March 2019). The relationship between surface thickness and tyre/road noise was initially found using the average L_{CPX} in each lane for each target thickness (30 mm, 40 mm and 50 mm). Following the discovery of a clear relationship between surface thickness and tyre/road noise core samples were taken at nine locations (3 cores per location) in October 2019 to verify the thickness relationship.

3.2 Material transfer vehicle effects

The effects of the material transfer vehicle on L_{CPX} , surface properties (macrotexture, dielectric constant and roughness) and construction properties (paving temperature, paving speed and paver stops) are investigated by considering the distributions of each property with and without the MTV (Section 5.2).

3.3 Longitudinal variability

Tyre/road noise is affected by macrotexture, void content and asphalt layer thickness (surface properties). In turn the surface properties are affected by the design and construction properties (see Figure 4). The design properties have remained constant across the WBB project (excluding thickness trial sections), meaning that any variability in tyre/road noise is due to the construction properties.

The approach used for the longitudinal variability study has been to quantify the local surface properties and construction properties and relate these to the local tyre/road noise (L_{CPX}). This is performed by plotting the 20 metre road segment $L_{CPX,P1:80}$ against each surface and construction property (Section 5.3).

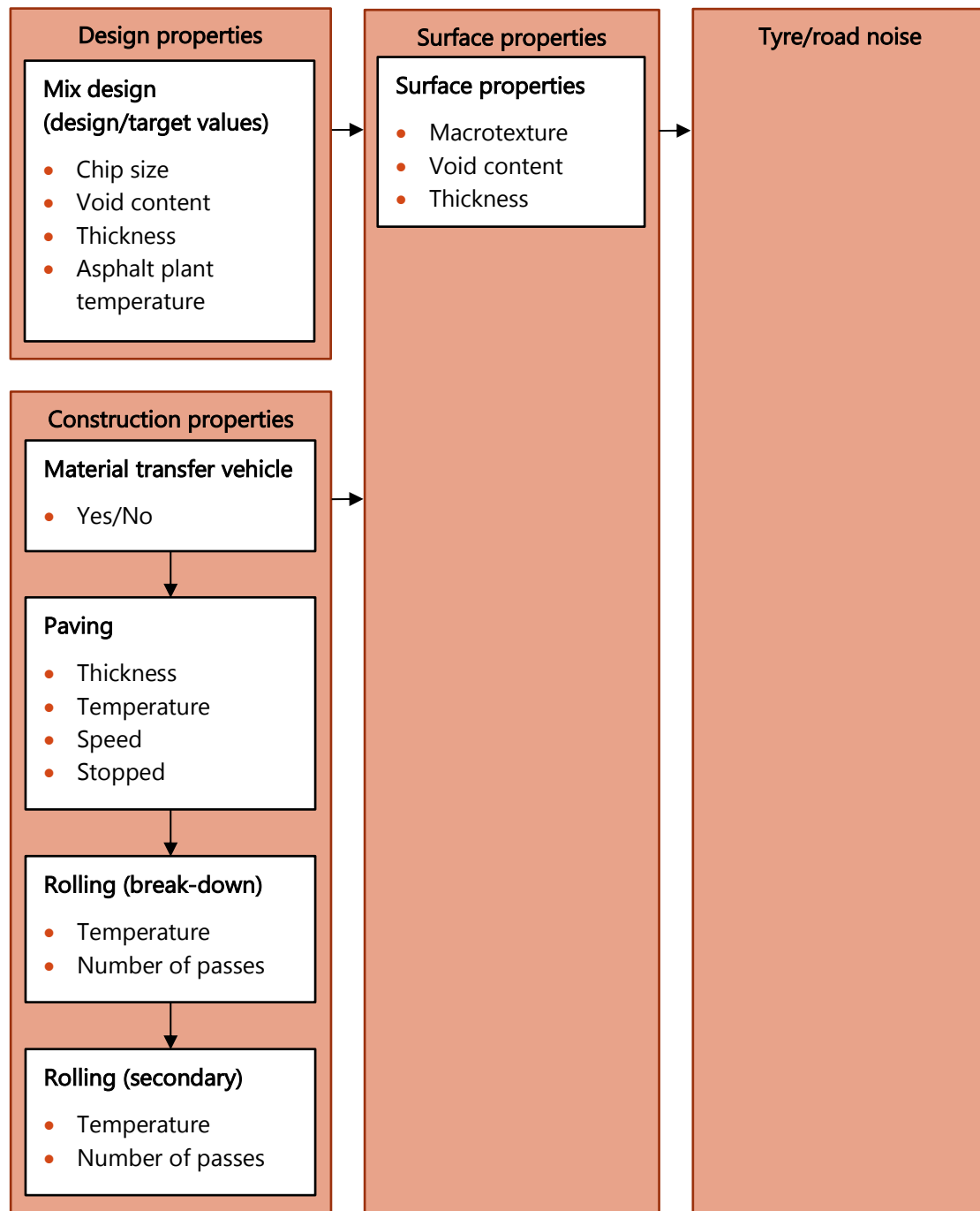


Figure 4 Relationship between tyre/road noise, surface properties and design and construction properties.

3.4 Data collection, storage and pre-processing

All of the raw data is GPS located and stored in a SQL database. The GPS coordinates of each row in the database are projected onto the RAMM [13] centreline model to find the linear reference associated with each raw data point (i.e. Rs/Rp). The linear references are then used to aggregate the raw data into discrete road segments. The data was processed at two scales for the current work. The 20 metre road segment lengths provide road segments consistent with ISO 11819-2 [14], while the 1 metre road segments provide a more detailed picture of the L_{CPX} distribution.

Tyre/road noise

The tyre/road noise was measured in December 2018 and March 2019 using the Transport Agency's CPX trailer. The CPX system records the raw audio data for each measurement run and outputs overall and one-third octave band CPX levels at the chosen road segment length.

For the current work the raw audio data was used instead of the 20 metre road segment values calculated directly and output by the CPX system. The raw audio data was processed into 1 and 20 metre road segments that align appropriately with the RAMM Rs/Rp points.

Three measurement runs were performed in each lane during each measurement session, and both the P1 and H1 test tyres were used.

Macrotexture

Surface macrotexture was measured in January 2019 using the vehicle mounted laser on the WDM high speed data collection truck as part of their annual network-wide survey. The macrotexture is reported as both mean profile depth over 1 metre and 10 metre road segments. The 1 metre road segment data was provided for the northbound carriageway only (see Figure 5); the detailed data does not form part of WDM's high-speed data collection contract with the Transport Agency and was provided in addition to the standard 10 metre road segments required under their contract. The 10 metre road segment data was available for the entire project area through RAMM.

The mean profile depth parameter contains no information concerning the texture wavelengths, which can be a critical piece of information when investigating road surface noise [15]. A 1 mm texture profile was provided by WDM; however, it was not possible to correctly align the profile with the other datasets. Only the 1 metre and 10 metre mean profile depth data has been included in the analyses to date.

Void content

The air void content of the asphalt surface was measured by proxy using a vehicle mounted ground penetrating radar ("GPR"), which measures a material's dielectric constant.

In order to quantify the absolute air void content of the surface from the measured dielectric constants a calibration process was performed (i.e. ground-truthing). This was attempted by extracting several core samples from the constructed surface and measuring the air void content in a laboratory (Appendix D, Section D.2).

GPR testing was performed in December 2018 using Fulton Hogan's 2GHz GPR system over the entire project area. The raw reflection amplitudes were converted to dielectric constants and then arithmetically averaged over the desired road segment lengths.

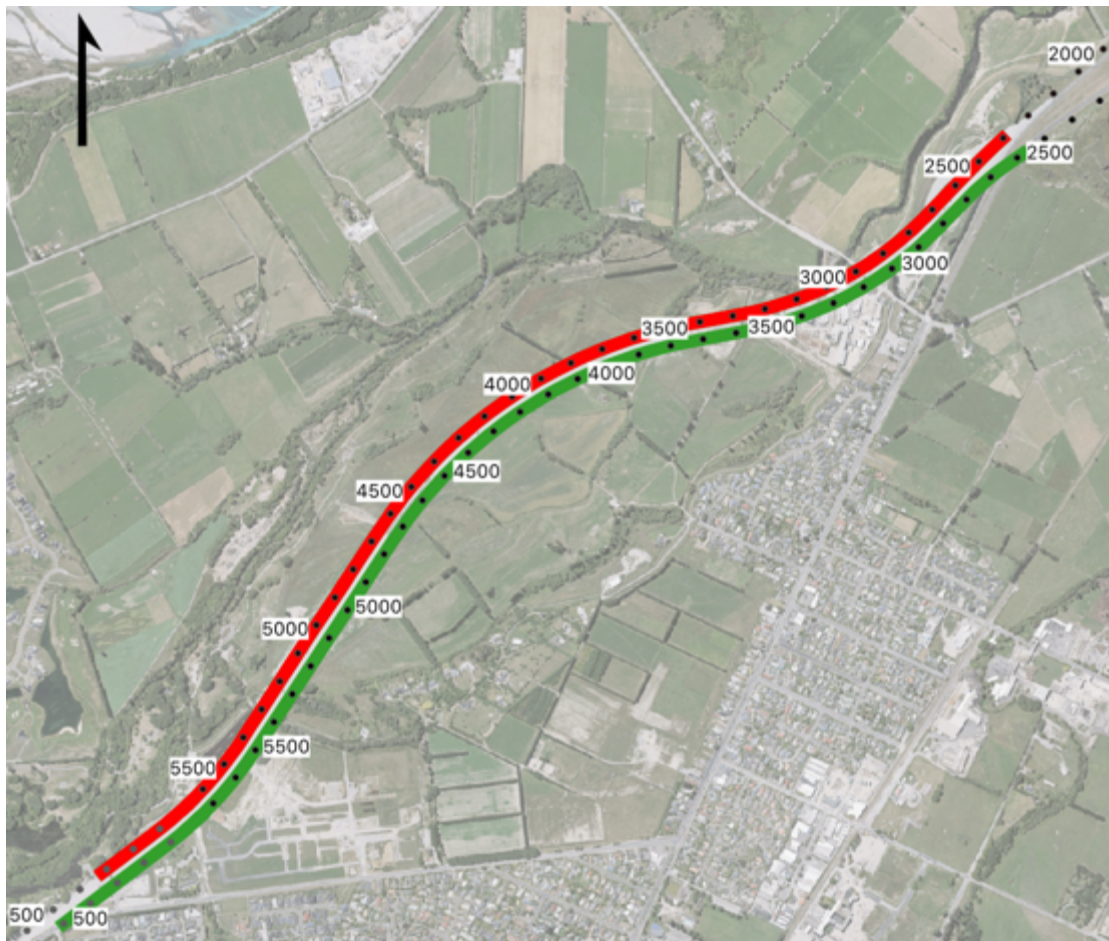


Figure 5 Extent of the detailed mean profile depth (1 metre road segments) and profile data is shown in red.

Roughness

Roughness is defined as road texture with wavelengths between 50 mm and 500 mm and is quantified by the NAASRA count parameter. Tyre/road noise is widely considered to be most influenced by texture in the macrotexture range (wavelengths between 0.5 mm and 50 mm); however, roughness is an important parameter for assessing ride quality and is expected to be influenced by the use of the material transfer vehicle. Roughness has therefore been included in the no-MTV / MTV analysis to determine the influence of the material transfer vehicle on roughness. 20 metre road segment data taken by WDM in January 2019 was available through RAMM.

Lidar thickness

A pre and post-construction height survey using a Lidar 3D scan was conducted by WSP over the thickness trial sections on the northbound carriageway (see Figure 6). WSP provided a detailed point cloud of both the original chipseal surface and the porous asphalt surface as well as cross-sections at 10 metre spacings.

The supplied point cloud data was used to generate long-section profiles for both the chipseal and porous asphalt surfaces. The thickness of the porous asphalt layer was found by subtracting the height of the chipseal surface from the height of the porous asphalt surface. The Altissimo results (calculated from the WSP point cloud data) were verified by comparing the calculated thicknesses to those in the 10 metre cross-sections supplied by WSP.

The thickness profiles are presented in Figure 7 below for the left and right lanes over the thickness trial sections. Inspection of the Lidar results shows that there is insufficient accuracy to assess small (<5mm) variations in surface thickness. In particular:

- The measured left lane asphalt thickness drops to 5 mm at its thinnest point. This is impossible given the mix design and visual inspection of the surface following paving. Assuming the surface is at least 20 mm thick, a measured thickness of 5 mm would suggest a measurement error of at least 15 mm.
- The measured left and right lane surface thicknesses show some correlation, at the 50-metre scale. Since the two lanes were paved in separate runs, correlation of surface thickness at the 50-metre scale is unlikely. While the base (chipseal) surface may contain bumps that run across the full width of the road, the paver's built in level control is only capable of smoothing out bumps up to 5-10 metres in length. The paver is unable to detect larger scale bumps in the base surface and hence will not correct for them. The observed correlation is most likely to be due to measurement error.
- The results show no difference between the 40 mm and 50 mm trial sections. The CPX measurement results presented in the later sections show a clear difference in L_{CPX} between the 40 mm and 50 mm trial sections and this difference can only be explained by a change in thickness.

Due to the above issues the Lidar thickness data is not considered an appropriate tool for determination of asphalt layer thickness and it has not been used in the current analysis.

Ground penetrating radar thickness

An alternative thickness measurement technique made use of the reflection return times from the ground penetrating radar measurements. When combined with the local dielectric constant, the reflection return times can be used to calculate the distance travelled by the radar pulse.

Significant effort was put into checking the validity of this technique and automating the processing of the raw radar measurements to provide a detailed survey of the asphalt thickness (every 0.25 metres). The process has not proven reliable for the current work involving thin asphalt layers; a summary of the findings is presented in Appendix D along with a discussion of ground penetrating radar measurements in general.

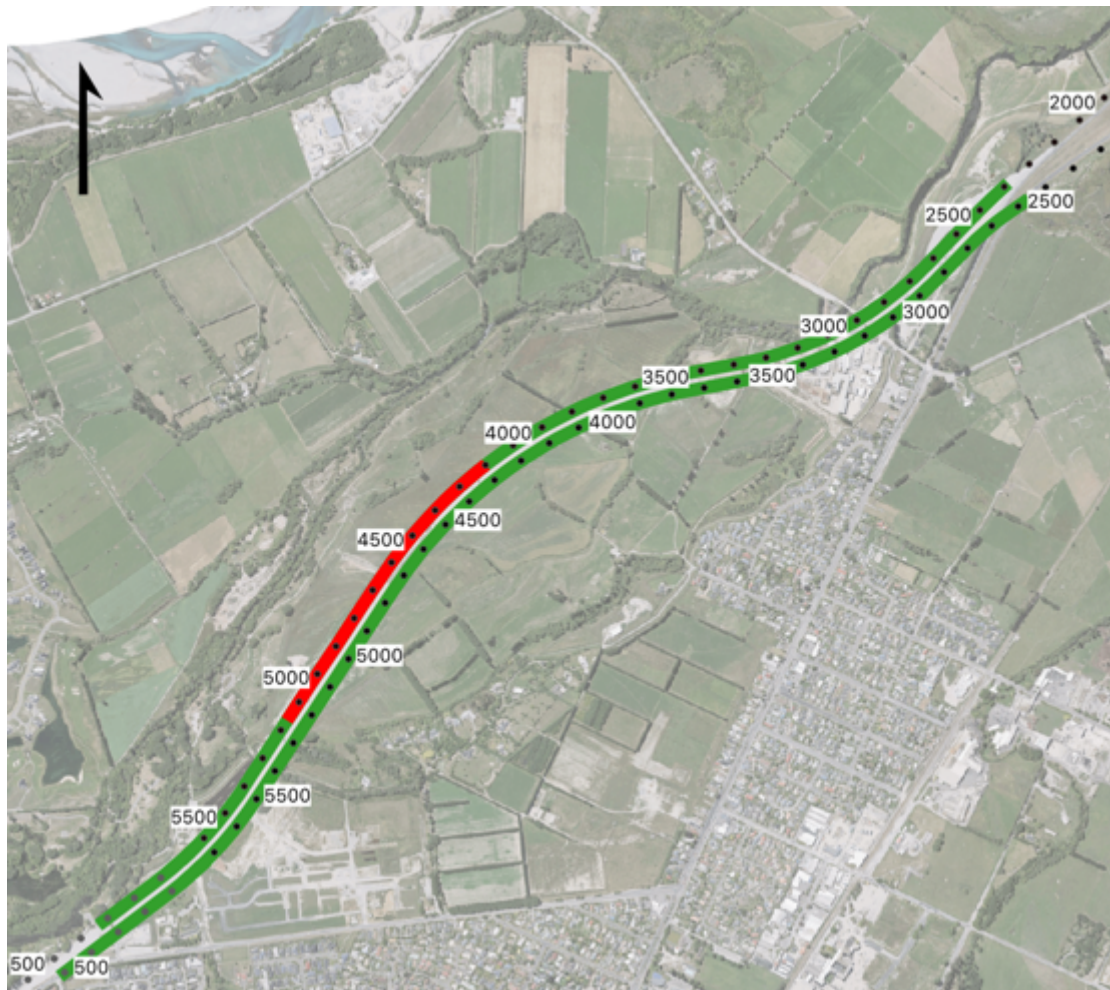


Figure 6 Extent of the WSP Lidar scan (limited to thickness trial sections).

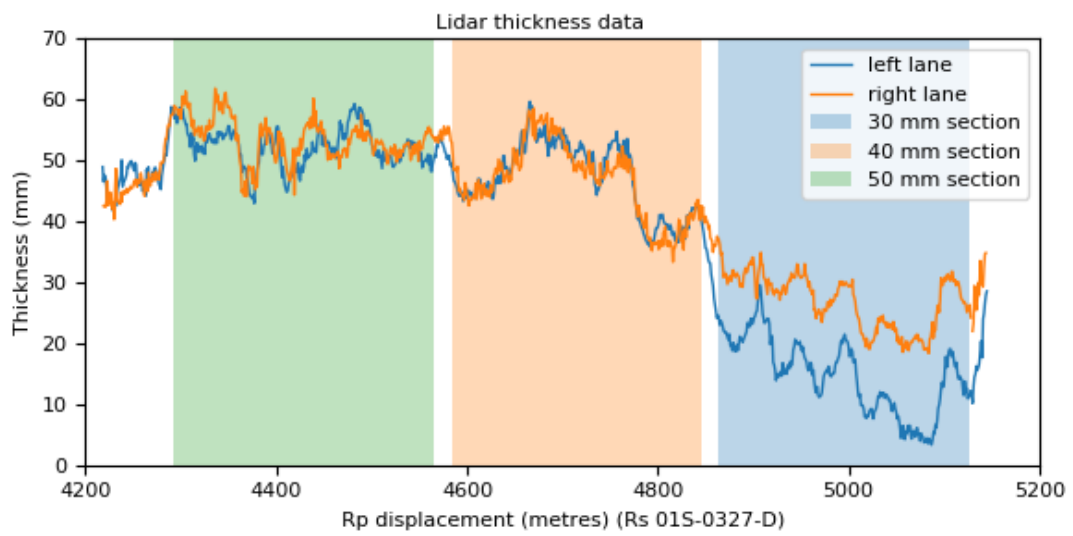


Figure 7 Left wheel path surface thickness profile

Tracesheet thickness

After failure of the Lidar and ground penetrating radar thickness measurement techniques a third method was trialled to calculate the average asphalt thickness between truck loads. This technique relied on GPS records of the paver position and manual records by contractor QC staff noting the arrival and departure times of each asphalt truck and the paving width (included in the tracesheet records).

During steady operation it can be assumed that the system (paver and MTV) is completely full of asphalt at the departure of each asphalt truck. Therefore, an amount of asphalt equivalent to the load of the current truck is laid between the departure of the previous truck and the departure of the current truck. Assuming a constant asphalt density of 1,800 kg/m³ and knowing the paving width at each truck departure, the average layer thickness can be calculated.

Again, the results of this technique proved unreliable, with the calculated asphalt thicknesses ranging from 10 mm to 150 mm. The main sources of error are thought to be the assumption that the MTV is full at the departure of each truck (the "full" condition is dependent on how the MTV is operated) and the manual recording of the truck departure times.

Core thickness

Core samples were taken at nine locations (3 cores per location) to provide a spot check of the asphalt layer thickness. The core samples had a diameter of 100 mm and were cut to the underlying chipseal depth. The thickness was measured at several locations around the circumference of each core and averaged.

Paving temperatures and speed

Temperature and position loggers were developed specifically for the current work (see Appendix E for details). One logger unit was installed on the paver, with up to three non-contact infrared temperature sensors directed at the surface 2 metres behind the paver. The surface temperatures, paver position and paver speed were logged every 2 seconds throughout each construction shift over the entire project area. The GPS records were also used in the tracesheet thickness calculations described above.

The GPS receiver used was a low-cost consumer-grade GPS. The absolute positioning accuracy of consumer grade GPS receivers is generally considered to be 3-5 metres.

Rolling temperatures, speed and number of passes

Two additional temperature and position loggers were installed on each of the two rollers, with a single non-contact infrared temperature sensor directed 2 metres in front of each roller. The surface temperatures, paver position and paver speed were logged every 2 seconds throughout each shift. Additional processing of the roller temperature and position data is required to extract useful parameters since each roller must make several passes across the width of the lane and is able to make multiple passes over the same patch of surface. The processing steps used are listed in Appendix E.

Infrared photographs

Infrared photographs were taken approximately every 10 metres along the length of the project using a hand-held infrared camera. These photographs provide a detailed record of the surface temperature distribution beyond that provided by the spot measurements of the paver temperature logger.

An infrared camera was mounted on the paver during shifts 5 to 8 to provide an alternative record of the temperature distribution. The photographs from the paver-mounted camera provide meaningful absolute temperatures.

The infrared photographs have not been reviewed as part of this work but will form part of the stored dataset should further analysis be undertaken.

Permeability

A permeability testing rig was developed based for the current work. The rig uses a 150 mm diameter ring and maintains a constant head on 5–15 mm. The time taken to drain 3.6L of water is recorded using a stop watch.

The permeability testing rig is based on the ASTM C1701 [16] permeability method; however, a smaller ring diameter of 150 mm was used to maintain consistency with the field permeability testing method described in the TNZ P/23: 2005 notes [17] and the sealing method was modified to allow for faster measurements. Further details of the test method are included in Appendix H.

Contractor QC information

QC information was provided by the contractor following construction. The QC data included asphalt lab test reports, compaction tests (during construction) and tracesheets. The tracesheets included the following information for each asphalt truck:

- Asphalt plant docket number
- Truck load time
- In MTV time
- Out MTV time
- Paving width
- Length of load
- Load size (tonnes)
- Average depth

Only the “truck load time”, “in MTV time”, “load size” and “paving width” information was used in the current analysis. The “truck load time” and “in MTV time” were used to determine the average elapsed time between truck loading at the asphalt plant and unloading into the MTV for each shift.

Both the “length of road” and “average depth” information is based on the project chainages, marked on the ground at a 10 metre spacing. There is a high chance of error due to the low precision of the chainage marks, manual error from reading the incorrect mark and error due to the staff member responsible being unavailable at the required time and estimating the distance upon their return. The tracesheet “length of road” and “average depth” has not been used in the current analysis.

Construction observations

Written notes were taken by John Bull (Altissimo Consulting) during all eight paving shifts. These included equipment details, general observations and events such as equipment breakdowns. See Appendix C for details.

Summary of data collected

Table 8 provides a summary of the data collected.

Table 8 Summary of data collected

Property	Parameters	Details
Macrotecture	1 metre mean profile depth	WDM annual high-speed data survey. (January 2019)
	10 metre mean profile depth	
	1 mm texture profile	
Void content	Dielectric constant (GPR reflection amplitudes)	Part of the current work, using Fulton Hogan 2.0GHz GPR unit. (December 2018)
	Core void content	Part of the current work, core samples taken at discrete locations in the left shoulder. (October 2019)
Roughness	20 metre NAASRA count	WDM annual high-speed data survey. (January 2019)
Thickness	Pre and post-construction height survey	WSP-Opus Lidar scan. (November 2018)
	Layer thickness (GPR reflection return times)	Part of the current work, using Fulton Hogan 2.0GHz GPR unit. (December 2018)
	Tracesheet thickness	Calculated for paver GPS records and truck departure times (contractor QC documentation).
	Core thickness	Part of the current work, core samples taken at discrete locations in the left shoulder. (October 2019)
Paver monitoring	Surface temperature (~2 metres behind paver)	Custom built loggers and non-contact IR temperature sensors. (taken during construction shifts)
	GPS position and speed	
Roller monitoring	Surface temperature (~2 metres in front of roller)	Custom built loggers and non-contact IR temperature sensors. (taken during construction shifts)
	GPS position and speed	
Infrared cameras	Hand-held camera	Flir One (hand-held) and Flir E4 (paver-mounted). (taken during construction shifts)
	Paver-mounted camera	
Permeability	Time to drain 3.6L	Part of the current work, measured at discrete locations in the left lane, left wheel path. (October 2019)
Construction trace sheets	Asphalt truck load details.	From contractor QC documentation.
Asphalt test reports	Asphalt laboratory test results (e.g. particle size distributions, air void content)	From contractor QC documentation.
Construction observations	Details of stops, breakdowns.	Written notes. (taken during construction shifts)

4 Thickness trial results

4.1 Thickness relationship using target thickness

Neither the Lidar scan nor ground penetrating radar techniques provided a reliable measurement of the asphalt layer thickness. The target thickness that the construction crew aimed for during construction was initially used to determine the presence or absence of any thickness effect.

The overall L_{CPX} (80 km/h) is presented below for each trial thickness, split by lane and test tyre for the December 2018 measurements. Figure 8 presents the data for the P1 test tyre. Figure 9 presents the data for the H1 test tyre.

There is a clear thickness effect, with L_{CPX} (80km/h) decreasing by 1.8–3.2dB for each 10 mm increase in target thickness. The thickness effect is present for all combinations of lane and tyre; however, the magnitude of the effect varies. The magnitude of the changes are presented in Table 9 for both test tyres.

The overall thickness to L_{CPX} (80 km/h) relationship for the December 2018 measurements is included below, for thickness t in millimetres. The thickness effect is -2.4 dB per 10 mm increase in thickness when considering the results from the P1 and H1 test tyres together.

$$L_{CPX} = -0.24t + 102.3$$

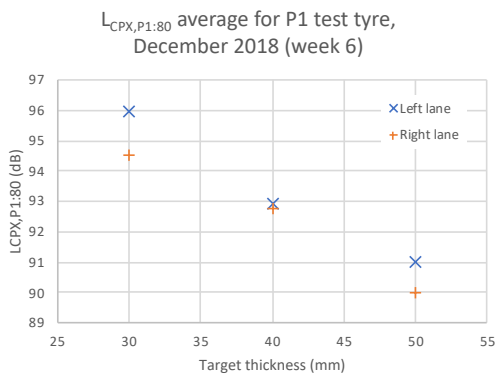


Figure 8 Average $L_{CPX,P1,80}$ for the thickness trial sections (December 2018).

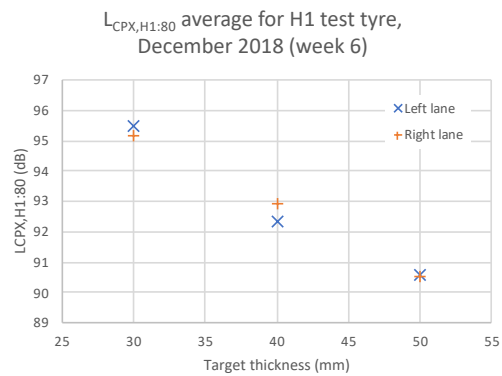


Figure 9 Average $L_{CPX,H1,80}$ for the thickness trial sections (December 2018).

Table 9 Thickness effect for P1 and H1 test tyres with 40 mm reference thickness

Lane	Target thickness	$L_{CPX,P1,80}$ (December 2018)	$L_{CPX,H1,80}$ (December 2018)
Left	30 mm	96.0 dB (+3.1)	95.5 dB (+3.2)
	40 mm	92.9 dB	92.3 dB
	50 mm	91.0 dB (-1.9)	90.5 dB (-1.8)
Right	30 mm	94.5 dB (+1.8)	95.1 dB (+2.2)
	40 mm	92.7 dB	92.9 dB
	50 mm	90.0 dB (-2.7)	90.5 dB (-2.4)

4.2 Thickness relationship from core samples

Spot checks of the asphalt layer thickness have been taken using a 100 mm core drill and these are compared to the corresponding 20 metre road segment $L_{CPX:P1:80}$ data (December 2018). The core samples were taken at nine locations in the left-hand shoulder. The locations were selected based on the above thickness to L_{CPX} relationship in order to collect cores for a range of asphalt thicknesses.

The core locations are provided in Table 10 and include sections of road both inside and outside of the thickness trial area. Three cores were taken at each location at a spacing of 5 metres with the middle core ("Core #2") being located at the Rs/Rp specified in the table.

Table 10 Spot check core locations and asphalt thickness

Location ID	Target thickness	Rs/Rp	Asphalt layer thickness (mm)			
			Core #1	Core #2	Core #3	Average
1	30 mm (thickness trial section)	01S-0327/04.950-D	26.7	24.9	26	25.9
2	40 mm (thickness trial section)	01S-0327/04.630-D	44.5	44.3	45.9	44.9
3	50 mm (thickness trial section)	01S-0327/04.390-D	60.6	55.6	53.7	56.6
4	40 mm	01S-0327/03.790-D	43.0	40.9	38.9	40.9
5	40 mm	01S-0327/03.610-I	52.5	52.7	50.0	51.7
6	40 mm	01S-0327/05.330-I	36.0	37.2	35.3	36.2
7	40 mm	01S-0327/05.250-D	50.6	45.9	53.2	49.9
8	40 mm	01S-0327/03.390-D	52.2	55.1	52.4	53.2
9	40 mm	01S-0327/04.650-I	41.3	39.6	40.8	40.6

The core sample results confirm that the as-built asphalt layer thickness can differ from the target asphalt thickness, with differences of up to 15 mm being observed.

The 20 metre $L_{CPX:P1:80}$ data (December 2018) corresponding to each core sample location is plotted against the core sample thicknesses in Figure 10. A linear regression of core sample thickness on $L_{CPX:P1:80}$ gives the following relationship:

$$L_{CPX:P1:80} = -0.22t + 103.0$$

The relationship is in general agreement with that found using the target thickness and average $L_{CPX:P1:80}$ above. The thickness effect using the core sample data is -2.2 dB $L_{CPX:P1:80}$ per 10 mm increase in thickness.

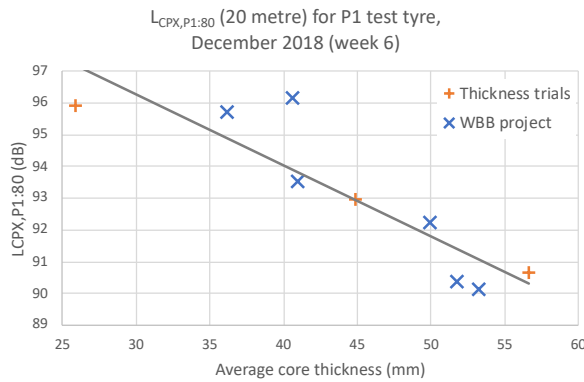


Figure 10 20 metre L_{CPX,P1:80} (December 2018) and core sample thickness.

4.3 Left-right lane differences in L_{CPX}

The left-right lane differences in L_{CPX} are presented in Table 11 for the December 2018 measurements. The P1 test tyre measurements show the left lane to have higher L_{CPX,P1:80} than the right lane for the 30 mm and 50 mm sections. The H1 test tyre measurements show the right lane to have higher L_{CPX,H1:80} for the 40 mm section, with insignificant lane differences for the 30mm and 50 mm sections.

Table 11 Left-right lane difference in L_{CPX} for the December 2018 measurements.

Measurement date	Target thickness	Left-right lane difference in L _{CPX}	
		P1 test tyre (L _{CPX,P1:80})	H1 test tyre (L _{CPX,H1:80})
December 2018 (week 6)	30 mm	+1.4 dB	+0.3 dB
	40 mm	+0.2 dB	-0.6 dB
	50 mm	+1.0 dB	+0.0 dB

Differences in macrotexture between lanes

Both the surface macrotexture and void content were kept as constant as possible during construction by maintaining the same asphalt mix design on all trial sections and constructing the trial sections in one continuous paving run per lane.

In previous studies it was hypothesised that any left-right lane differences in L_{CPX} were due to differences in macrotexture caused by differences in early trafficking between the lanes, with left lanes generally experiencing higher traffic volumes than right lanes.

The average and standard deviation of the 1 metre road segment mean profile depth (macrotexture) are presented in Table 12 below for each thickness and lane (measured 12 weeks after construction). The results show no significant variations in mean profile depth between trial thicknesses or between lanes and provide no evidence of differences in macrotexture.

Table 12 Mean profile depth by lane and trial thickness (measured 12 weeks after construction)

Lane	Target thickness	Mean profile depth (mm)	
		Average	Standard deviation
Left	30 mm	1.19	0.07
	40 mm	1.13	0.07
	50 mm	1.12	0.08
Right	30 mm	1.18	0.06
	40 mm	1.17	0.06
	50 mm	1.20	0.09

Differences in thickness between lanes

While the target thickness is known for each trial section, there is a possibility that the left-right lane thicknesses differed slightly during construction. With an average thickness effect of -2.2 dB per 10mm increase in thickness, a 5 mm difference in surface thickness between lanes could cause a 1.1 dB difference in L_{CPX} .

The average and 95% confidence interval one-third octave band $L_{CPX:P1,80}$ values from the December 2018 measurements are presented in Figure 11 to Figure 13 for each thickness.

While there are clear differences in the frequency content of the $L_{CPX:P1,80}$ between the three target thicknesses, there are no substantial differences in frequency content between the lanes that would support the hypothesis that the lane differences are the result of differences in thickness. Core sampling would be required to determine whether or not there are differences in thickness between the lanes.

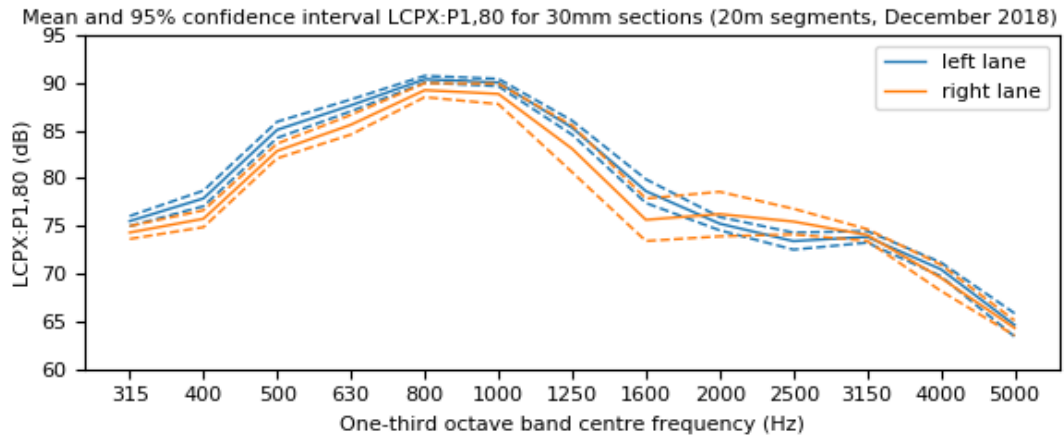


Figure 11 One-third octave band $L_{CPX:P1,80}$ (December 2018) for the 30 mm thickness sections.

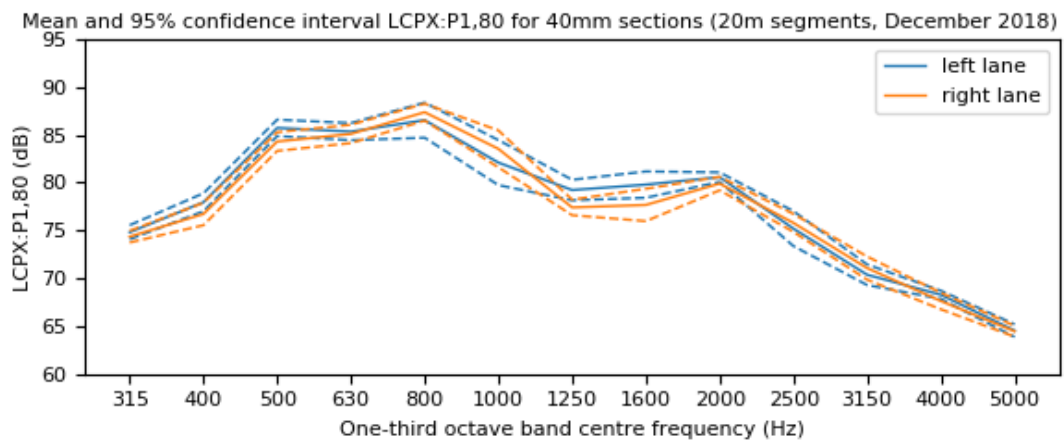


Figure 12 One-third octave band $L_{CPX:P1,80}$ (December 2018) for the 40 mm thickness sections.

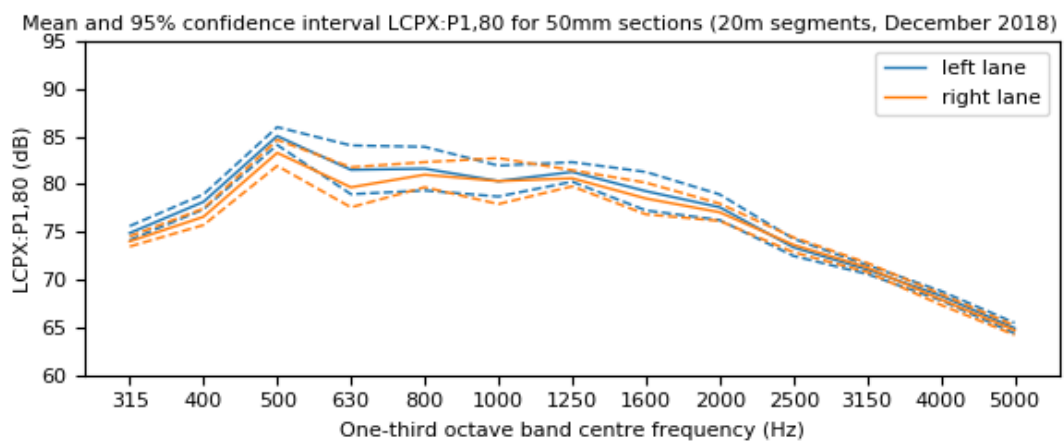


Figure 13 One-third octave band $L_{CPX:P1,80}$ (December 2018) for the 50 mm thickness sections.

5 Longitudinal variability trial results

5.1 Heatmaps

The tyre/road noise, surface and construction properties are shown as “heatmaps” below to provide an overview of the dataset. Each property includes a left and right lane measurement in both carriageways. The longitudinal variability study has only made use of the $L_{CPX:P1,80}$ data from the December 2018 measurements.

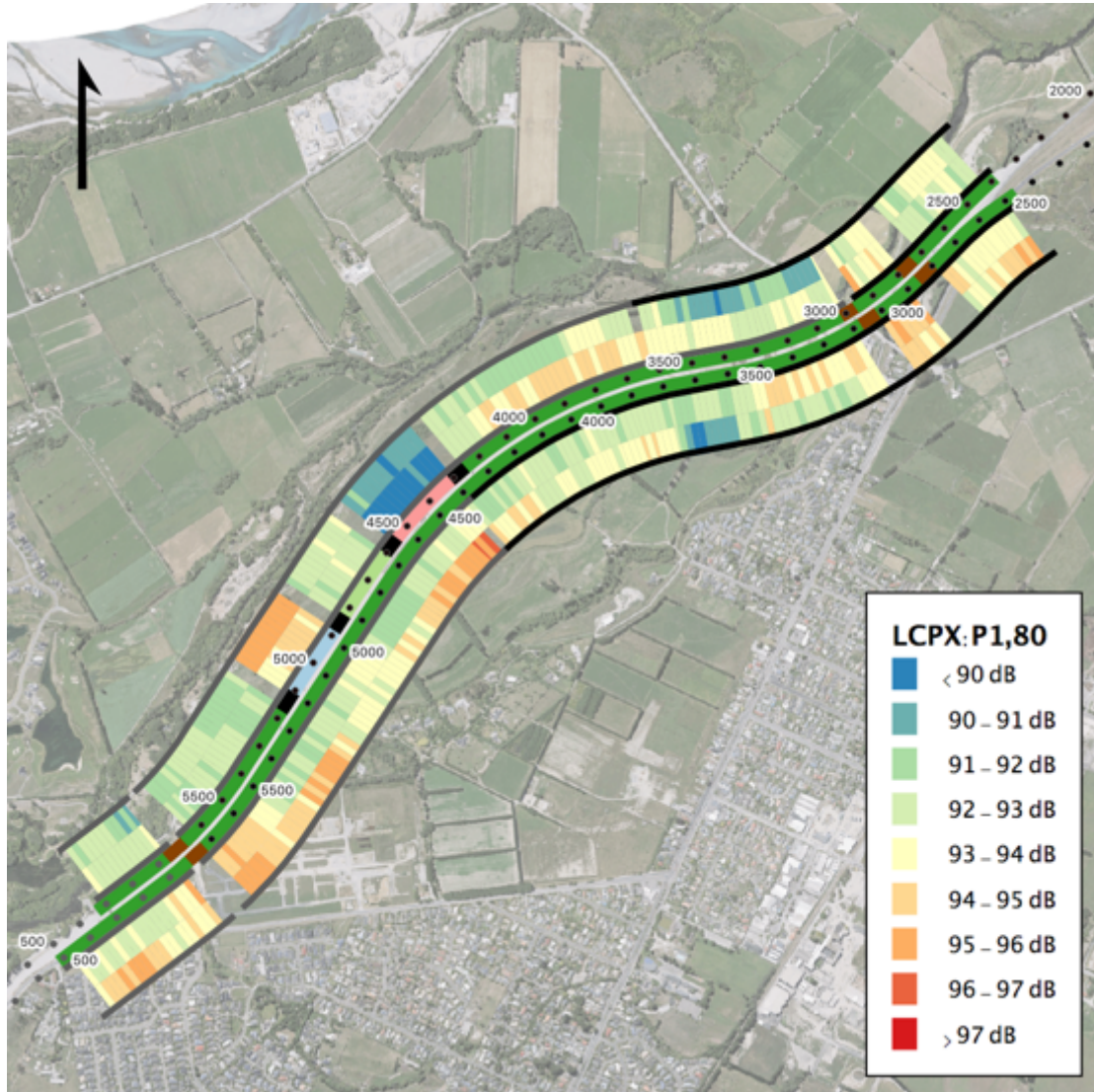


Figure 14 $L_{CPX:P1,80}$ for WBB (20 metre segments). The thickness trial sections are marked on the dotted centreline as pale blue (30 mm), pale green (40 mm) and pale red (50 mm). The construction shifts are marked as northern half (black) and southern half (grey).

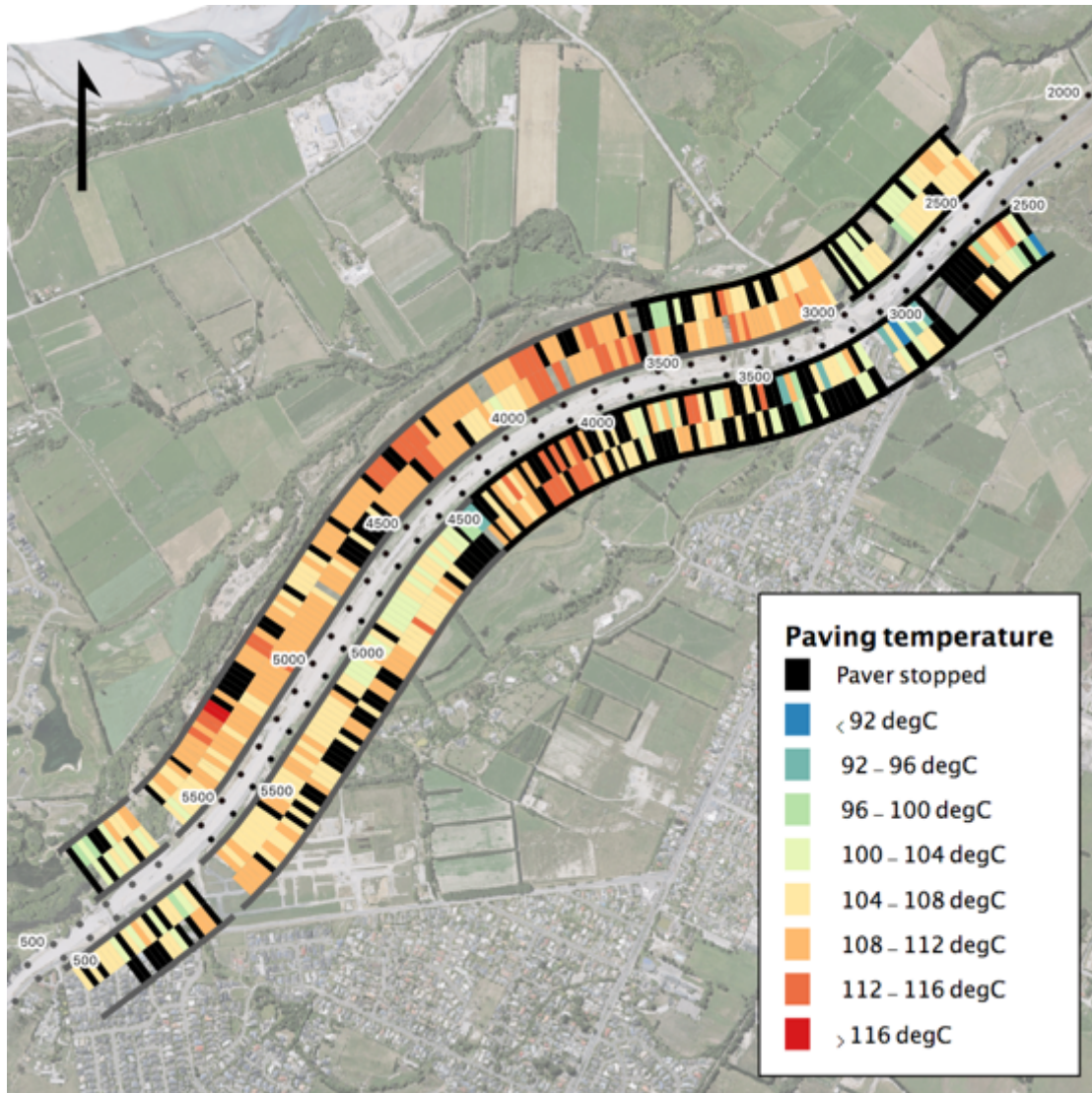


Figure 15 Paving temperature and stops for WBB (20 metre segments). The construction shifts are marked as northern half (black) and southern half (grey).



Figure 16 Paving speed and stops for WBB (20 metre segments). The construction shifts are marked as northern half (black) and southern half (grey).

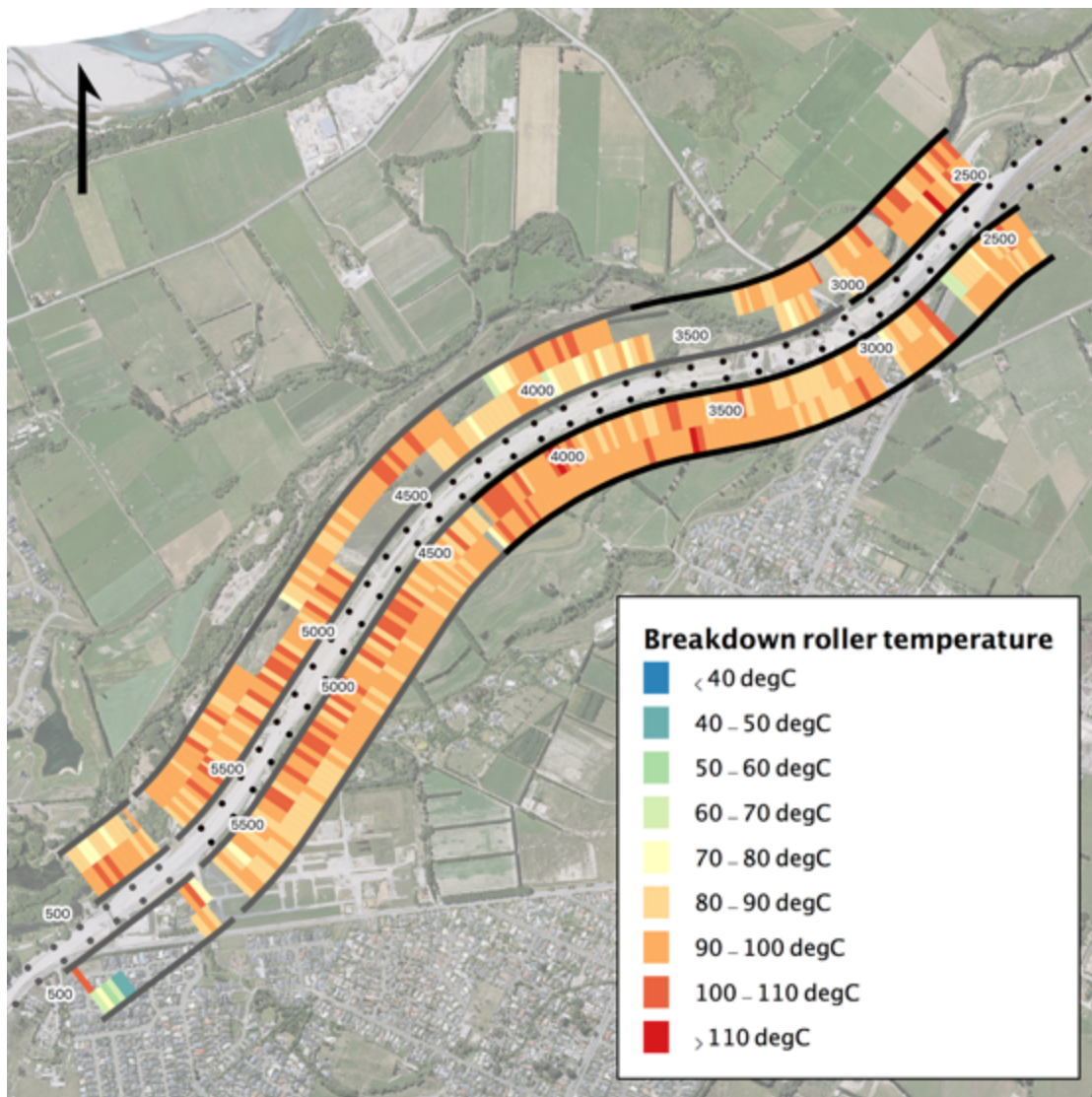


Figure 17 Breakdown roller temperature (maximum) for WBB (20 metre segments). The construction shifts are marked as northern half (black) and southern half (grey).

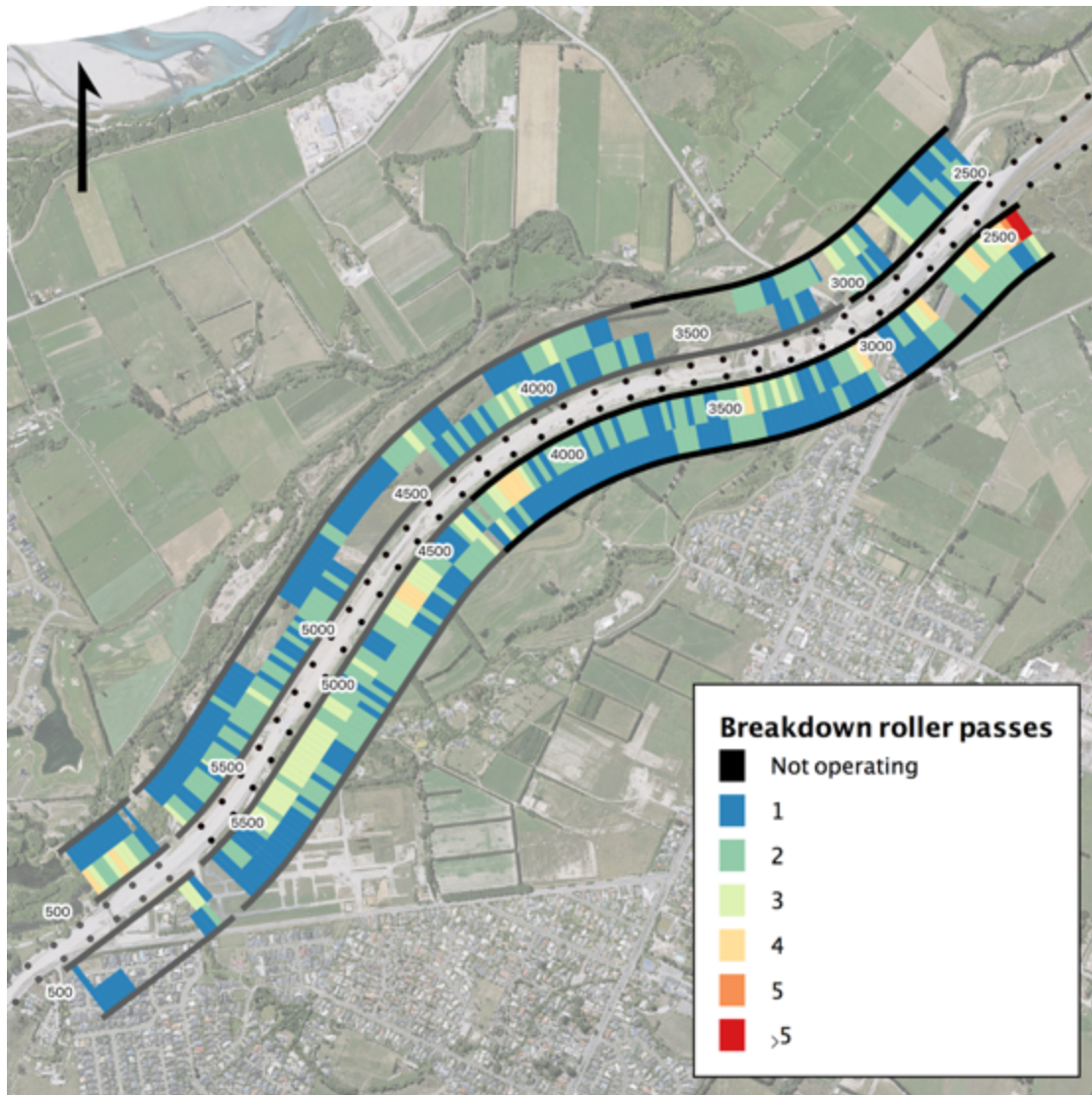


Figure 18 Number of breakdown roller passes for WBB (20 metre segments). The construction shifts are marked as northern half (black) and southern half (grey).

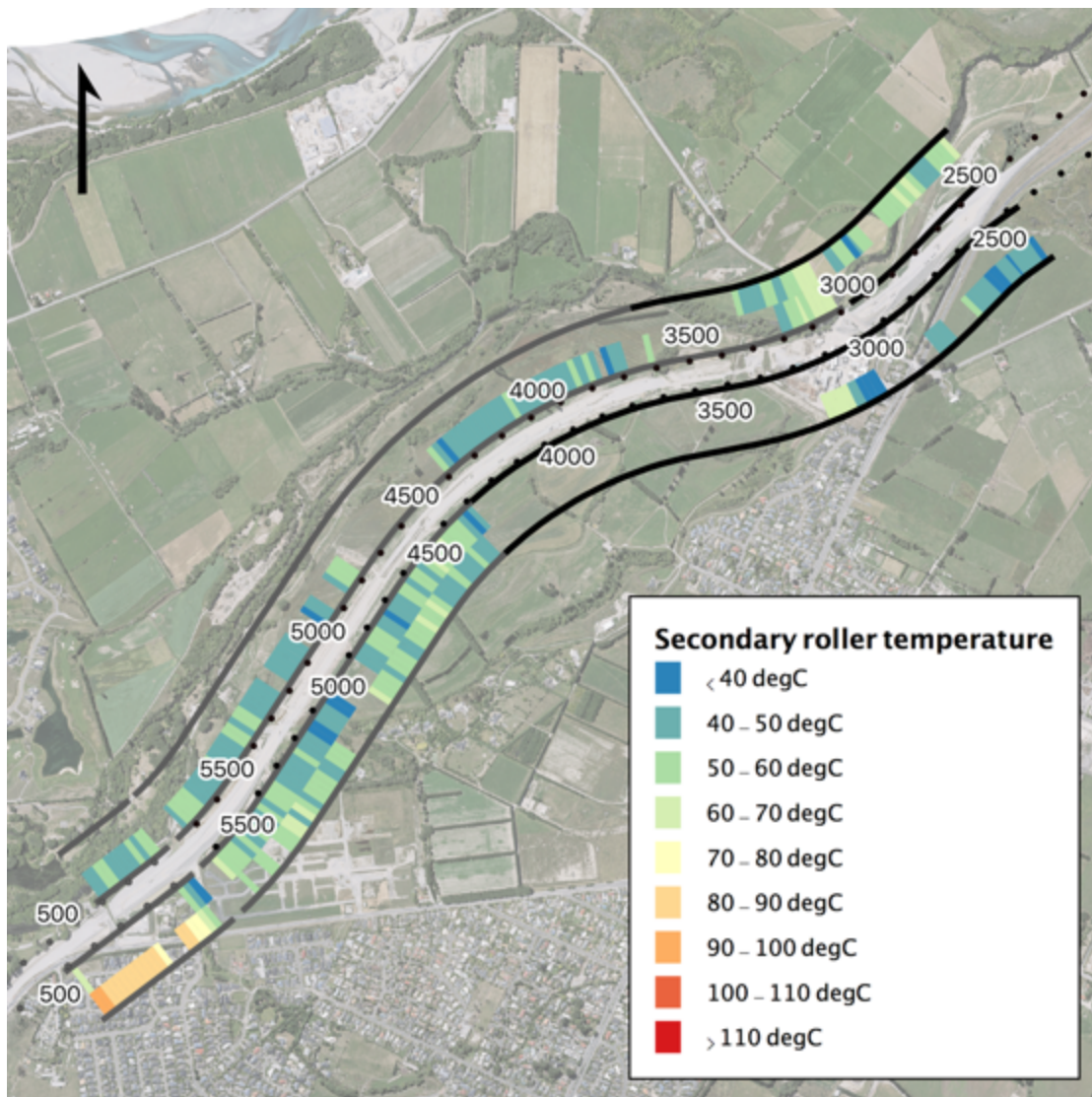


Figure 19 Secondary roller temperature (maximum) for WBB (20 metre segments). The construction shifts are marked as northern half (black) and southern half (grey).

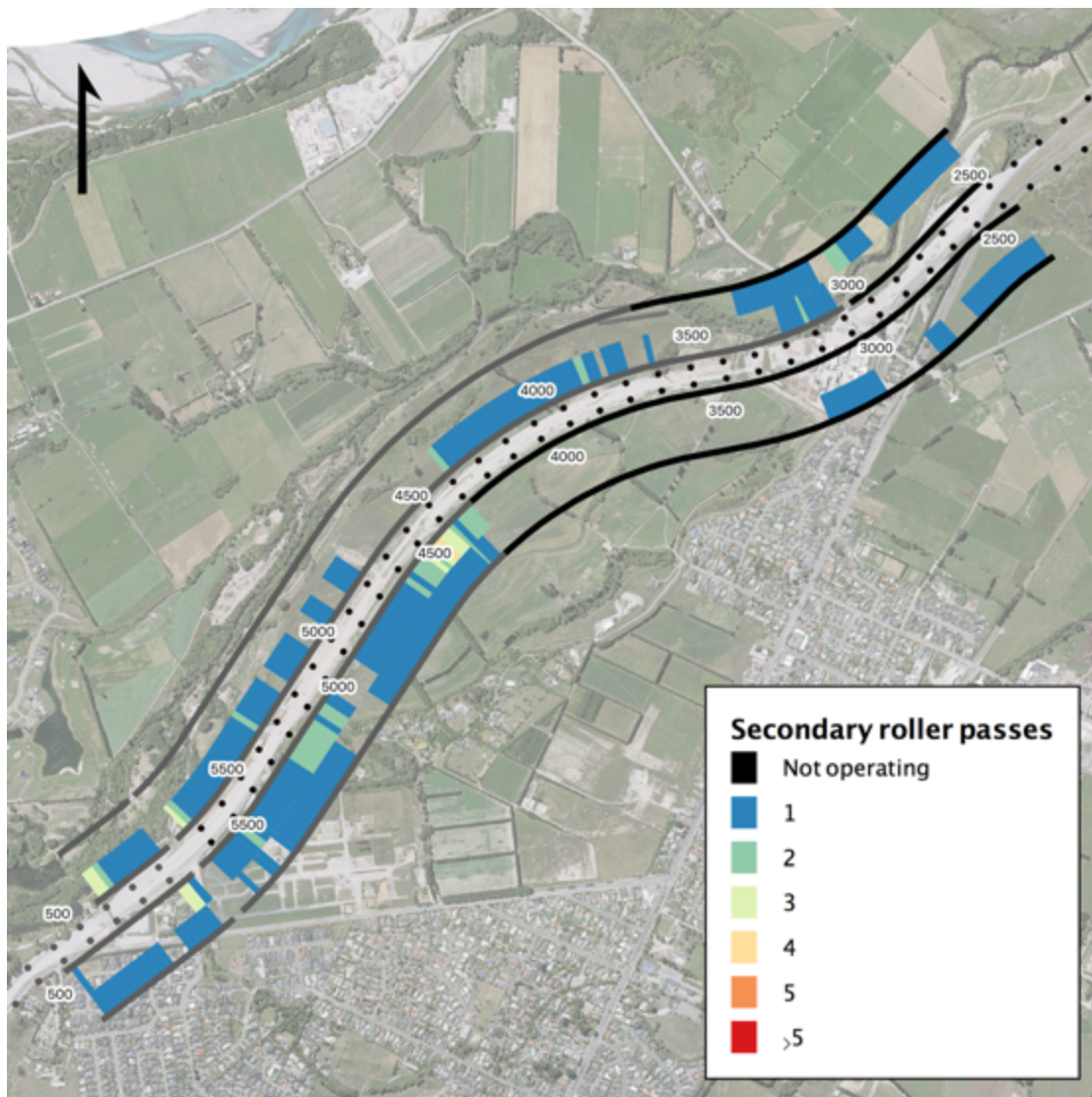


Figure 20 Number of secondary roller passes for WBB (20 metre segments). The construction shifts are marked as northern half (black) and southern half (grey).

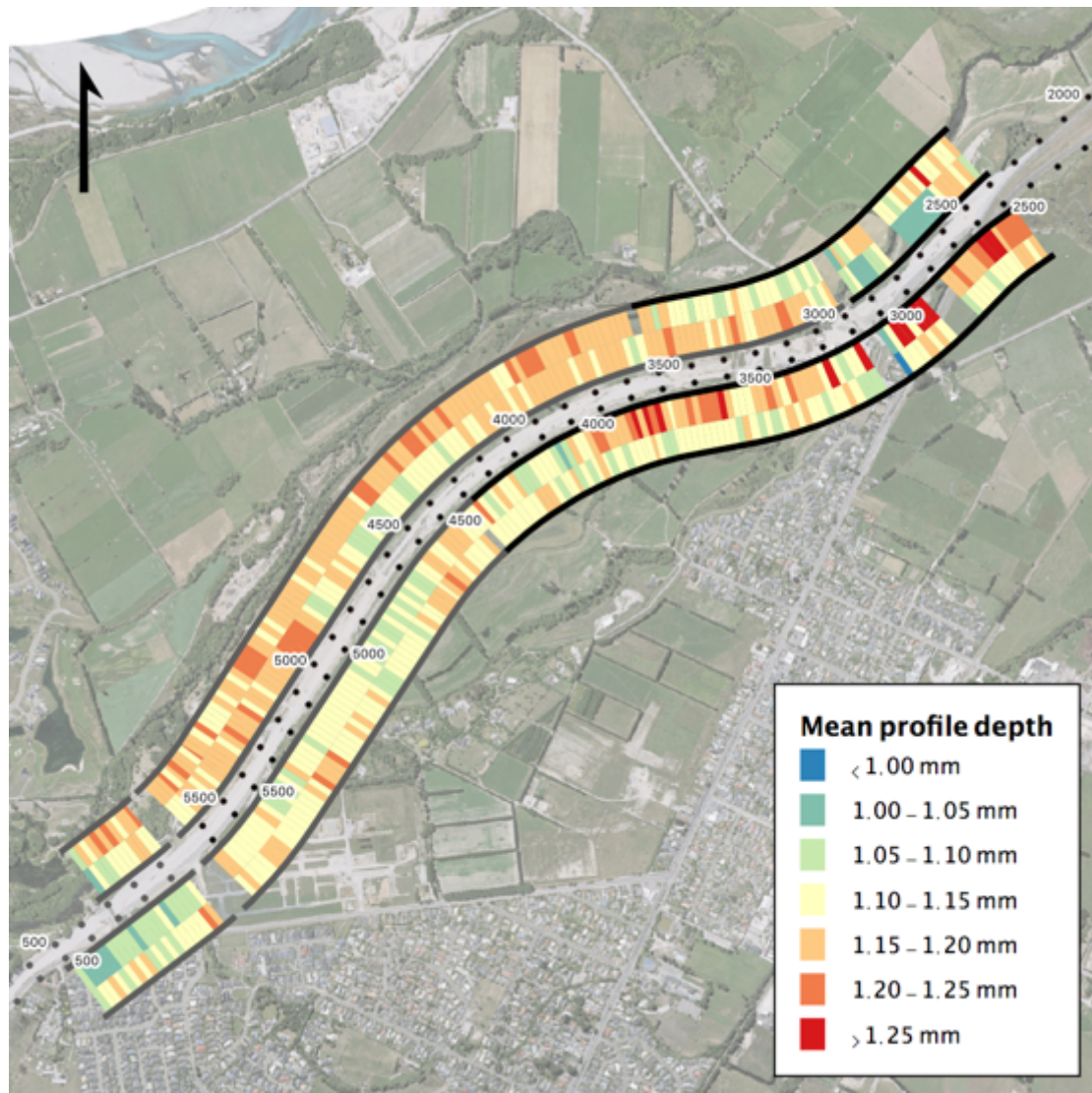


Figure 21 Left wheel path mean profile depth for WBB (20 metre segments), calculated from 2019 WDM 10 metre dataset. The construction shifts are marked as northern half (black) and southern half (grey).

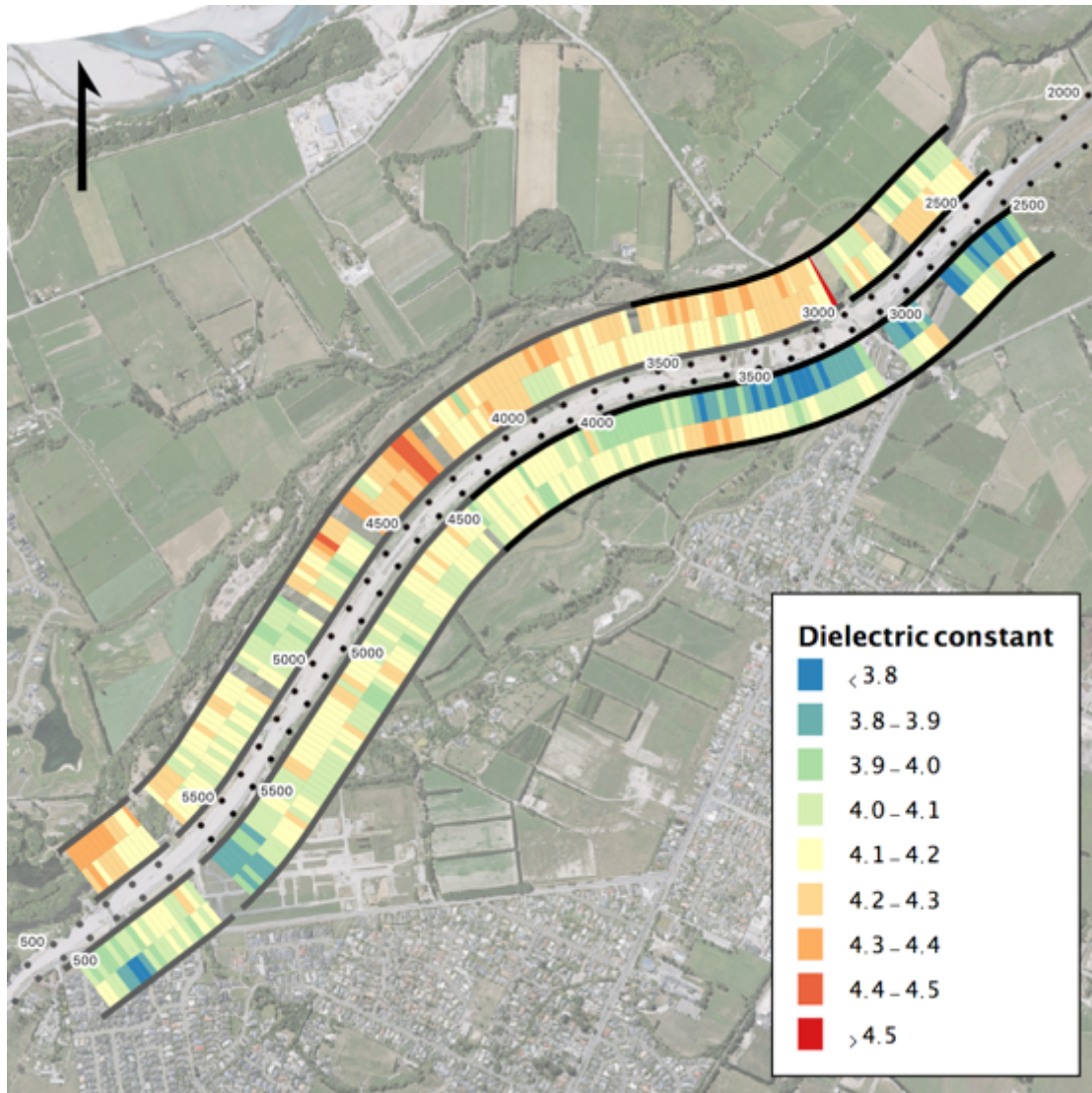


Figure 22 Surface dielectric constant for WBB (20 metre segments). The construction shifts are marked as northern half (black) and southern half (grey).

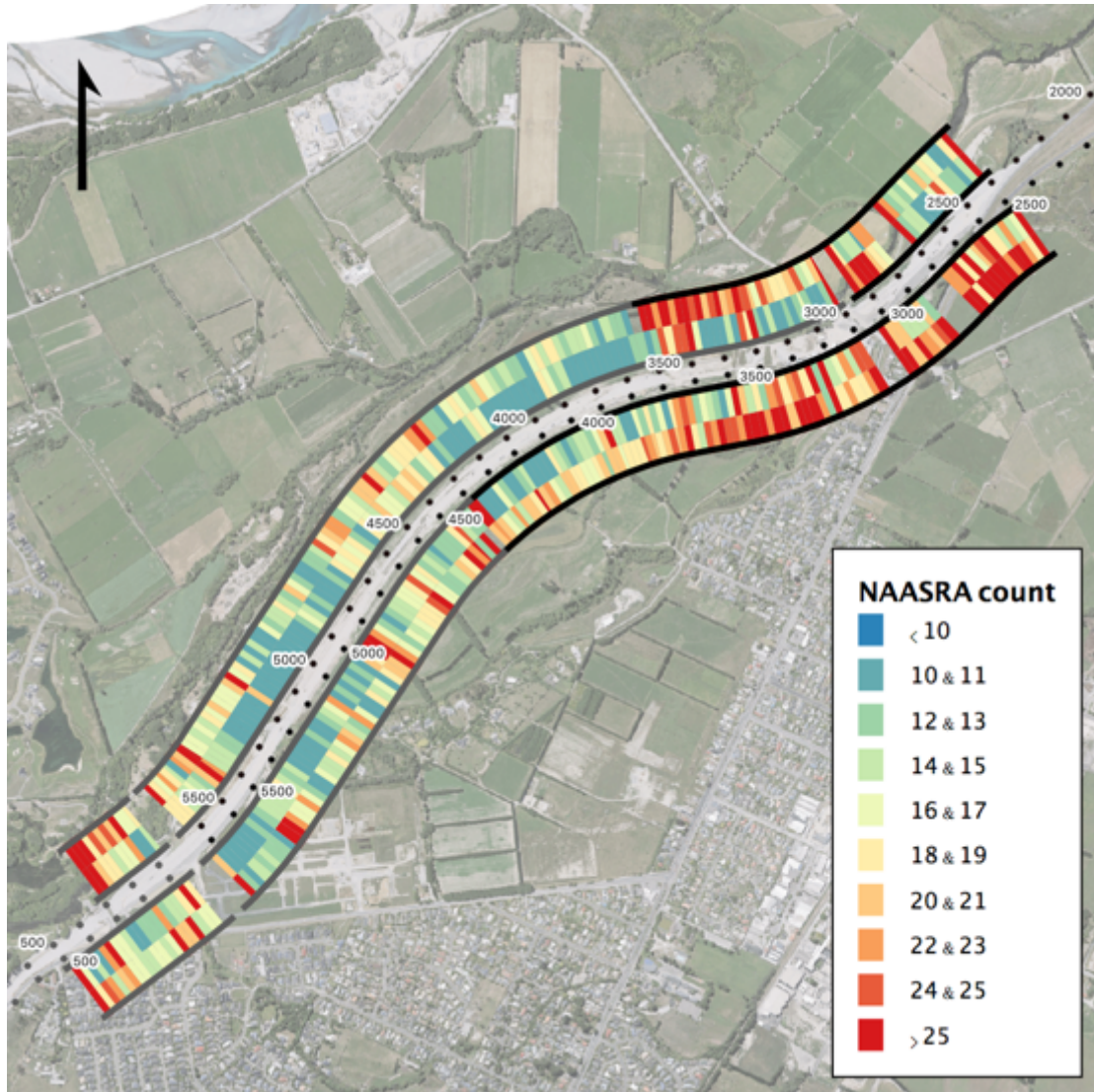


Figure 23 NAASRA count for WBB (20 metre segments). The construction shifts are marked as northern half (black) and southern half (grey).

5.2 $L_{CPX:P1,80}$, surface properties and construction properties with and without MTV

The effects of the material transfer vehicle on tyre/road noise, road surface properties and operating behaviour of the paver are investigated using the right lane southbound carriageway between Dickey's Road bridge and Groynes Road bridge.

The section of road was chosen for the following reasons:

- It is free from features that would usually cause the paving process to slow or stop (key-ins, manholes and complex edge detailing),
- Both MTV and no-MTV sections lie in the same lane (and carriageway) so experience similar traffic behaviour, and
- There are approximately equal numbers of MTV and no-MTV 20 metre road segments.

Table 13 lists the start and end positions of the no-MTV and MTV sections. The segments within 50 metres of each bridge key-in have been excluded as these generally involve some edge detailing. Similarly, the segments within 50 metres of the junction between the two shifts have been excluded due to the slow paving and paver stops usually associated with the start and end of paving shifts.

Table 13 Start and end Rs/Rp for the no-MTV and MTV sections.

	Start Rs/Rp	End Rs/Rp	Length
No MTV section (shift 1)	01S-0327/03.150-I	01S-0327/04.350-I	1,200 metres
MTV section (shift 3)	01S-0327/04.450-I	01S-0327/05.700-I	1,250 metres

Table 14 provides a summary of the mean and standard deviation for each available surface and construction property. Also included in the table are details of the number of paver stops, asphalt plant-to-paver time, truck load size and the total number of trucks. Where applicable the distributions of each property are plotted (see Figure 24 to Figure 37).

Key differences between the no-MTV and MTV sections are as follows:

- The results show that there is no significant difference in $L_{CPX:P1,80}$ between the no-MTV and MTV sections, both in terms of average level and standard deviation.
- The average and standard deviation of the mean profile depth for the MTV section is slightly lower than the no-MTV section. It is unclear whether or not this is a significant difference. Analysis of a similar system provided mean profile depth repeatability of 0.1 mm [18].
- The average surface dielectric constant is slightly higher for the MTV section, suggesting that the MTV section has a lower void content than the no-MTV section. The relationship between surface dielectric constant and void content was investigated using the core samples from nine locations (3 cores per location); however, no clear relationship was found (refer to Appendix D, Section D.2).
- There is a small change in average NAASRA count between the no-MTV and MTV sections. The magnitude of the change is minimal and should not represent a perceptible difference in ride quality.
- The average paving temperature is slightly lower for the MTV section. This could be explained by the fact that the asphalt has to travel through the MTV (without reheating) before reaching the paver; however, there was also a difference in ambient air temperature between the two paving shifts (11°C for no-MTV, 7°C for MTV), which may be another reason for the faster asphalt cooling within the MTV section. The 20 metre segments within the MTV section experienced lower variations in paving temperature than those within the no-MTV section, which can be explained by the temperature smoothing effect caused by the large thermal mass of the MTV.
- The no-MTV section involved more paver stops. This is due to the paver being stopped at every truck change-over, compared to the MTV section that generally involved continuous paving.

- The 20 metre segment paving speed is consistent for both no-MTV and MTV sections. The paving speed calculation includes paver stops, hence, the no-MTV section has more <4 metre/minute segments due to the higher number of stops.
- The average asphalt plant-to-paver time is significantly longer for the no-MTV section, which is put down to the reasons listed below and supported by the piecemeal distribution in Figure 36.
 1. The no-MTV section was the first paving shift of the project and there were multiple delays getting paving underway while staff and equipment settled in to their roles. Later paving shifts involved fewer start-of-shift delays.
 2. The no-MTV section follows on from a complex area involving bridge key-ins and edge detailing that caused the paving process to slow and significant wait times for the asphalt trucks.
- The truck load size was consistent between the no-MTV and MTV sections. With the MTV section using three more trucks, which is consistent with it being slightly longer.

Table 14 Summary statistics for the no-MTV and MTV sections.

Property	Statistic	No-MTV (shift 1)	MTV (shift 3)
L _{CPX:P1,80} (20 metre segments, December 2018)	Mean	93.1 dB	93.0 dB
	Std. dev.	0.87 dB	0.97 dB
Mean profile depth (20 metre segments, WDM January 2019)	Mean	1.17 mm	1.12 mm
	Std. dev.	0.06 mm	0.03 mm
Surface dielectric constant (20 metre segments, December 2018)	Mean	3.96	4.11
	Std. dev.	0.13	0.09
NAASRA count (20 metre segments, WDM January 2019)	Mean	16.2	14.3
	Std. dev.	5.2	4.4
Paving temperature (1 metre segments, excludes stops)	Mean	107.5°C	105.6°C
	Std. dev.	6.7°C	3.0°C
Paving speed (20 metre segments, includes stops)	Mean	6.8 metres/minute	6.6 metres/minute
	Std. dev.	1.7 metres/minute	1.5 metres/minute
Paver stops (1 metre segments)	Total	40	8
Asphalt plant-to-paver time	Mean	79.5 minutes	36.8 minutes
	Std. dev.	43.3 minutes	5.3 minutes
Asphalt truck load size	Mean	12.8 tonnes	13.1 tonnes
	Std. dev.	3.6 tonnes	3.3 tonnes
Number of trucks	Total	32	35
Paved length per truck load	Average	37.5 metres	35.7 metres

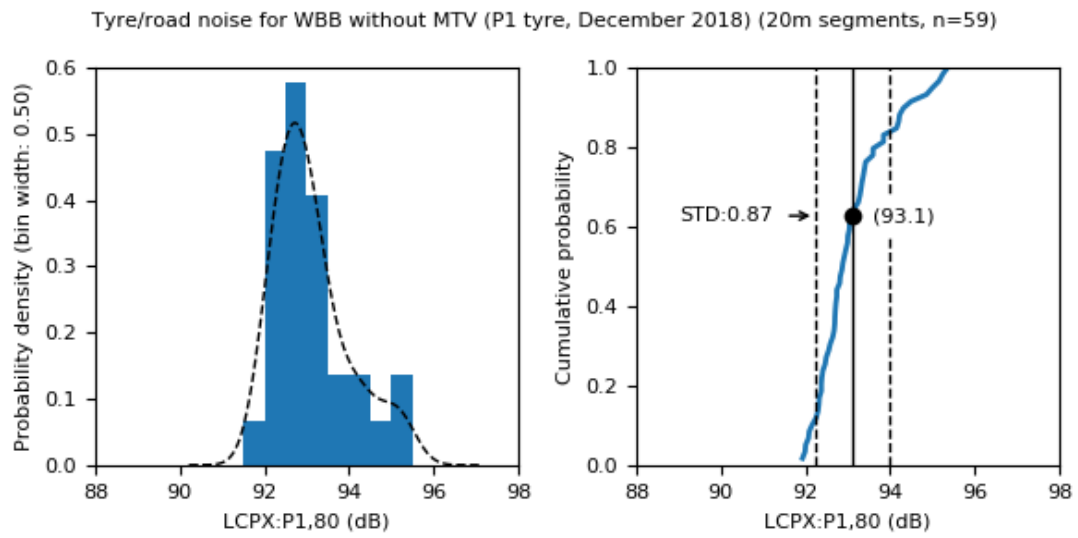


Figure 24 $L_{CPX:P1,80}$ (December 2018) for the no-MTV section.

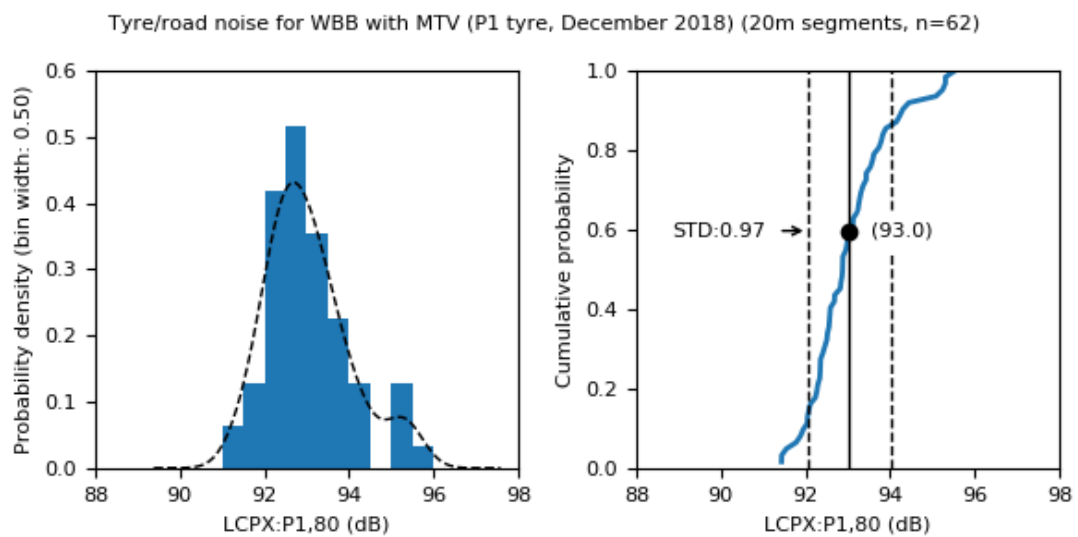


Figure 25 $L_{CPX:P1,80}$ (December 2018) for the MTV section.

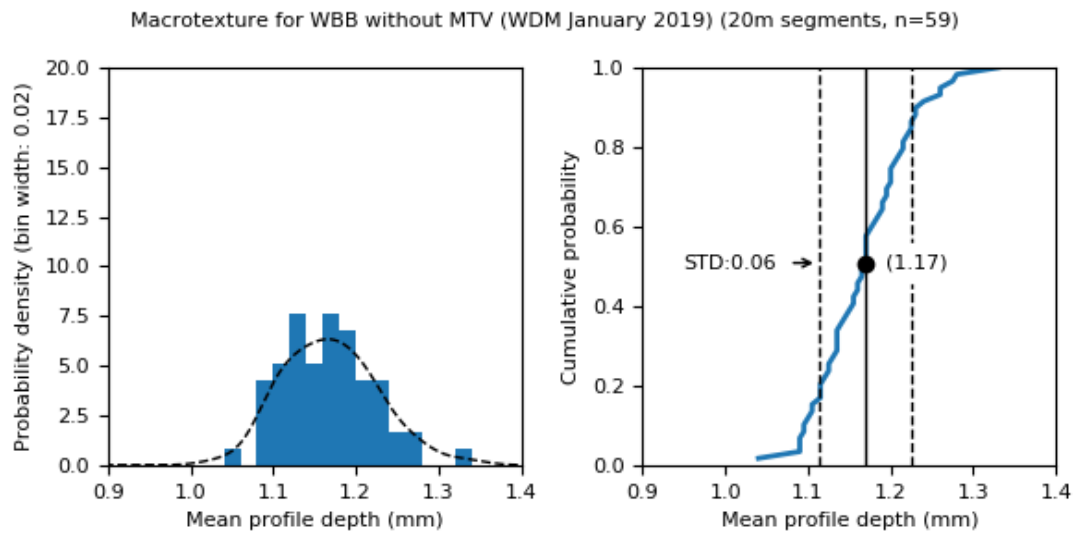


Figure 26 Mean profile depth (WDM, January 2019) for the no-MTV section.

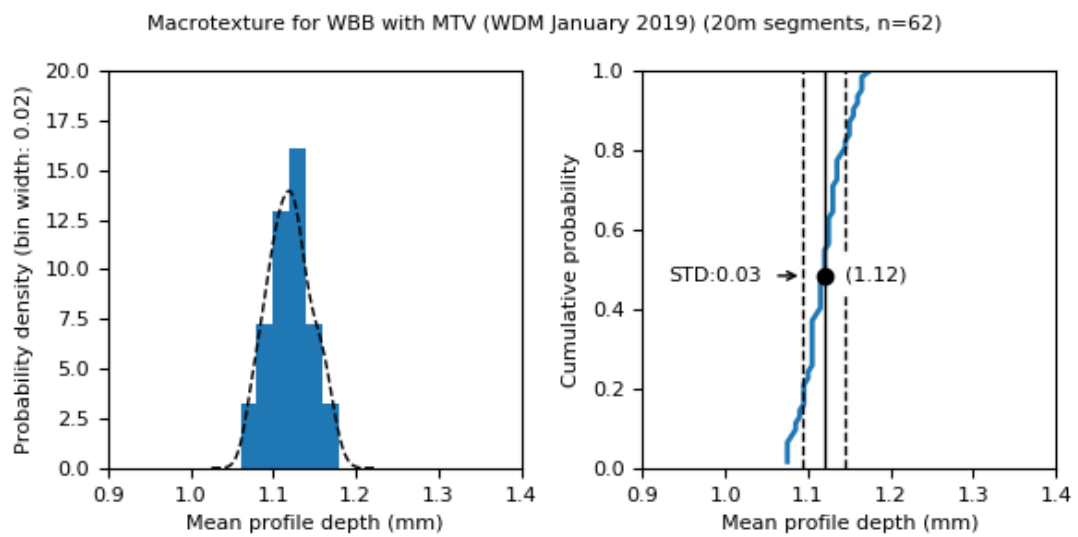


Figure 27 Mean profile depth (WDM, January 2019) for the MTV section.

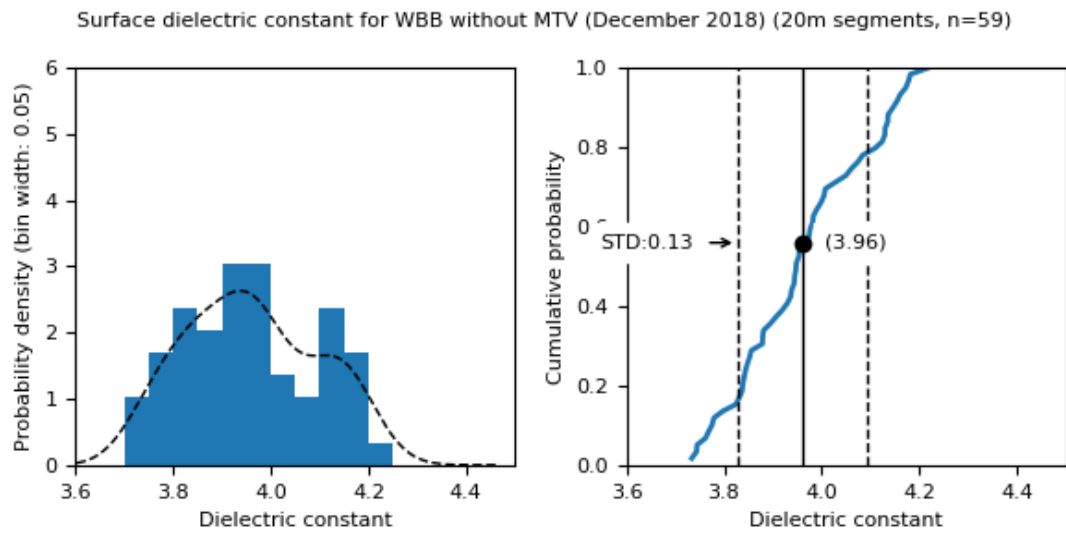


Figure 28 Surface dielectric constant (December 2018) for the no-MTV section.

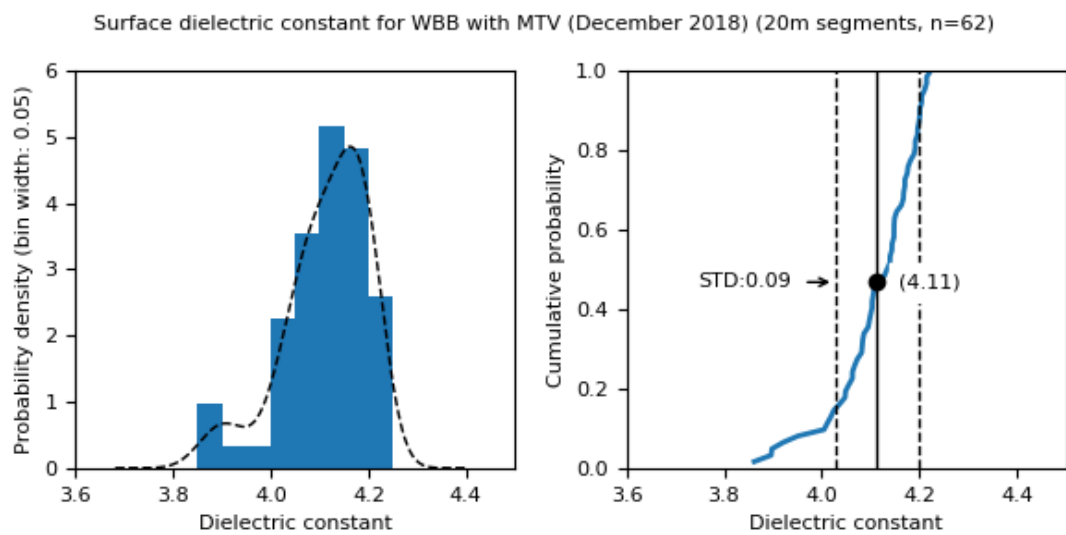


Figure 29 Surface dielectric constant (December 2018) for the MTV section.

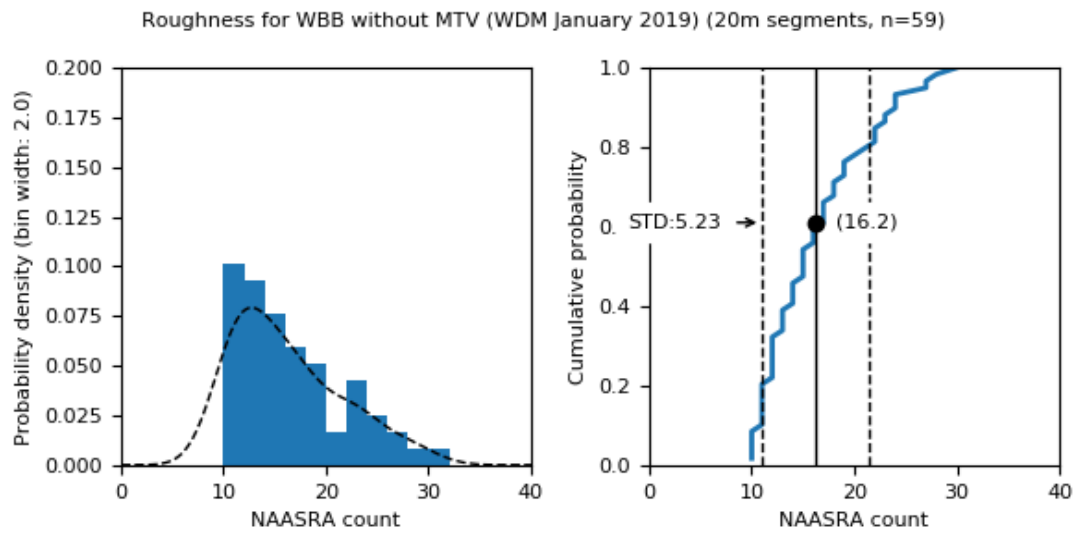


Figure 30 NAASRA count (WDM, January 2019) for the no-MTV section.

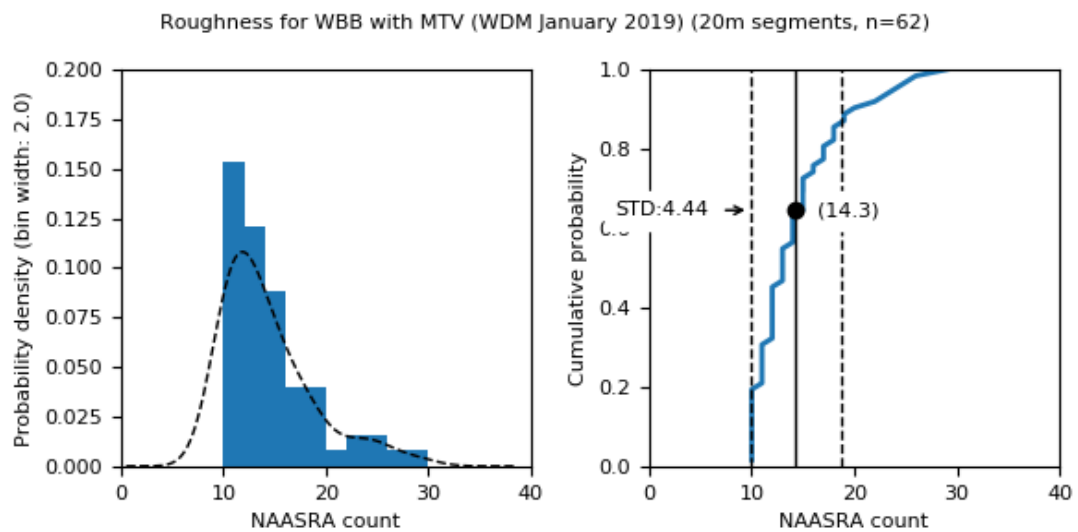


Figure 31 NAASRA count (WDM, January 2019) for the MTV section.

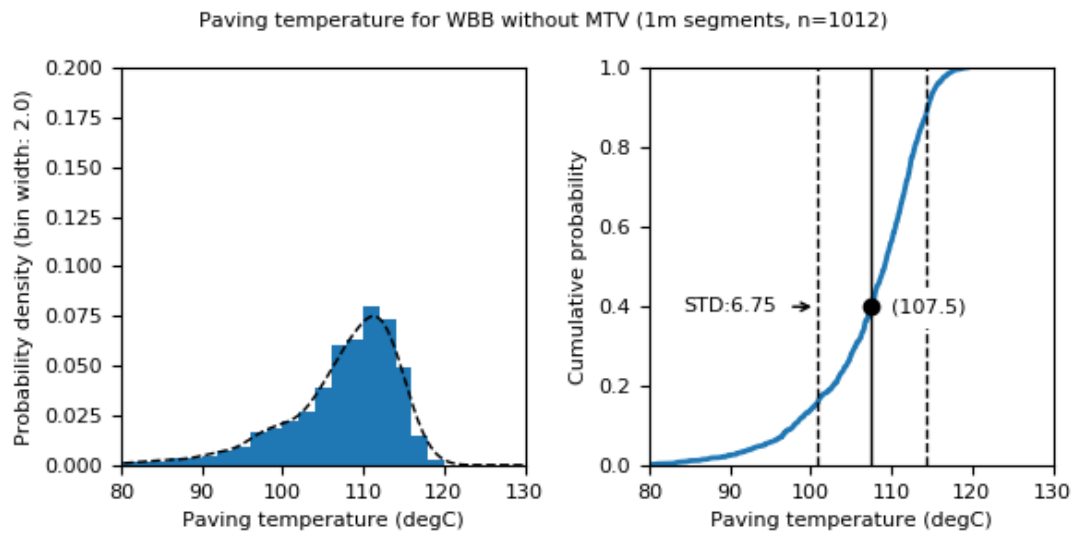


Figure 32 Paving temperature, 1 metre segments excluding stops for the no-MTV section.

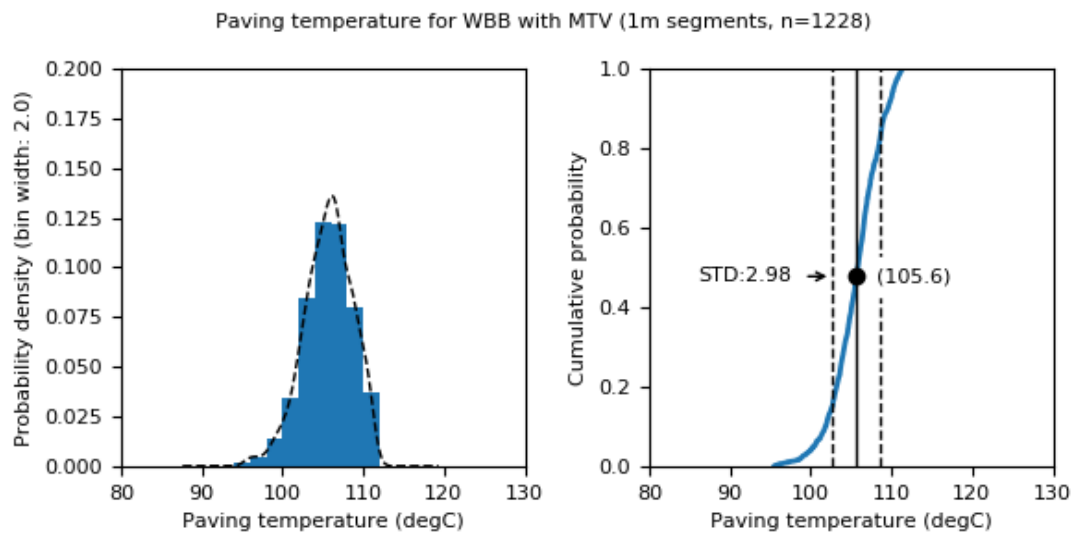


Figure 33 Paving temperature, 1 metre segments excluding stops for the MTV section.

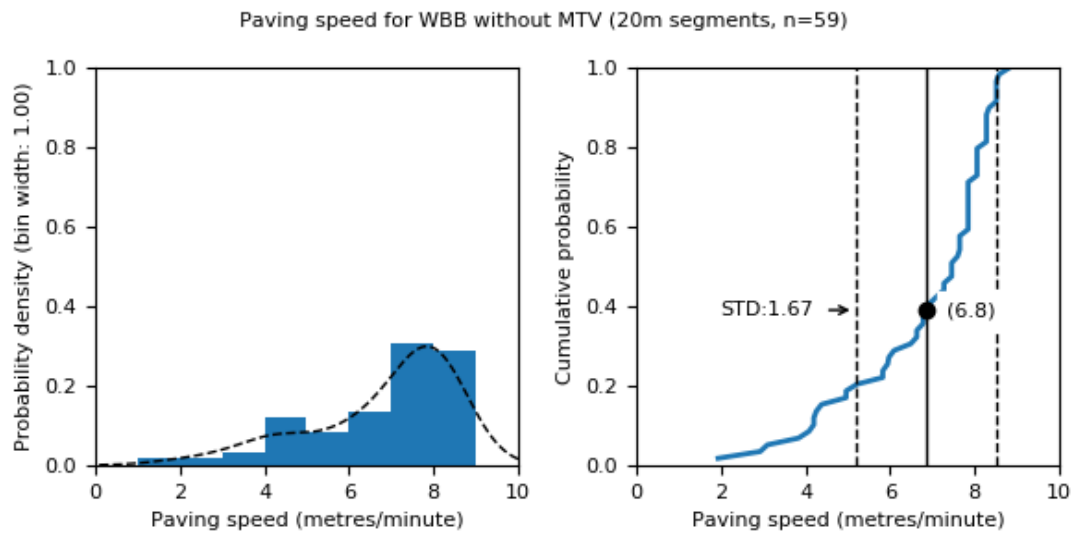


Figure 34 Paving speed, 20 metre segments including stops for the no-MTV section.

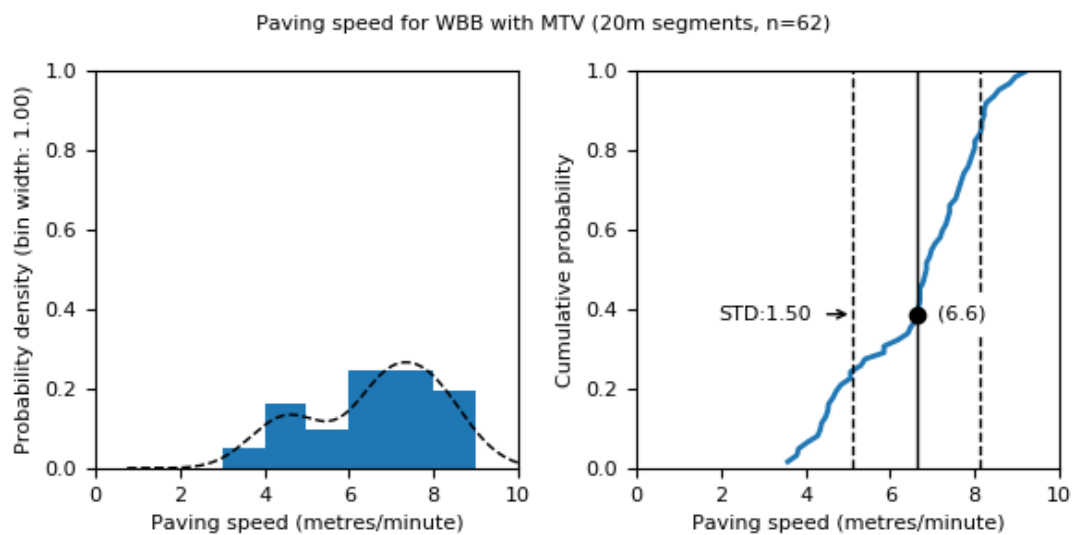


Figure 35 Paving speed, 20 metre segments including stops for the MTV section.

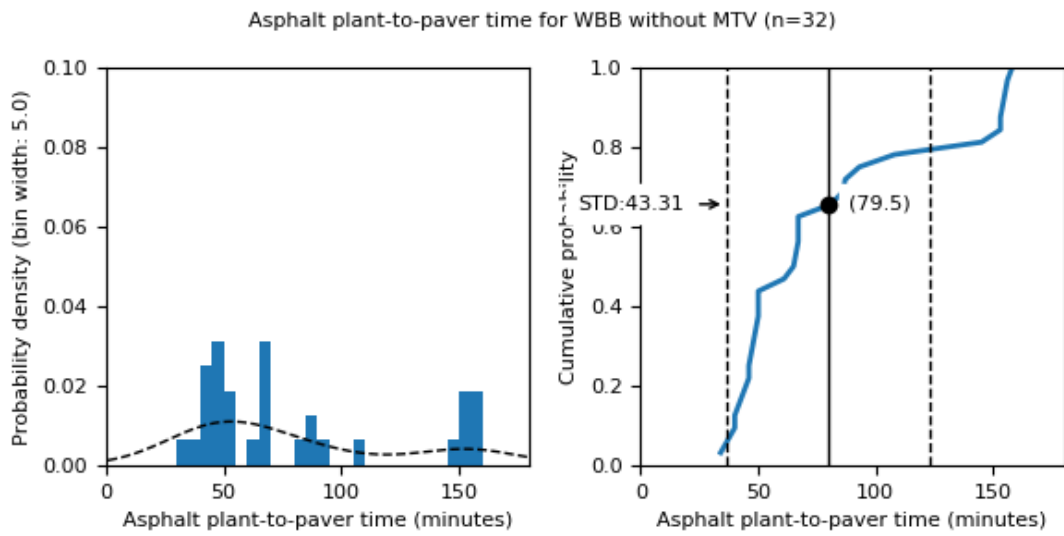


Figure 36 Asphalt plant-to-paver time for the no-MTV section.

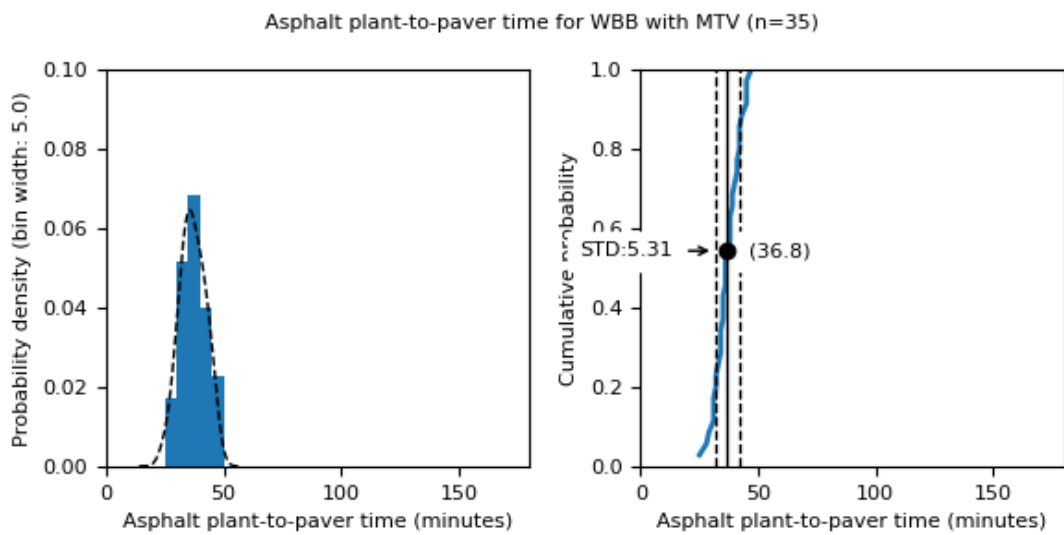


Figure 37 Asphalt plant-to-paver time for the MTV section.

5.3 Effect of surface and construction properties on $L_{CPX:P1,80}$

From the above thickness trial results it is hypothesised that the majority of variability in tyre/road noise is associated with variations in the as-built asphalt thickness. The lack of a comprehensive as-built thickness dataset significantly limits the ability to investigate additional (less significant) sources of variability. Consequently, this section simply presents the distribution of each construction property along with a comparison between each property and the tyre/road noise.

The sections of road used are limited to the MTV sections (shifts 2–8) with 40 mm target thickness.

Table 15 presents the average and standard deviation of $L_{CPX:P1,80}$, surface and construction properties. The distributions of each property are plotted in Figure 38 to Figure 46. Each property is plotted against the tyre/road noise in Figure 47 to Figure 55.

Apart from a weak correlation between surface dielectric constant and $L_{CPX,P1:80}$ no clear relationships are observed. Current work to calibrate the dielectric to void content relationship has not proved successful.

Table 15 Summary of available surface properties for WBB project, 40 mm nominal thickness with MTV.

Type	Property	Statistic	Value
Tyre/road noise	$L_{CPX:P1,80}$ (20 metre segments, December 2018)	Mean	93.4 dB
		Std. dev.	1.2 dB
Surface	Mean profile depth (20 metre segments, WDM January 2019)	Mean	1.14 mm
		Std. dev.	0.04 mm
	Surface dielectric constant (20 metre segments, December 2018)	Mean	4.14
		Std. dev.	0.11
Construction	Paving temperature (20 metre segments, includes stops)	Mean	106.2°C
		Std. dev.	4.5°C
	Paving speed (20 metre segments, includes stops)	Mean	6.5 metres/minute
		Std. dev.	1.8 metres/minute
	Paving stops (number of 20 metre segments affected by at least one stop)	Total	119 (out of 502 segments)
	Breakdown roller temperature (20 metre segments, maximum value)	Mean	90.8°C
		Std. dev.	11.3°C
	Breakdown roller passes (20 metre segments, average across lane)	Mean	2.0 passes
		Std. dev.	0.8 passes
	Secondary roller temperature (20 metre segments, maximum value)	Mean	52.3°C
Std. dev.		11.2°C	
Secondary roller passes (20 metre segments, average across lane)	Mean	1.3 passes	
	Std. dev.	0.7 passes	

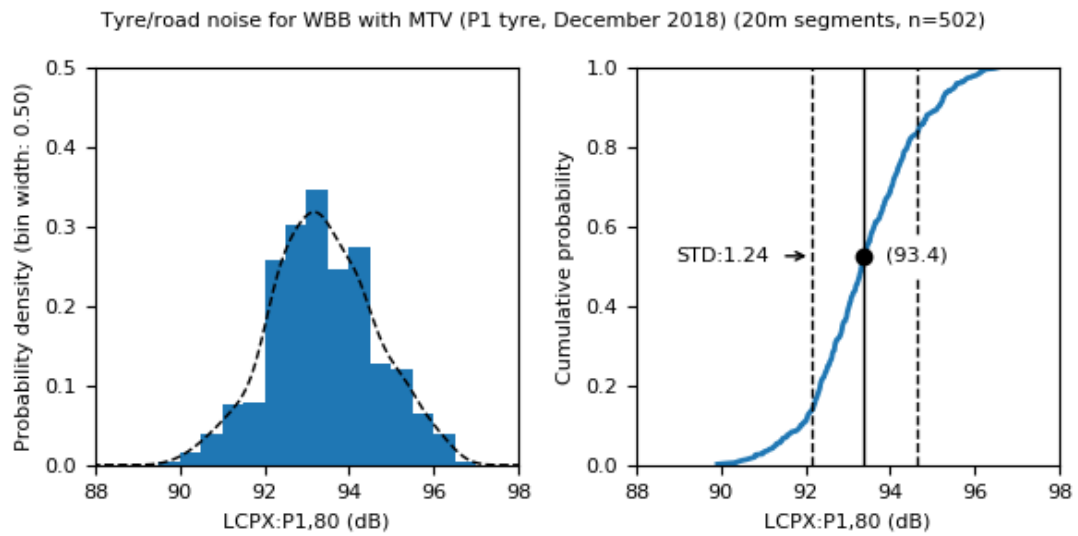


Figure 38 $L_{CPX:P1,80}$ (December 2018) for WBB project, 40 mm nominal thickness with MTV.

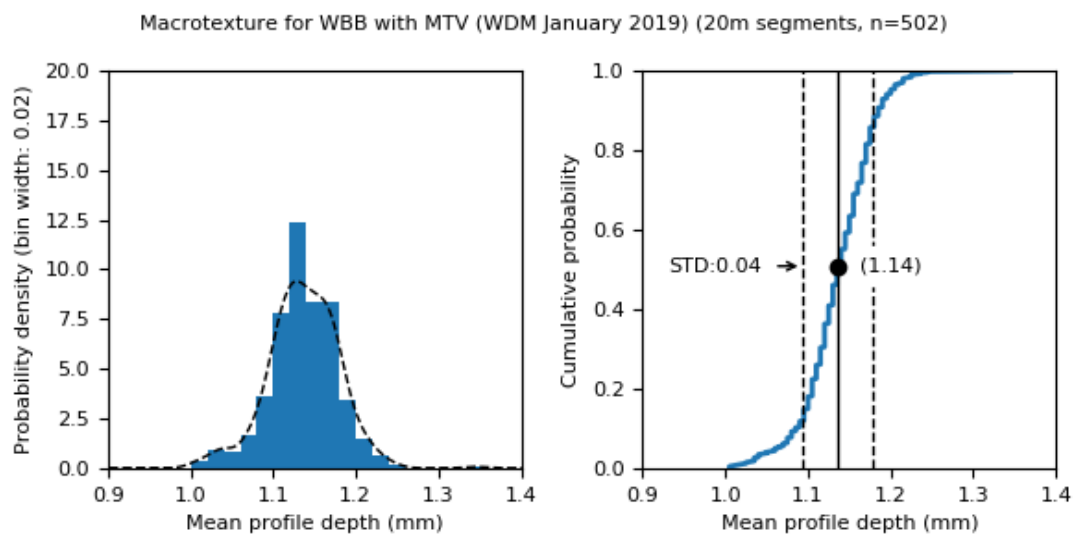


Figure 39 Mean profile depth (WDM, January 2019) for WBB project, 40 mm nominal thickness with MTV.

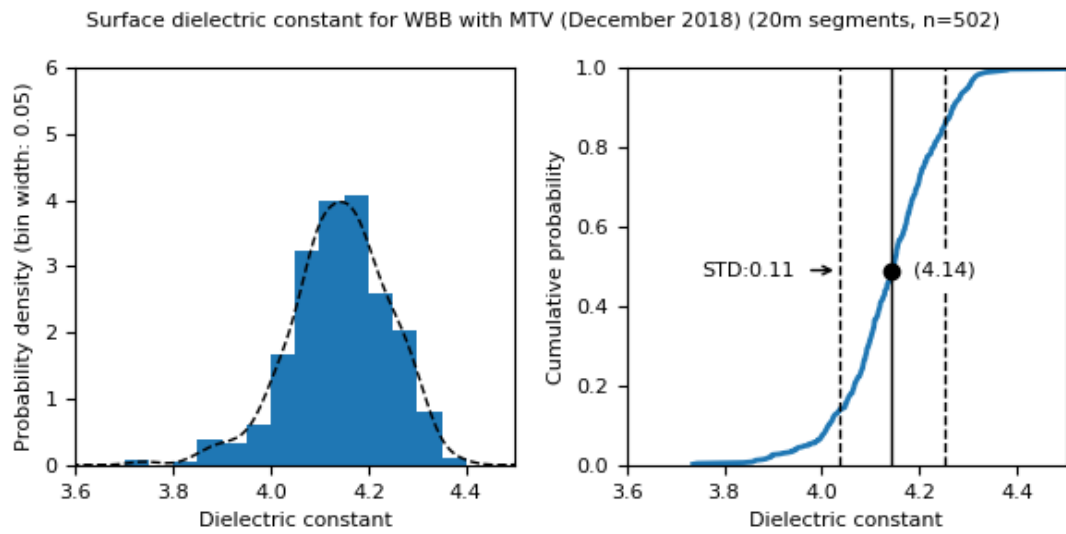


Figure 40 Surface dielectric constant (December 2018) for WBB project, 40 mm nominal thickness with MTV.

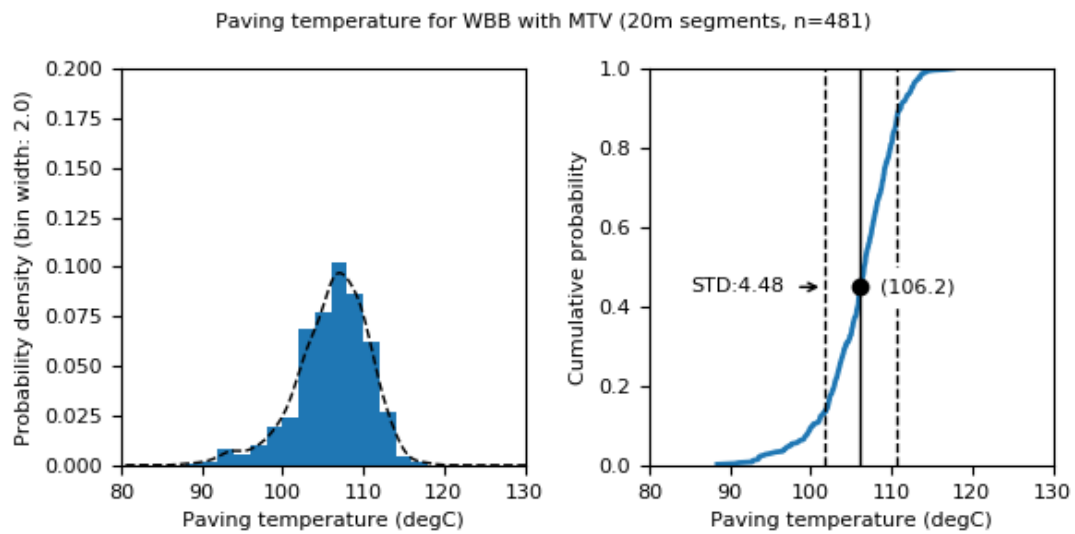


Figure 41 Paving temperature (including stops) for WBB project, 40 mm nominal thickness with MTV.

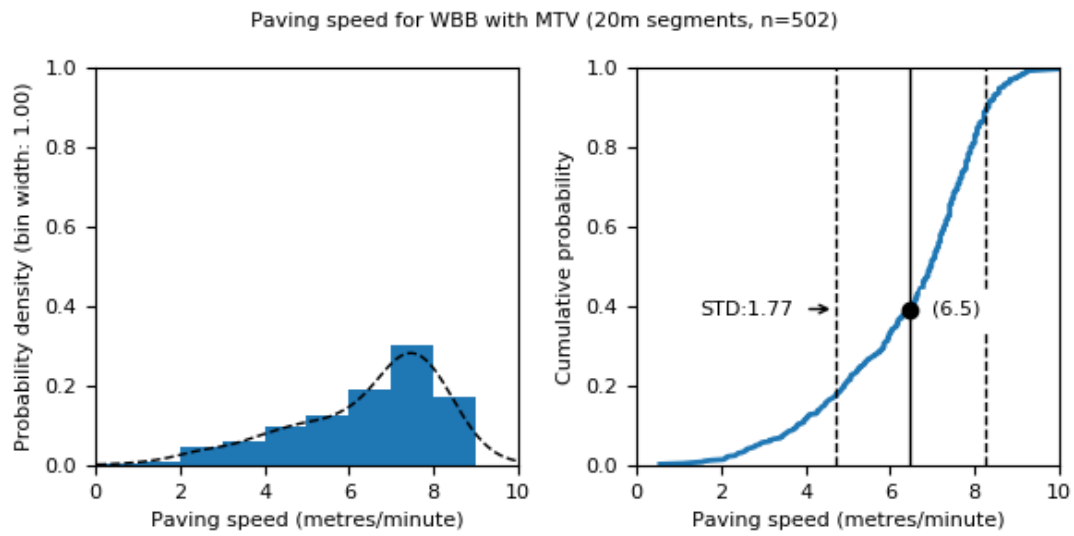


Figure 42 Paving speed (including stops) for WBB project, 40 mm nominal thickness with MTV.

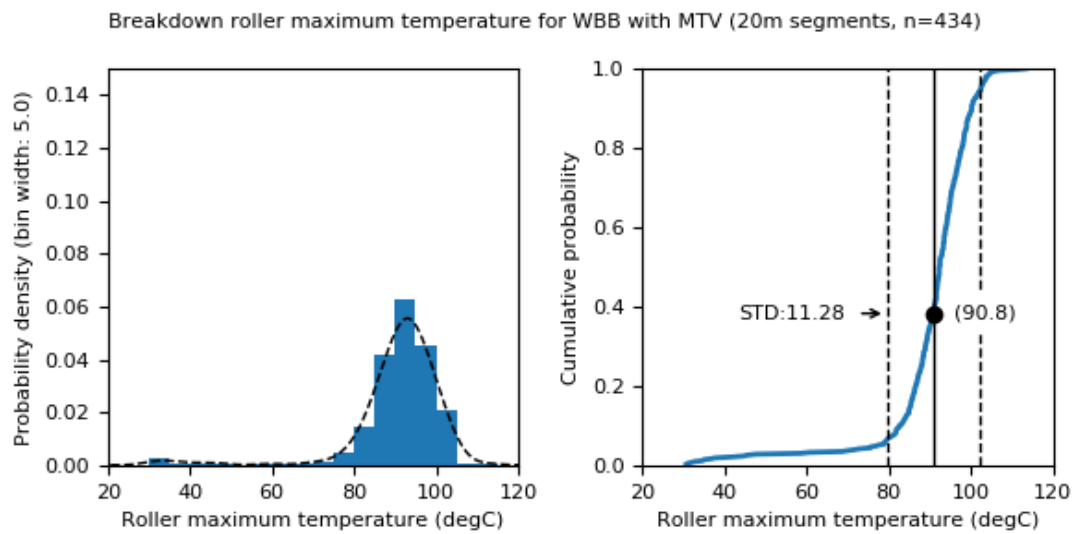


Figure 43 Breakdown roller temperature for WBB project, 40 mm nominal thickness with MTV.

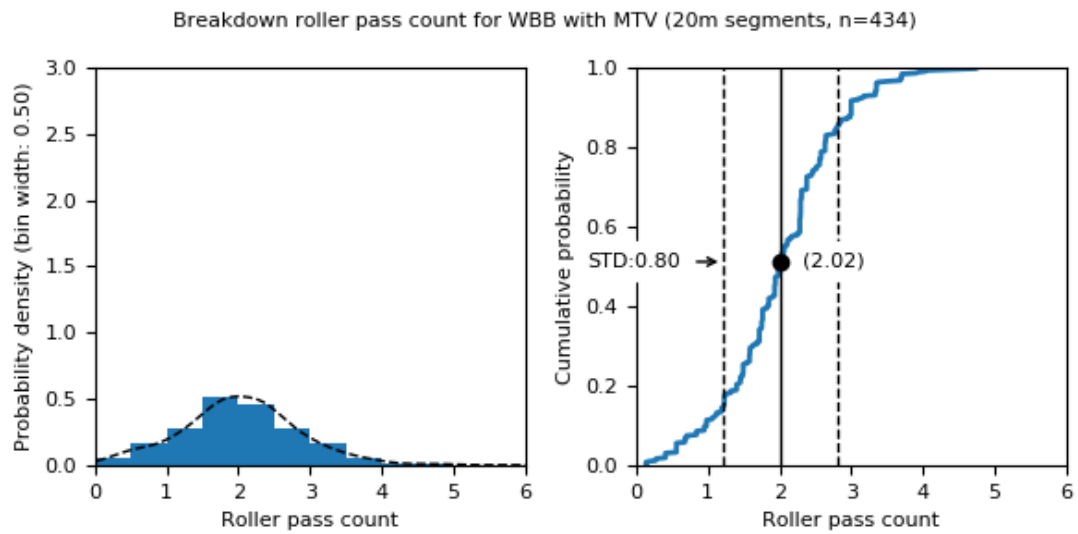


Figure 44 Number of breakdown roller passes for WBB project, 40 mm nominal thickness with MTV.

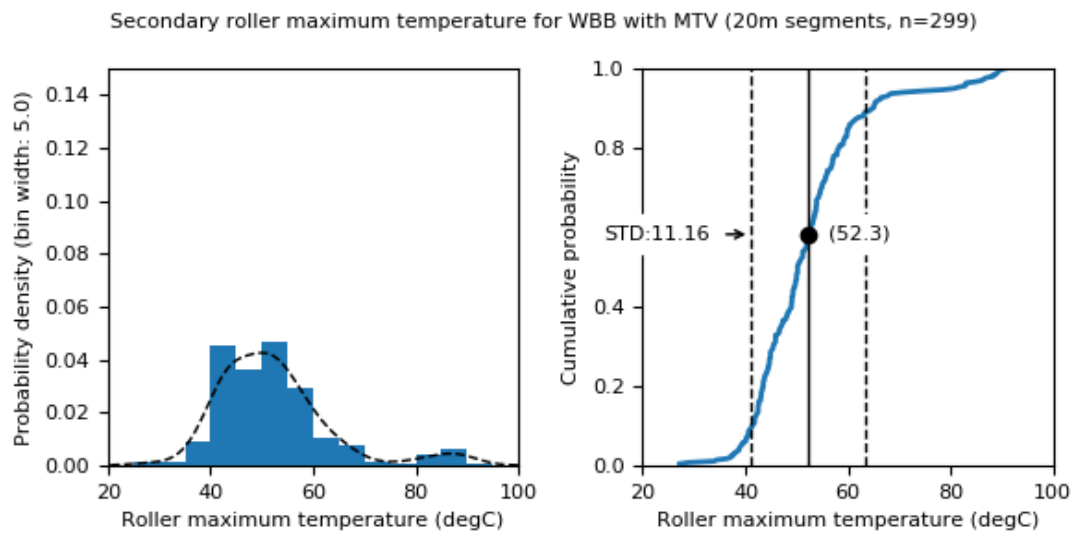


Figure 45 Secondary roller temperature for WBB project, 40 mm nominal thickness with MTV.

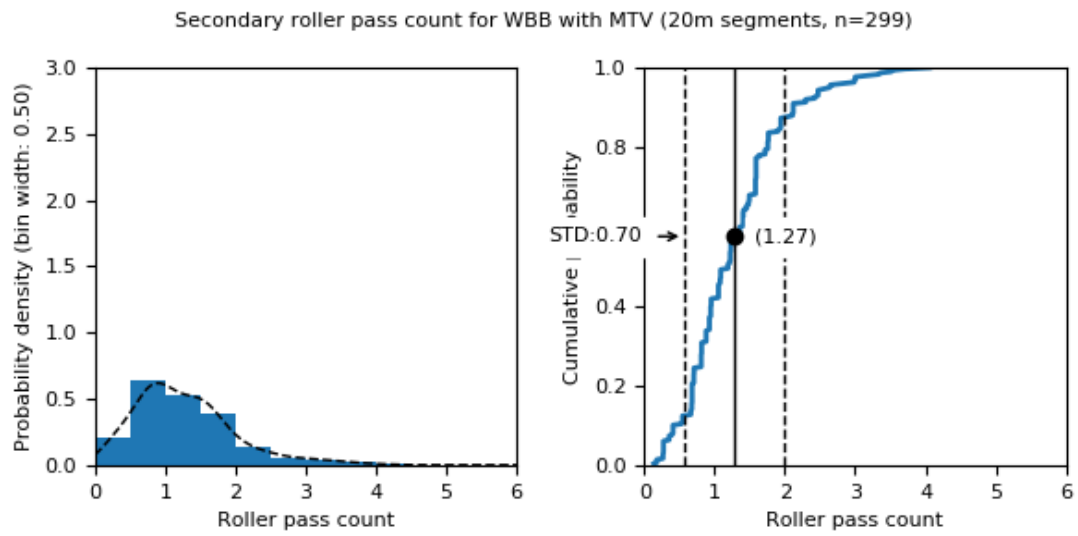


Figure 46 Number of secondary roller passes for WBB project, 40 mm nominal thickness with MTV.

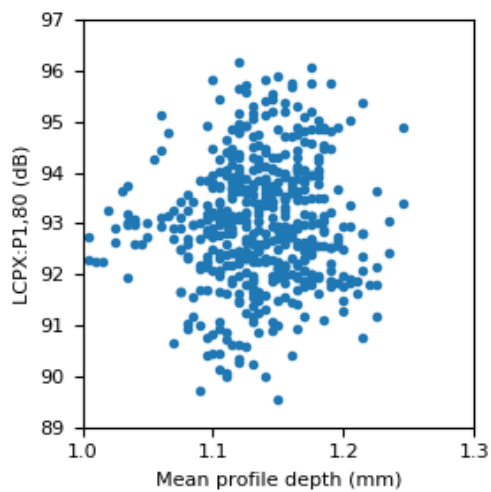


Figure 47 Left wheel path mean profile depth (2019 WDM 10 metre dataset) vs LCPX:P1,80 (December 2018).

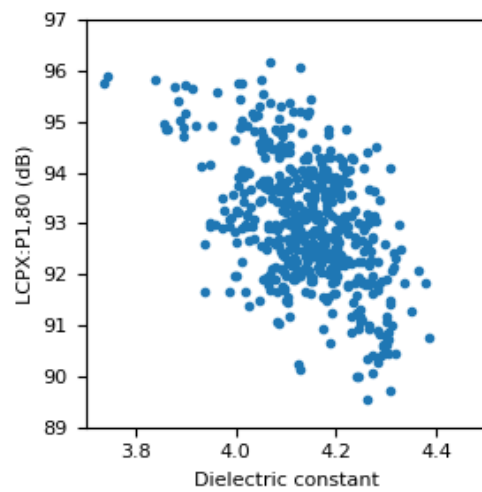


Figure 48 Surface dielectric constant vs LCPX:P1,80 (December 2018).

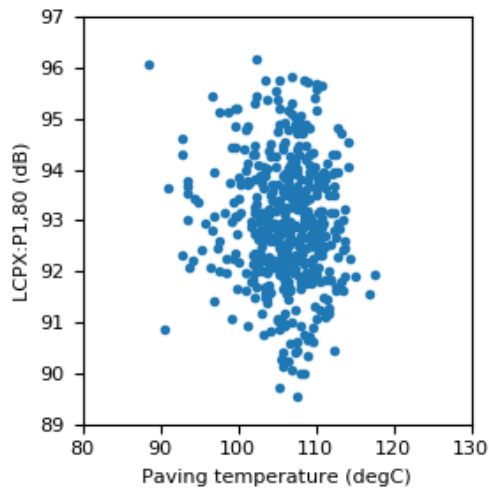


Figure 49 Paving temperature vs $L_{CPX:P1,80}$ (December 2018).

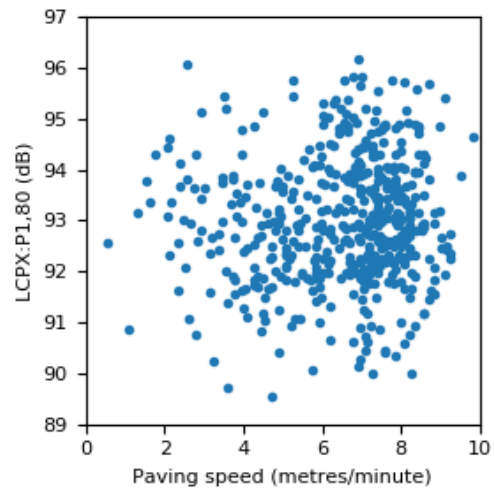


Figure 50 Paving speed vs $L_{CPX:P1,80}$ (December 2018).

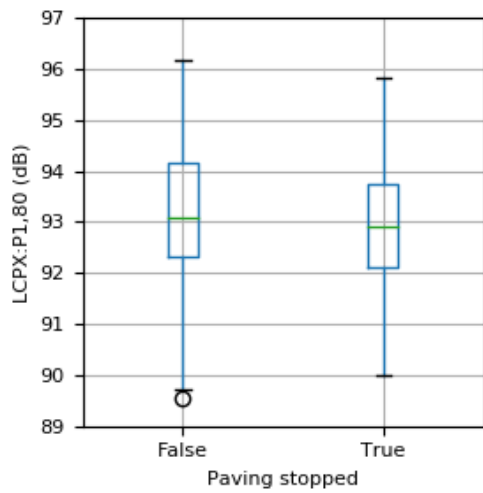


Figure 51 Paver stopped vs $L_{CPX:P1,80}$ (December 2018).

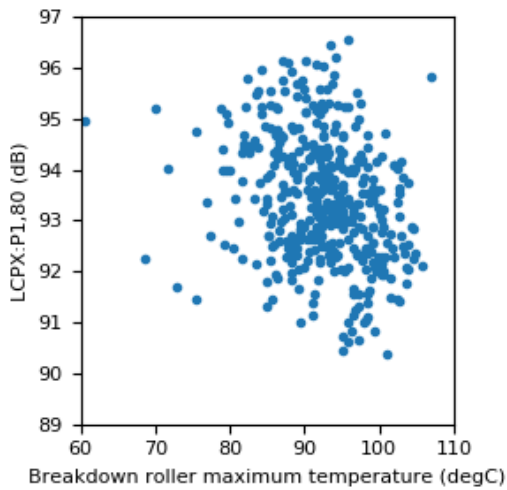


Figure 52 Breakdown roller maximum temperature vs $L_{CPX:P1,80}$ (December 2018).

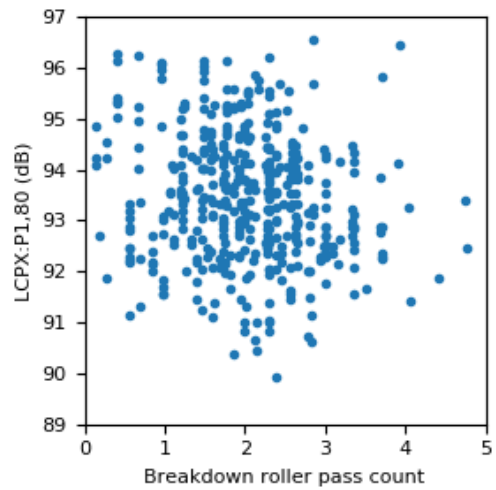


Figure 53 Breakdown roller average passes vs $L_{CPX:P1,80}$ (December 2018)

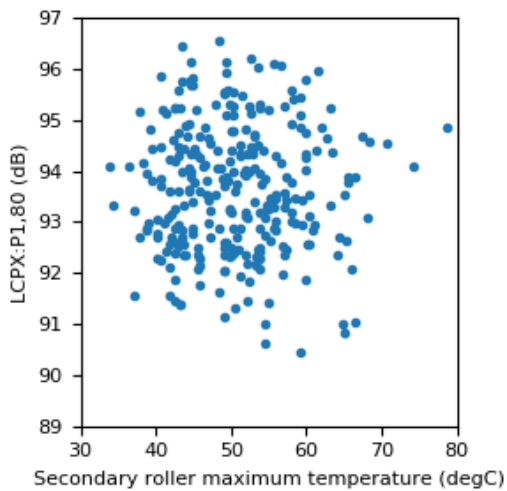


Figure 54 Secondary roller maximum temperature vs $L_{CPX:P1,80}$ (December 2018).

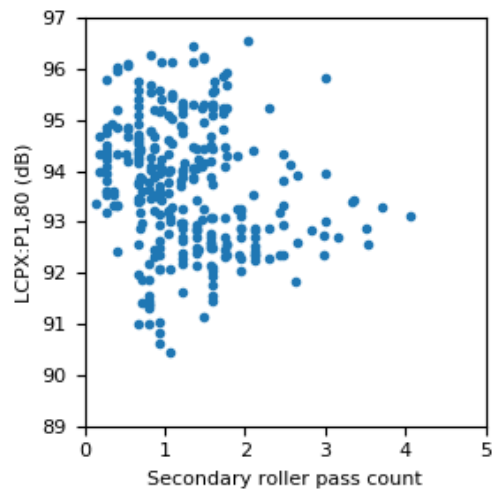


Figure 55 Secondary roller average passes vs $L_{CPX:P1,80}$ (December 2018)

5.4 Thickness as determined by $L_{CPX:P1,80}$

The $L_{CPX:P1,80}$ "heatmap" (Figure 14) shows that there are local areas of high and low tyre/road noise, generally varying between 90 and 97 dB. Differences of up to 15 mm have been observed between the target and as-built asphalt layer thickness (core samples). Therefore, it is hypothesised that the variations in $L_{CPX:P1,80}$ over the main WBB project (40 mm target thickness) are primarily due to deviations of the as-built thickness from the target thickness.

Using the below thickness to $L_{CPX:P1,80}$ (December 2018) relationship, developed as part of the thickness study and rearranged for thickness, the as-built asphalt thickness has been estimated. The distribution of the estimated as-built thickness is shown in Figure 56.

$$t = -4.47L_{CPX:P1,80} + 460.23$$

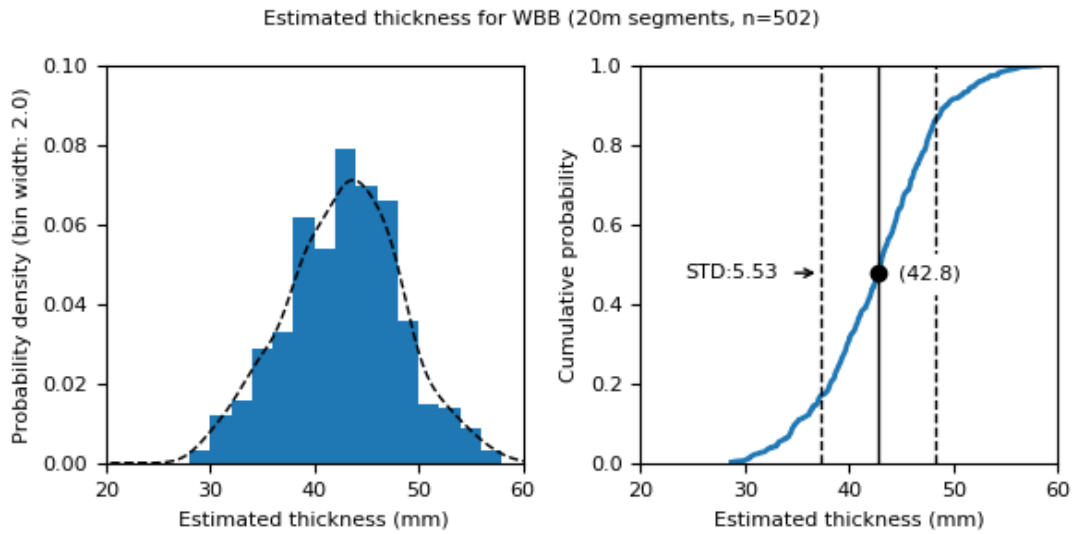


Figure 56 Estimated thickness for WBB (excludes thickness trial sections).

5.5 Field permeability

Field permeability measurements were taken alongside the core samples in October 2019. The permeability measurements were taken in the left lane, left wheel path. A description of the permeability test method used is included in Appendix H.

The field permeability results are shown in Table 16 and plotted against the adjacent core sample thickness in Figure 57.

The results show a general trend of short drain times (high permeability) in thicker sections and long drain times (low permeability) in thinner sections of road.

Table 16 Field permeability results for Western Belfast Bypass (left lane, left wheel path).

Location	Position	Permeability (time to drain 3.6L)
1	A	>300 sec
	B	>300 sec
	C	-
2	A	250 sec
	B	230 sec
	C	240 sec
3	A	180 sec
	B	196 sec
	C	215 sec
4	A	-
	B	280 sec
	C	>300 sec
5	A	235 sec

Location	Position	Permeability (time to drain 3.6L)
6	B	275 sec
	C	260 sec
	A	-
7	B	>300 sec
	C	>300 sec
	A	225 sec
8	B	238 sec
	C	192 sec
	A	176 sec
9	B	226 sec
	C	235 sec
	A	231 sec
9	B	206 sec
	C	204 sec
	A	204 sec

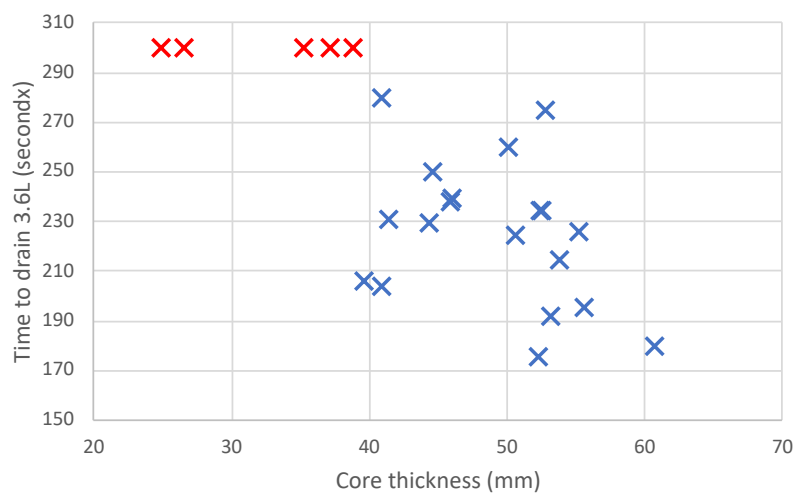


Figure 57 Core thickness vs time to drain 3.6L. Measurements in red were cut short at 300 seconds (5 minutes).

6 Conclusions

Thickness study

The overall thickness effect is determined using $L_{CPX,P1,80}$ at the nine core sample locations. The average thickness effect is -2.2 dB $L_{CPX,P1,80}$ per 10 mm increase in thickness when considering the measurement results from December 2018.

Differences in $L_{CPX,P1,80}$ of up to 1.4 dB are seen between the lanes; however, the left-right lane differences are not consistent between each thickness section or between the two test tyres. There are no significant variations in mean profile depth between the lanes. Investigation of the one-third octave band $L_{CPX,P1,80}$ shows clear differences between thickness sections; however, the differences in spectra between the lanes are only small and insufficient to confirm the presence of a thickness difference for the same sections. Alternative thickness measurement procedures should be investigated for future work.

Thickness as a source of tyre/road noise variability

The range of $L_{CPX,P1,80}$ across the WBB project (40 mm target thickness) matches the range in $L_{CPX,P1,80}$ found at the thickness trial area and core sample thickness measurements showed differences between target and as-built thicknesses of up to 15 mm in the thickness trial sections (equivalent to 3.3 dB change in $L_{CPX,P1,80}$). Therefore, it is hypothesised that the variations in $L_{CPX,P1,80}$ over the main WBB project are primarily due to deviations of the as-built thickness from the target thickness.

The surface thickness is estimated using the relationship derived from the thickness study and provides an average thickness of 43 mm, with values ranging between approximately 30 mm and 55 mm on the main project area (40 mm target thickness).

Effect of material transfer vehicle

The right lane southbound carriageway between Dickey's Road bridge and Groynes Road bridge was used to investigate the effect of the material transfer vehicle as it provided a section of road free from complex features and has consistent traffic behaviour. No significant differences in average $L_{CPX,P1,80}$ and acoustic variability were measured, indicating that use of the MTV during paving has no effect on $L_{CPX,P1,80}$.

Differences in the consistency of the paving temperature were observed, with the MTV section exhibiting a narrower distribution of paving temperatures. There are small differences in mean profile depth and surface dielectric constant between the no-MTV and MTV sections; however, it is unclear whether or not these differences are significant. The no-MTV section involved 40 paver stops, compared to the eight that occurred within the MTV section. This is due to the paver being stopped at every truck change-over for the no-MTV section. The no-MTV section experienced significantly longer average asphalt plant-to-paver times, which is attributed to the start-of-shift delays and complex edge detailing that caused long wait times for the asphalt trucks.

Effect of surface and construction properties on tyre/road noise

It is clear from the thickness trial sections and core samples that the as-built asphalt thickness can vary from the target thickness, and that these variations can have a significant effect on the tyre/road noise. The lack of a comprehensive as-built thickness dataset therefore limits the ability to investigate other (less significant) sources of variability.

The effect of local surface and construction properties on tyre/road noise was investigated by simply plotting the 20 metre road segment data for each property against the tyre/road noise.

Apart from a weak correlation between the surface dielectric constant and tyre/road noise there were no clear relationships observed, which should be expected given the magnitude of the thickness effect.

The relationship between surface dielectric constant and air void content was investigated using the core samples from nine locations (3 cores per location). No clear relationship was observed and it was not possible to perform a reliable calibration of the dielectric constant measurement.

Permeability testing

Field permeability measurements were undertaken during the coring process in October 2019. The results show a general trend of short drain times (high permeability) in thicker sections and long drain times (low permeability) in thinner sections of asphalt.

7 Further work

As-built thickness

- There is a clear relationship between porous asphalt thickness and tyre/road noise. New QA/QC processes during surface construction should focus on reducing the variability in thickness and/or achieving a minimum asphalt thickness.
- Additional techniques for measuring the thickness of porous asphalt surfaces should be investigated to provide a means of verifying the as-built asphalt thickness.
- The lack of a comprehensive as-built thickness dataset has limited the ability to investigate other less significant sources of tyre/road noise variability and there may be value in revisiting some of the other surface and construction properties should a reliable as-built thickness measurement technique become available, or should there be sufficient QA/QC processes put in place to reduce the thickness variability.

Surface macrotexture

- The mean profile depth parameter may not be suitable for describing the surface texture properties that affect tyre/road noise. In particular, the texture wavelength information is not captured in the mean profile depth parameter. Future work involving macrotexture should look at alternative texture parameters.

Acknowledgements

We would like to thank Geoff Griffiths (NZ Transport Agency), Fulton Hogan and WSP for accommodating this tyre/road noise study into the Western Belfast Bypass project and agreeing to include the use of the material transfer vehicle. We thank WDM for reprocessing and supplying detailed data from their January 2019 network survey. And finally, the NZ Transport CAPTIF staff for their ongoing support and commitment to the road surface noise research programme.

References

- [1] S. Chiles and J. I. Bull, "Road surface noise research 2016-2018," NZ Transport Agency, 2018.
- [2] NZ Transport Agency, "Close proximity (CPX) road surface noise measurement trailer guide," 2018.
- [3] J. I. Bull and S. Chiles, "Mackays to Peka Peka road surface noise survey," NZ Transport Agency, 2017.
- [4] J. I. Bull and S. Chiles, "SH25 Tairua road surface noise measurements," NZ Transport Agency, 2017.
- [5] R. Jackett, "NZTA road surface noise research programme – Task A: Close proximity versus wayside measurements," WSP, 2019.
- [6] R. Wareing, "Road surface noise measurements of porous asphalt on the Waikato Expressway and Tauranga Eastern Link," Altissimo Consulting, 2019.
- [7] R. Jackett, "NZTA road surface noise research programme 2018/2019 – Preliminary chipseal study," WSP, 2019.
- [8] R. Wareing, "Road surface noise – Measurements of porous asphalt on the Auckland Motorways," Altissimo Consulting, 2019.
- [9] NZ Transport Agency, "Guide to state highway road surface noise," 2014.
- [10] D. I. Hanson and R. S. James, "Colorado DOT Tire/Pavement Noise Study," Department of Transportation Research, 2004.
- [11] M. Berengier, J. F. Hamet and P. Bar, "Acoustical Properties of Porous Asphalts: Theoretical and Environmental Aspects," *Transportation Research Record*, pp. 9-24, 1990.
- [12] A. Ongel, E. Kohler and J. Harvey, "Principal components regression of onboard sound intensity levels," *Journal of Transportation Engineering*, no. 134, pp. 459-466, 2008.
- [13] "RAMM Software Limited," [Online]. Available: <http://www.ramm.com/>.
- [14] *ISO 11819-2:2017. Acoustics – Measurement of the influence of road surfaces on traffic noise – Part 2: The close-proximity method.*, International Organization for Standardization.
- [15] U. Sandberg and G. Descornet, "Road surface influence on tire/road noise – Part I," in *Internoise*, Miami, 1980.
- [16] ASTM, ASTM C1701 - Standard Test Method for Infiltration Rate of In Place Pervious Concrete.

[17] Transit New Zealand, TNZ P/23 notes: 2005 - Notes to the performance based specification for hotmix asphalt wearing course surfacing, 2005.

[18] J. N. Keeney, *Evaluation of the Repeatability and Reproducibility of Network-Level Pavement Macrotecture Measuring Devices. Masters Thesis*, Virginia Polytechnic Institute and State University, 2017.

Appendix A Summary of previous porous asphalt trials

A.1 High void and texture trials

Based on previous pass-by measurements showing potential noise reduction, trials to investigate high void porous asphalt surfaces were organised and laid in February 2017 on the northbound carriageway of State Highway 1 between the Sawyers Arms Road roundabout and the Greywacke Road exit in Christchurch. Four mix designs were initially investigated:

- EPA10 – standard epoxy modified porous asphalt, with 10 mm chips
- EPA14 – epoxy modified porous asphalt, with 14 mm chips
- EPA10HV – epoxy modified porous asphalt, with 10 mm chips and increased void content
- EPA14HV – epoxy modified porous asphalt, with 14 mm chips and increased void content

The EPA14HV mix failed its preliminary laydown test and was excluded from the trials.

The high void trial sections were laid on the right and left lanes on 11 and 12 February 2017, respectively. CPX measurement dates are listed below:

- 21 February 2017 (10 days old)
- 10 April 2017 (8 weeks old)
- 26 April 2017 (10 weeks old)
- 21 March 2018 (13 months old)
- 18 July 2018 (17 months old)
- 17 December 2018 (22 months old)
- 21 March 2019 (25 months old)
- 11 September 2019 (31 months old)

The average results for each lane are presented in Table 17.

The results show consistent ranking of each mix with the EPA10 surface exhibiting the lowest $L_{CPX:P1,80}$ values and the EPA14 surface having the highest $L_{CPX:P1,80}$ values.

Comparisons between $L_{CPX:P1,80}$ values for the left and right lanes show consistently higher $L_{CPX:P1,80}$ values for the left lane, despite identical mixes being used, laid one day apart by the same equipment and crew.

Mean profile depth (“MPD”) measurements were taken by Downer on 13 February 2017 for each lane. The $L_{CPX:P1,80}$ and MPD values show a good correlation, with the mean profile depth varying between the lanes and between the mixes (see Figure 58).

Discussions with NZ Transport Agency and Downer staff regarding the differing mean profile depth values between the lanes highlighted the differences in traffic management in the 36 hours following paving and differences in the width of paving. These are summarised as follows:

- Right lane paved Saturday, 11 February. Opened to traffic ~18 hours later with temporary traffic management in place. This resulted in well controlled rolling by traffic within the wheel paths during the 18-36 hours following paving. Fully opened to traffic ~36 hours after paving.
- Left lane paved Sunday, 12 February. Fully opened to traffic ~18 hours after paving (no temporary traffic management). Initial traffic was able to wander within the lane reducing the amount of rolling within the wheel paths compared to the right lane.
- Right lane narrower than left lane, and potentially receives a longer duration of rolling by the 7-ton roller during construction, and had the paver screed extensions largely retracted.

- By the time the mean profile depth measurements were taken on Monday, 13 February, the right lane wheel paths had effectively received a longer duration of rolling than the left lane wheel paths, resulting in a smoother surface.

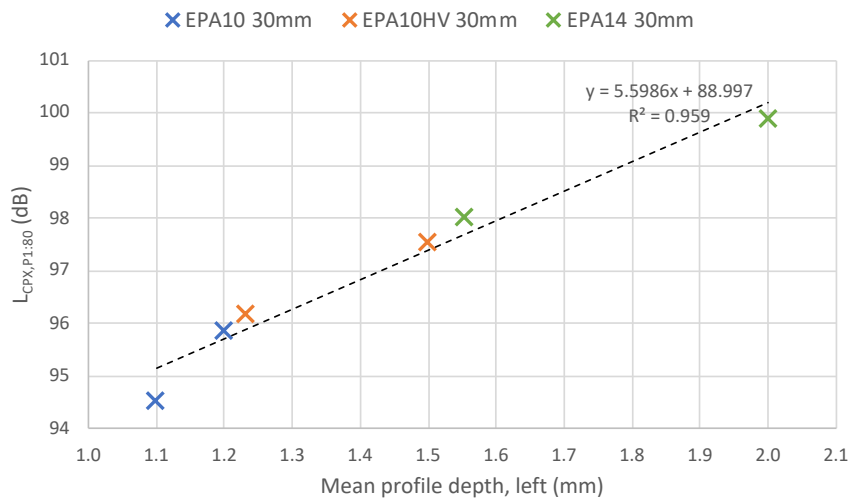


Figure 58 High-void trial sections – relationship between mean profile depth and L_{CPX:P1,80}.

Statistical pass-by (“SPB”) testing was performed by WSP in July 2018 to check for noise reduction effects at the way-side that may not be detectable using the CPX method; no additional way-side noise reduction was observed¹.

The results of the trial demonstrate how macrotexture is a strong driver of differences in tyre/road noise between different porous asphalt mixes. It also shows how an increase in void content results in an increase in macrotexture, and that any noise reduction due to increased void content is insufficient to make up for the increase in noise due to macrotexture.

CPX measurements will continue to be taken for this section of road to investigate age effects.

A.2 Small chip trials

Initial results from the Sawyers to Groynes sections showed that surfaces with higher mean profile depth values (i.e. EPA14 compared to EPA10) produced higher noise levels. It was expected that a reduction in chip size, and hence mean profile depth, would result in a quieter surface.

A section of EPA7 (40 mm nominal thickness) was laid by Fulton Hogan in late 2017 at the southern extent of Western Belfast Bypass (Clearwater to Groynes) to investigate the effect of reduce chip sizes in a porous asphalt surface. CPX measurements were taken on:

- 21 March 2018
- 18 July 2018
- 17 December 2018
- 21 March 2019
- 11 September 2019

¹ WSP (2019). NZTA road surface noise research programme – Task A: Close proximity versus wayside measurements.

A further section of EPA7 (30 mm nominal thickness) was laid by Downer along SH1 at the Memorial Avenue bridge on 7 April 2018 (descending abutment) and 14 April 2018 (ascent abutment). CPX measurements were taken on:

- 8 June 2018
- 4 July 2018
- 11 September 2019

The average results for each lane at each trial location are included in Table 17.

As was the case with the high void trial sections, the EPA7 sections show higher noise levels in the left lane compared to the right lane, although the difference at Memorial Avenue bridge is only minor. It should be noted that the Clearwater surface was laid before the road was opened to the public, so any degradation of the left lane has occurred after the surface finished curing.

The Clearwater EPA7 surface (40 mm thick) shows a 2-3 dB improvement over the previous EPA10 trial surface; however, some of the improvement is likely due to the slightly increased thickness of the layer.

The Memorial Avenue bridge EPA7 surface (30 mm thick) shows a 0.5-1.5 dB improvement over the previous EPA10 trial surface and represents a more reliable comparison given the common thicknesses of the two surfaces.

Table 17 $L_{CPX,t,80}$ for each trial section (average of all measurement sessions)

Mix	Location	Lane	$L_{CPX:P1,80}$ (dB)	$L_{CPX:H1,80}$ (dB)
EPA10 30 mm	S2G high void trial	Left	95.9	94.5
		Right	94.5	93.7
EPA10HV 30 mm	S2G high void trial	Left	97.6	96.0
		Right	96.2	95.1
EPA14 30 mm	S2G high void trial	Left	99.9	98.8
		Right	98.0	97.0
EPA7 40 mm	Clearwater small chip trial	Left	93.6	92.9
		Right	91.4	91.6
EPA7 30 mm	Memorial Ave bridge	Left	94.3	-
		Right	94.0	-

Appendix B

Porous asphalt trial results

B.1 Introduction

A number of porous asphalt trial sections were constructed in Christchurch during 2017 and 2018 as part of the low noise road surface programme. Additionally, several epoxy modified porous asphalt trials already existed on the Christchurch Southern Motorway and those trial sections have been incorporated into the surface noise programme.

Intermittent CPX testing has been performed on each trial section; however, some of the data was either not previously processed, affected by errors in the on-board CPX trailer measurement software or processed using outdated correction procedures.

Raw CPX measurement data in the form of calibrated wav files has been collected since early 2018, which has allowed the affected measurements to be re-processed. Previously collected but unprocessed data has also been processed.

This appendix presents the CPX testing results for the Christchurch porous asphalt trial sections as at January 2020.

B.2 Trial section details

The porous asphalt trial sections are located on SH1 and SH73 in Christchurch. Table 18 to Table 21 provide details of the trial sections, broken down by location.

Table 18 High void trial sections – Sawyers Arms Rd to Greywacke Rd ("S2G")

Mix	Thickness	Carriageway	Rs	Start	End	Length	Lanes	Contractor	Construction date	Notes
EPA10	30 mm	Northbound	01S-0333 (D)	3,640 m	3,880 m	240 m	Both	Downer	Feb 2017	
EPA10HV	30 mm			3,320 m	3,630 m	310 m				
EPA14	30 mm			3,040 m	3,300 m	260 m				

Table 19 Small chip trial sections

Mix	Thickness	Carriageway	Rs	Start	End	Length	Lanes	Contractor	Construction date	Notes
EPA7	40 mm	Northbound	01S-0333 (D)	518 m	1,007 m	489 m	Both	Fulton Hogan	Oct 2017	
EPA7	30 mm	Northbound	01S-0333 (D)	7,322 m	7,660 m	338 m	Both	Downer	Apr 2018	Descending abutment
EPA 7	30 mm			6,895 m	7,260 m	365 m				Ascending abutment

Table 20 Thickness trial sections – Western Belfast Bypass ("WBB")

Mix	Thickness	Carriageway	Rs	Start	End	Length	Lanes	Contractor	Construction date	Notes
EPA7	30 mm	Northbound	01S-0327 (D)	4,864 m	5,126 m	262 m	Both	Fulton Hogan	Nov 2018	
EPA7	40 mm			4,585 m	4,845 m	260 m				
EPA7	50 mm			4,292 m	4,566 m	274 m				

Table 21 Epoxy dilution trial sections – Christchurch Southern Motorway ("CSM")

Mix	Thickness	Carriageway	Rs	Start	End	Length	Lanes	Contractor	Construction date	Notes
EPA10 (SB, 25% epoxy)	40 mm	Southbound	076-0003 (I)	7,250 m	7,466 m	216 m	Left	Fulton Hogan	Jun 2012	
EPA10 (SB, 50% epoxy)	40 mm			6,842 m	7,050 m	208 m				
EPA10 (SB, 100% epoxy)	40 mm			5,685 m	5,900 m	215 m				
PA10 (SB, control)	40 mm			5,900 m	6,100 m	200 m				100% epoxy control
PA10 (SB, control)	40 mm			7,050 m	7,250 m	200 m				25% and 50% epoxy control
EPA10 (NB, 25% epoxy)	40 mm	Northbound	076-0003 (D)	6,232 m	6,530 m	298 m	Left	Fulton Hogan	Jun 2012	
PA10 (NB, control)	40 mm			5,670 m	6,164 m	494 m				

B.3 Measurement details

Details of the CPX testing sessions are given in Table 22.

The table includes measurements taken before raw data capture was incorporated into the CPX trailer system. The early measurements are affected by an error in the on-board trailer software and enclosure reflections; the affected measurement results are not presented in this letter but are included in *italics* in Table 22.

Table 22 CPX testing sessions

Location	Trial section	Date	Age	Tyres	Notes		
S2G	High void	<i>21/02/2017</i>	<i>1 week</i>	<i>P1</i>	<i>Early measurement s(affected by averaging error and enclosure reflections)</i>		
		<i>10/04/2017</i>	<i>8 weeks</i>	<i>P1</i>			
		<i>26/04/2017</i>	<i>10 weeks</i>	<i>P1</i>			
				21/03/2018	13 months	P1	Early measurement (affected by averaging error) 1 run of raw data
				18/07/2018	17 months	P1	Left lane only
				17/12/2018	22 months	P1, H1	
				21/03/2019	2 years	P1, H1	
		11/09/2019	2½ years	P1, H1			
Clearwater to Groyne	Small chip	21/03/2018		P1	Early measurement (affected by averaging error) 1 run of raw data		
		18/07/2018		P1	Left lane only		
		17/12/2018		P1, H1			
		07/03/2019		P1	Single run, left lane only		
		21/03/2019		P1, H1			
		11/09/2019		P1, H1			
Memorial Ave bridge	Small chip	08/06/2018	7 weeks	P1			
		04/07/2018	3 months	P1			
		11/09/2019	17 months	P1			
WBB	Thickness	17/12/2018	6 weeks	P1, H1			
		07/03/2019	4 months	P1, H1	Single run, left lane only		

Location	Trial section	Date	Age	Tyres	Notes
		21/03/2019	4½ months	P1, H1	
		11/09/2019	10 months	P1, H1	
CSM	Epoxy dilution	26/04/2017	5 years	P1	Early measurement (affected by averaging error and enclosure reflections)
		10/09/2019	7½ years	P1	

B.4 Results

Average results for each surface mix and thickness are given in Table 23, Figure 59 and Figure 60.

Measurement session results by location and trial section are presented in Table 24 to Table 31. The tables include $L_{CPX;t,80}$ and s_t (acoustic variability) for each measurement date and test tyre, "t" (P1 or H1). The average air temperature and average testing speed are included for information. All corrections required by ISO 11819-2:2017 have been applied; however, the hardness correction procedure has been modified according to a recent conference paper².

The new hardness correction procedure is expected to become part of a future version of ISO 11819-2.

Table 23 $L_{CPX;t,80}$ for each trial section (average of all measurement sessions)

Mix	Location	Lane	$L_{CPX:P1,80}$ (dB)	$L_{CPX:H1,80}$ (dB)
EPA7 30 mm	Memorial Ave bridge	Left	94.3	-
		Right	94.0	-
	WBB thickness trial	Left	96.2	95.8
		Right	94.5	95.0
EPA7 40 mm	Clearwater small chip trial	Left	93.6	92.9
		Right	91.4	91.6
	WBB thickness trial	Left	93.0	92.4
		Right	92.6	92.9
EPA7 50 mm	WBB thickness trial	Left	91.4	91.0
		Right	90.3	91.2
EPA10 30 mm	S2G high void trial	Left	95.9	94.5
		Right	94.5	93.7

² Bühlmann, E., Mioduszewski, P., Sandberg, U., An in-depth look at the tire rubber hardness influence on tire/road noise measurements. Inter-Noise 2018. Chicago.

Mix	Location	Lane	L _{CPX:P1,80} (dB)	L _{CPX:H1,80} (dB)
EPA10HV 30 mm	S2G high void trial	Left	97.6	96.0
		Right	96.2	95.1
EPA14 30 mm	S2G high void trial	Left	99.9	98.8
		Right	98.0	97.0

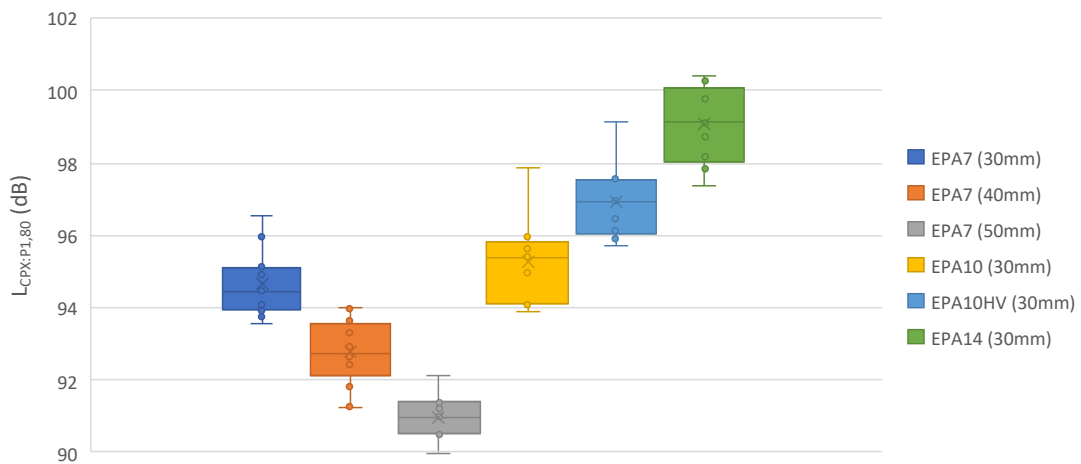


Figure 59 $L_{CPX:P1,80}$ for all available measurement sessions, arranged by surface mix type

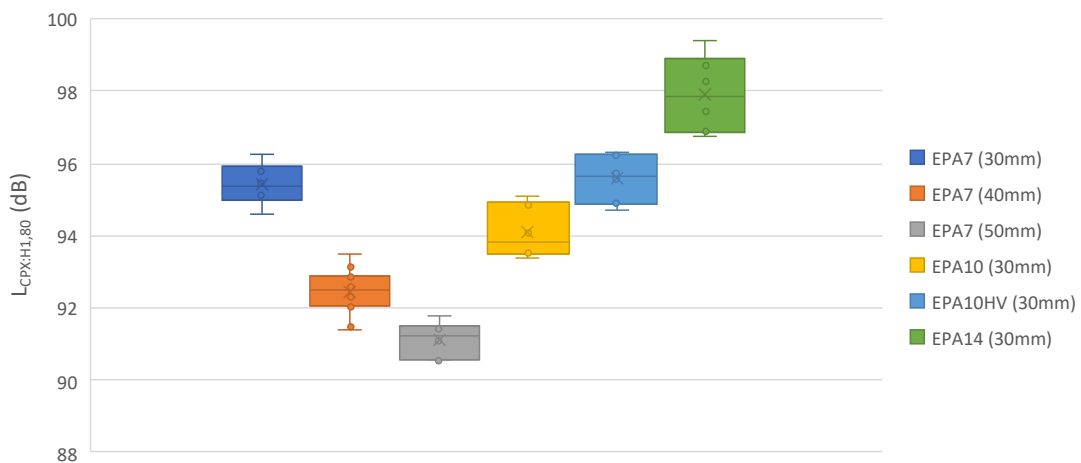


Figure 60 $L_{CPX:H1,80}$ for all measurement sessions, arranged by surface mix type

Table 24 High void trial sections – Sawyers Arms Rd to Greywacke Rd ("S2G") – P1 tyre

Mix	Lane	Date	Runs	L _{CPX:P1,80} (dB)	S _{P1} (dB)	Speed (km/h)	Air temperature (C)
EPA10 (30 mm thick)	Left	21/03/18	1	97.9	0.4	77.3	23.0
		18/07/18	3	95.4	0.5	80.3	17.5
		17/12/18	4	94.9	0.5	79.3	22.9
		21/03/19	4	95.7	0.5	78.6	18.0
		11/09/19	8	95.5	0.6	79.8	7.7
	Right	21/03/18	3	96.0	0.4	77.5	26.5
		17/12/18	3	93.9	0.5	79.6	23.1
		21/03/19	3	94.1	0.4	79.1	17.9
		11/09/19	3	94.2	0.4	80.3	8.8
		EPA10HV (30 mm thick)	Left	21/03/18	1	99.2	0.4
18/07/18	3			97.6	0.6	80.3	17.3
17/12/18	4			97.1	0.5	79.6	23.0
21/03/19	4			97.5	0.4	78.7	18.1
11/09/19	8			96.5	0.6	79.9	7.6
Right	21/03/18		3	96.9	0.3	77.9	26.1
	17/12/18		3	96.1	0.6	80.2	23.2
	21/03/19		3	95.9	0.5	79.2	18.0
	11/09/19		3	95.7	0.4	80.0	8.7
	EPA14 (30 mm thick)		Left	21/03/18	1	99.9	1.0
18/07/18		3		100.4	1.0	79.8	17.2
17/12/18		4		99.8	0.9	78.8	23.0
21/03/19		4		100.3	0.8	78.3	18.0
11/09/19		8		99.1	0.9	78.2	7.6
Right		21/03/18	3	98.7	0.6	77.6	25.9
		17/12/18	3	98.2	0.4	78.7	23.1
		21/03/19	3	97.8	0.6	77.8	18.0
		11/09/19	3	97.4	0.6	79.8	8.6

Table 25 High void trial sections – Sawyers Arms Rd to Greywacke Rd ("S2G") – H1 tyre

Mix	Lane	Date	Runs	L _{CPX:H1,80} (dB)	S _{H1} (dB)	Speed (km/h)	Air temperature (C)
EPA10 (30 mm thick)	Left	17/12/18	3	93.5	0.6	79.4	19.4
		21/03/19	3	94.9	0.6	78.9	17.8
		10/09/19	3	95.1	1.1	80.2	7.5

Mix	Lane	Date	Runs	L _{CPX:H1,80} (dB)	S _{H1} (dB)	Speed (km/h)	Air temperature (C)
	Right	17/12/18	3	93.4	0.5	79.6	20.7
		21/03/19	3	94.1	0.5	79.3	17.9
		10/09/19	3	93.5	0.4	79.7	6.6
EPA10HV (30 mm thick)	Left	17/12/18	3	95.5	0.6	79.8	19.2
		21/03/19	3	96.2	0.8	79.8	18.0
		10/09/19	3	96.3	0.8	79.5	7.5
	Right	17/12/18	3	94.9	0.5	80.1	20.5
		21/03/19	3	95.7	0.5	78.4	18.1
		10/09/19	3	94.7	0.5	79.3	6.5
EPA14 (30 mm thick)	Left	17/12/18	3	98.3	1.0	79.2	19.1
		21/03/19	3	99.4	0.9	78.5	18.0
		10/09/19	3	98.7	1.4	79.1	7.5
	Right	17/12/18	3	96.9	0.4	79.0	20.5
		21/03/19	3	97.4	0.6	77.7	18.1
		10/09/19	3	96.7	0.7	78.7	6.4

Table 26 Small chip trial sections – Clearwater Roundabout to Groynes Rd offramp – P1 tyre

Mix	Lane	Date	Runs	L _{CPX:P1,80} (dB)	S _{P1} (dB)	Speed (km/h)	Air temperature (C)
EPA7 (40 mm thick)	Left	21/03/18	3	94.0	1.1	77.6	24.3
		18/07/18	3	93.4	1.0	81.1	17.5
		17/12/18	3	93.5	1.0	80.5	22.4
		7/03/19	1	93.7	0.6	81.8	30.9
		21/03/19	3	93.3	0.8	80.2	18.0
		11/09/19	3	94.0	0.9	79.0	9.3
	Right	21/03/18	3	91.8	0.7	79.1	25.6
		17/12/18	3	91.3	0.6	80.8	20.8
		21/03/19	3	91.3	0.6	79.9	18.3
		11/09/19	3	91.3	0.6	81.4	6.6

Table 27 Small chip trial sections – Clearwater Roundabout to Groynes Rd offramp – H1 tyre

Mix	Lane	Date	Runs	L _{CPX:H1,80} (dB)	S _{H1} (dB)	Speed (km/h)	Air temperature (C)
EPA7 (40 mm thick)	Left	17/12/18	3	92.6	0.9	80.1	19.5
		21/03/19	3	93.1	0.8	80.2	18.1
		10/09/19	3	92.9	0.8	80.0	7.2
	Right	17/12/18	3	91.4	0.7	80.4	20.3
		21/03/19	3	92.0	0.6	79.8	18.3
		10/09/19	3	91.5	0.5	80.0	5.7

Table 28 Small chip trial sections – Memorial Ave bridge – P1 tyre

Mix	Lane	Date	Runs	L _{CPX:P1,80} (dB)	S _{P1} (dB)	Speed (km/h)	Air temperature (C)
EPA7 (30 mm thick, ascending)	Left	8/06/18	3	95.1	1.0	79.4	14.4
		4/07/18	3	93.9	0.8	80.2	15.2
		11/09/19	4	94.9	0.6	77.6	8.9
	Right	8/06/18	3	93.9	1.0	80.2	14.5
		4/07/18	3	94.1	0.8	79.8	15.3
		11/09/19	3	94.2	0.7	78.5	8.3
EPA7 (30 mm thick, descending)	Left	8/06/18	3	94.5	1.1	81.2	14.4
		4/07/18	3	93.7	0.8	79.8	15.2
		11/09/19	4	93.5	0.7	78.7	8.9
	Right	8/06/18	3	94.1	0.8	83.3	14.4
		4/07/18	3	93.9	0.8	80.1	15.3
		11/09/19	3	94.0	0.5	79.0	8.4

Table 29 Thickness trial sections – Western Belfast Bypass (“WBB”) – P1 tyre

Mix	Lane	Date	Runs	L _{CPX:P1,80} (dB)	S _{P1} (dB)	Speed (km/h)	Air temperature (C)
EPA7 (30 mm thick)	Left	17/12/18	3	96.0	0.2	80.2	22.1
		7/03/19	1	96.5	0.4	79.0	29.9
		21/03/19	3	96.1	0.3	78.6	18.1
		11/09/19	3	96.1	0.4	78.9	9.3
	Right	17/12/18	3	94.5	0.5	79.4	20.7
		21/03/19	3	94.5	0.3	78.9	18.3
		11/09/19	3	94.6	0.5	78.6	6.9
	EPA7 (40 mm thick)	Left	17/12/18	3	92.9	0.4	79.9
7/03/19			1	93.6	0.4	77.8	29.5
21/03/19			3	92.7	0.5	79.9	18.2
11/09/19			3	92.7	0.7	79.5	9.2
Right		17/12/18	3	92.7	0.4	79.6	20.5
		21/03/19	3	92.6	0.4	80.0	18.3
		11/09/19	3	92.4	0.5	79.6	6.8
EPA7 (50 mm thick)		Left	17/12/18	3	91.0	0.4	79.6
	7/03/19		1	92.1	0.4	79.2	29.0
	21/03/19		3	91.2	0.3	79.1	18.1
	11/09/19		3	91.4	0.3	80.1	9.1
	Right	17/12/18	3	90.0	0.2	80.2	20.3
		21/03/19	3	90.5	0.3	78.8	18.3
		11/09/19	3	90.5	0.2	79.0	6.6

Table 30 Thickness trial sections – Western Belfast Bypass (“WBB”) – H1 tyre

Mix	Lane	Date	Runs	L _{CPX:H1,80} (dB)	S _{H1} (dB)	Speed (km/h)	Air temperature (C)
EPA7 (30 mm thick)	Left	17/12/18	3	95.5	0.4	79.1	18.8
		21/03/19	3	96.2	0.3	78.8	18.2
		10/09/19	3	95.8	0.4	79.3	7.4
	Right	17/12/18	3	95.1	0.4	79.6	19.7
		21/03/19	3	95.3	0.5	78.0	18.4
		10/09/19	3	94.6	0.3	79.3	5.9
EPA7 (40 mm thick)	Left	17/12/18	3	92.3	0.4	80.2	18.3
		21/03/19	3	92.9	0.5	79.5	18.2
		10/09/19	3	92.1	0.3	79.8	7.2

Mix	Lane	Date	Runs	L _{CPX:H1,80} (dB)	S _{H1} (dB)	Speed (km/h)	Air temperature (C)
	Right	17/12/18	3	92.9	0.4	80.5	19.4
		21/03/19	3	93.5	0.5	77.7	18.3
		10/09/19	3	92.3	0.4	79.9	5.7
EPA7 (50 mm thick)	Left	17/12/18	3	90.5	0.3	80.4	18.0
		21/03/19	3	91.4	0.3	78.2	18.2
		10/09/19	3	91.1	0.3	79.8	7.0
	Right	17/12/18	3	90.5	0.2	79.1	19.3
		21/03/19	3	91.8	0.3	78.5	18.4
		10/09/19	3	91.4	0.4	79.1	5.6

Table 31 Epoxy dilution trial sections – Christchurch Southern Motorway (“CSM”) – P1 tyre

Mix	Lane	Date	Runs	L _{CPX:P1,80} (dB)	S _{P1} (dB)	Speed (km/h)	Air temperature (C)
EPA10 (SB, 25% epoxy)	Left	10/09/19	3	99.3	1.1	79.2	5.6
EPA10 (SB, 50% epoxy)	Left	10/09/19	3	100.8	0.2	80.2	5.9
EPA10 (SB, 100% epoxy)	Left	10/09/19	3	101.0	0.3	79.5	6.2
PA10 (SB, 100% epoxy control)	Left	10/09/19	3	101.7	0.2	78.0	6.1
PA10 (SB, 25% and 50% epoxy control)	Left	10/09/19	3	101.0	0.3	79.8	5.7
EPA10 (NB, 25% epoxy)	Left	10/09/19	3	100.8	0.6	79.8	5.8
PA10 (NB, 25% epoxy control)	Left	10/09/19	3	101.1	0.4	80.8	6.0

Appendix C Construction observations

C.1 Shift 1 – Tuesday, 23 October 2018

Carriageway	Southbound
Lane	Right
Start position	01S-0327/02.472-l
End position	01S-0327/04.400-l
Start time	2018-10-23 2206h
End time	2018-10-24 0443h
Weather conditions	Cool and foggy (11°C min)
Length paved	1,798 metres
Average width	4.75 metres
Total asphalt	611 tonnes
Paver	logger-01 (ch1 left wheel path, ch2 right wheel path)
Break-down roller	logger-03
Secondary roller	logger-02

No material transfer vehicle ("MTV") – the ring feeders on the asphalt trucks meant that the trucks could not access the MTV hopper and the MTV was abandoned for shift 1. The ring feeders were removed from the trucks for shift 2.

Notes

A small patch of SMA was repaired at the start of the shift (2040h).

The secondary roller broke down shortly after paving began. The temperature logger unit could not be moved to the back-up roller and as a result secondary roller temperature and position information was only recorded for a small section of road. The secondary roller struggled to keep up with the break-down roller and was generally at least 300 metres behind (on subsequent shifts the secondary roller generally kept up with the break-down roller).

The break-down roller performed a single pass (forward and back) across the lane width. One of the passes was generally under vibration; however, there was no clear pattern to the extent of vibration and it was generally performed in a piecemeal fashion. While the majority of the road experienced a single vibration pass some section will have experience multiple vibration passes. The forward extent of break-down rolling was controlled by contractor QC staff who targeted a maximum surface temperature of 90°C. The break-down roller operator frequently rolled beyond the position specified by the QC staff into the hot (>90°C) area.

There were 5 key-ins on this stretch (shift start and two SMA bridge decks) as well as delays getting paving started due to issues with the asphalt truck ring feeders getting in the way of the MTV hopper. This led to numerous disruptions during the first 600 metres of the shift and many asphalt trucks were delayed in unloading (at most there were 10 trucks waiting on site). The paver stopped on every truck that arrived resulting in a brief pause to paving every 30-40 metres. There was a mechanical fault on the right-hand screed that had to be repaired and caused approximately 30 minute delay.

Traffic management

The lane was opened to traffic (50km/h signs) at 0600h on Wednesday, 24 October. A line of cones was placed between the lanes to protect the asphalt edge. The lane was opened to 100 km/h traffic at 0600h on Thursday, 25 October.

C.2 Shift 2 –Wednesday, 24 October 2018

Carriageway	Southbound
Lane	Left lane
Start position	01S-0327/02.472-I
End position	01S-0327/04.400-I
Start time	2018-10-24 2102h
End time	2018-10-25 0446h
Weather conditions	Light mist from 0100h (8°C min)
Length paved	1,836 metres
Average width	6.35 metres
Total asphalt	840 tonnes
Paver	logger-01 (ch1 left wheel path, ch2 right wheel path)
Break-down roller	logger-03
Secondary roller	Logger-02

Notes

The set-up time for shift 2 was shorter as the construction equipment was already on site. There was some initial coordination between the MTV operators and the paver operator. The paver operator would drive as per usual and the MTV operators would adjust their speed to suit.

There were numerous disruptions to paving due to manual edge detailing, removal of unmixed binder from the asphalt mat, asphalt truck breakdown (approximately 60 minutes), paver hopper overflows and MTV hopper/truck spills.

The secondary roller stayed closer to the break-down roller than during shift 1. The secondary roller performed two slow non-vibration passes over each section of road.

Traffic management

The lane was opened to traffic (100km/h signs) at 0600h on Thursday, 25 October.

C.3 Shift 3 – Friday, 26 October 2018

Carriageway	Southbound
Lane	Right lane
Start position	01S-0327/04.400-I
End position	01S-0333/0.510-I
Start time	2018-10-26 1950h
End time	2018-10-27 0109h
Weather conditions	Cold wind (7°C min)
Length paved	1,802 metres
Average width	4.7 metres
Total asphalt	660 tonnes
Paver	logger-01 (ch1 left wheel path, ch2 right wheel path)
Break-down roller	logger-03
Secondary roller	logger-02

Notes

The shift was delayed until Friday, 26 October due to rain on Thursday.

Paving generally went smoothly. There were four key-ins (Groynes bridge SMA and start/end of shift). There were only a few stops to paving (excluding the bridge key-ins), but these were all limited to 1-2 minutes. The asphalt trucks ran smoothly, and there were never more than three trucks on site at any one time. There was a cold wind for the first few hours of the shift and this caused the asphalt to cool much faster than on previous nights. During this period, the asphalt dropped to rolling temperature (90°C) only 5-10 metres behind the paver. The secondary roller was further behind the break-down roller compared to shift 2.

Even with the MTV there were still times when cold asphalt could be seen in the mat. In one case it was visible to the naked eye. The larger ("Trout River") asphalt trucks appeared to provide a more uniform temperature asphalt than the standard asphalt trucks.

Traffic management

The lane was opened to traffic (50km/h signs) at 0600h on Saturday, 27 October. The lane was opened to 100km/h at 0600h on Sunday, 28 October.

C.4 Shift 4 – Sunday, 28 October 2018

Carriageway	Southbound
Lane	Left lane
Start position	01S-0327/04.400-I
End position	01S-0333/0.507-I
Start time	2018-10-28 2120h
End time	2018-10-29 0300h
Weather conditions	Cold, drizzle prior to paving (10°C min)
Length paved	1,763 metres
Average width	6.2 metres
Total asphalt	806 tonnes
Paver	logger-01 (ch1 left wheel path, ch2 right wheel path)
Break-down roller	logger-02
Secondary roller	logger-03 (with temperature display)

Notes

Note that logger-02 and logger-03 were swapped between the rollers on this shift.

There were a few spots of rain during the setup period, but by the time the paving started the rain had cleared completely. There were four key-ins (Groynes bridge SMA and start/end of shift. There were approximately 6 stops (excluding bridge key-ins). One of the stops was due to running out of asphalt and there was a delay of around 10 minutes until the next truck arrived.

The mat held its heat longer than the previous shift and the break-down roller was generally at least 50 metres behind the paver.

Traffic management

The lane was opened to traffic (100km/h signs) at 0600h on Monday, 29 October.

C.5 Shift 5 – Sunday, 4 November 2018

Carriageway	Northbound
Lane	Right lane
Start position	01S-0333/0.310-D
End position	01S-0327/02.995-D
Start time	2018-11-04 2053h
End time	2018-11-05 0427h
Weather conditions	Clear (5°C min)
Length paved	2,898 metres
Average width	4.8 metres
Total asphalt	1101 tonnes
Paver	01 (ch1 left wheel path (long arm), ch2 right wheel path (short arm), ch3 middle (long arm))
Break-down roller	logger-02
Secondary roller	logger-03 (with temperature display)

Notes

Paving was delayed for a week due to rain.

The lane was narrow meaning slightly longer intervals between trucks, rarely running out of asphalt (only once during the shift) and trucks only waiting a short time to unload (1-2 trucks waiting for most of the shift). The lack of kerb detailing and manhole lids meant a relatively smooth paving run. There were some delays at the very start of the shift that saw 5-7 trucks waiting before paving commenced.

There were four key-ins (Groynes bridge SMA and start/end of shift). The final key-in was at the Dickey's Rd bridge.

The secondary roller took over from the break-down roller when the break-down roller ran out of water. The break-down roller assisted the secondary roller at times.

The break-down roller picked up part of the mat at 01S-0327/04.681-D (within the 40mm trial section). Most of the damage was in the median shoulder, apart from a 2-metre section in the right wheel path about 50 metres behind where the roller first picked up. Observed temperatures reached 103°C immediately before the roller picked-up, however, the high rolling temperature was not uncommon. The cause was attributed to the break-down roller operator feathering the water supply to delay returning to the water truck to refill.

Traffic management

The road was opened to traffic (50km/h signs) at 1000h Monday, 5 November. The lane was opened to 100km/h at 1000h on Tuesday, 6 November.

C.6 Shift 6 – Monday, 5 November 2018

Carriageway	Northbound
Lane	Left lane
Start position	01S-0333/0.310-D
End position	01S-0327/03.624-D
Start time	2018-11-06 0053h
End time	2018-11-06 0814h
Weather conditions	Clear (7°C min)
Length paved	2,274 metres
Average width	6.0 metres
Total tonnes	1102 tonnes
Paver	logger-01 (ch1 left wheel path (long arm), ch2 right wheel path (short arm), ch3 middle (long arm))
Break-down roller	logger-03
Secondary roller	not monitored

Notes

Logger-02 was not working during this shift and logger-03 was moved from the secondary roller to the break-down roller.

The secondary roller took over from the break-down roller when the break-down roller ran out of water. The break-down roller assisted the secondary roller at times.

There were three key-ins (Groynes bridge SMA and start of shift) and numerous stops due to kerb detailing and manhole lids. Paving was intentionally slowed down during the final 90 minutes of the shift to allow the asphalt trucks extra time to negotiate the morning traffic, which minimised stoppage time due to running out of asphalt.

The shift was completed in the daylight. The line markers later commented that the surface was still sticky when they marked the lines mid-morning.

The lane was opened to traffic (100km/h signs) at 1000h on Tuesday, 6 November.

C.7 Shift 7 – Tuesday, 6 November 2018

Carriageway	Northbound
Lane	Left lane
Start position	01S-0327/03.624-D
End position	01S-0327/02.386-D
Start time	2018-11-07 0053h
End time	2018-11-07 0505h
Weather conditions	Clear (6°C min)
Length paved	1,116 metres
Average width	6.2 metres
Total asphalt	562 tonnes
Paver	logger-01 (ch1 left wheel path (long arm), ch2 right wheel path (short arm), ch3 middle (long arm))
Break-down roller	logger-02
Secondary roller	logger-03 (with temperature display)

Notes

The left lane was continued with from the previous shift as it was the longest remaining section. This left the shortest stretch to be paved during the final shift.

The secondary roller took over from the break-down roller when the break-down roller ran out of water. The break-down roller assisted the secondary roller at times.

There were numerous stops due to manhole lid and edge detailing, particularly around the concrete barriers at the bridges. There were six key-ins (two SMA bridges and start/end of shift).

Traffic management

The lane was opened to traffic (50km/h signs) at 1000h on Wednesday, 7 November. The lane was opened to 100km/h at 1000h on Thursday, 8 November.

C.8 Shift 8 – Wednesday, 7 November 2018

Carriageway	Northbound
Lane	Right lane
Start position	01S-0327/02.949-D
End position	01S-0327/02.386-D
Start time	2018-11-08 0010h
End time	2018-11-08 0151h
Weather conditions	Clear (14°C min)
Length paved	494 metres
Average width	5.3 metres
Total asphalt	182 tonnes
Paver	logger-01 (ch1 left wheel path (long arm), ch2 right wheel path (short arm), ch3 middle (long arm))
Break-down roller	logger-02
Secondary roller	logger-03 (with temperature display)

Notes

The shift started at the northern side of the Dickey's Rd bridge. Paving began as soon as the first asphalt truck arrived on site and ran smoothly with some brief stops due to edge detailing on the centre median. There were four key-ins (one bridge and start/end) and the asphalt trucks had to wait while the paver traversed the bridge.

Traffic management

The lane was opened to traffic (100km/h signs) at 1000h on Thursday, 8 November.

Appendix D Ground Penetrating Radar

D.1 Background

General information

Ground penetrating radars (“GPR”) measure the travel time and reflection amplitudes of electromagnetic pulses generated by a horn. Reflections occur due to electrical interferences (changes in a material’s dielectric constant) at the interface between two layers caused by:

- Differences in materials,
- Areas of differing moisture content, and/or
- Areas of differing density or void content.

The dielectric constants of some common materials are listed below³. The measured dielectric constant is the volumetric ratio of dielectric constants of the layer’s component materials, meaning that a change in air void content will be seen as a change in dielectric constant.

Table 32 Dielectric constants of common materials

Material	Dielectric constant
Air	1
Asphalt (dry)	2–4
Asphalt (wet)	6–12
Clay (dry)	2–6
Clay (wet)	5–40
Concrete (dry)	4–10
Concrete (wet)	10–20

Figure 61 shows the reflections that occur at various layer interfaces. The recorded signal (measured by the GPR receiver) contains reflection time information (t_1 and t_2) and peak reflection amplitude (A_0 , A_1 and A_2). The reflection time and amplitude information can be used to determine the layer thicknesses (d_1 and d_2) and layer dielectric constants ($\epsilon_{r,1}$, $\epsilon_{r,2}$, $\epsilon_{r,3}$) using the following equations^{5,4}:

$$d_i = \frac{ct_i}{2\sqrt{\epsilon_{r,i}}}$$

$$\epsilon_{r,1} = \left[\frac{A_{inc} + A_0}{A_{inc} - A_0} \right]^2$$

where

- c is the speed of light in free space ($\sim 3 \times 10^8$ m/s),
- i is the layer number,
- A_{inc} is the peak amplitude of the incident wave, obtained by performing a measurement over a metal plate (assumed to be a perfect reflector).

Calculation of the dielectric constants of layers 2 and below (base and subgrade) are based on the calculated dielectric constants for the layers above (equations not included here). These relationships are simplifications and do not account for attenuation within the layer above the

³ D.J. Daniels, Ground Penetrating Radar, Institution of Engineering and Technology (2004)

⁴ Lahouar, S. Development of data analysis algorithms for interpretation of ground penetrating radar data. PhD Thesis. Virginia Polytechnic Institute and State University. (2003)

interface. This results in an underestimation of the dielectric constant of the layer below the interface and hence an overestimation of the thickness of the layer below the interface.

Inhomogeneities within a layer due to defects, repairs, moisture accumulation or multiple lifts are also not accounted for. Each feature can cause a small reflection due to a small change in dielectric constant, hence GPR measurements taken on existing roads can be unreliable or difficult to interpret. Inhomogeneity issues are generally less of a concern for GPR measurements taken on newly constructed roads.

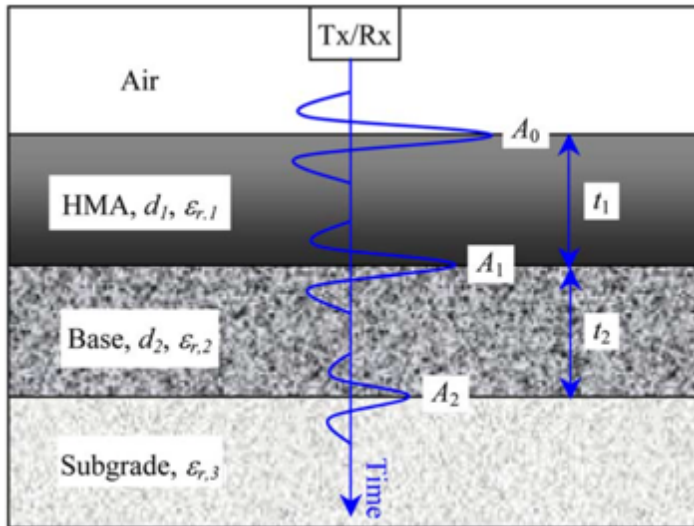


Figure 61 Reflections due to changes in material dielectric constant (from [5]).

Depth resolution limitations

The minimum resolvable layer depth is limited by the width of the transmitted radar pulse, which is a function of the GPR system being used. Layers that are too thin will be obscured by the larger reflection from the interface at the top of the layer.

The minimum resolvable layer depth can be calculated using:

$$\Delta d = \frac{cT}{2\sqrt{\epsilon_r}}$$

where

- *T* is the transmitted radar pulse width in seconds.

The width of the radar pulse for the Fulton Hogan 2.0 GHz GPR system is approximately 1.0 ns. Assuming a typical porous asphalt dielectric constant of 4.0 the minimum resolvable asphalt layer depth will be 75 mm. This rules out use a standard GPR assessment for asphalt thickness measurements in New Zealand where asphalt layers are typically 20-50 mm thick.

Lahouar proposed several solutions to the depth resolution problem and found the power cepstrum and iterative decomposition techniques to be the best performing⁴. The power cepstrum involves calculating the power spectrum of the logarithm of a signal's power spectrum. The resulting signal is composed of peaks that correspond to the reflection times. The iterative decomposition technique involves the detection and subtraction of the largest

⁵ AL-Qadi & Lahouar, Measuring layer thicknesses with GPR – Theory to practice, Construction and Building Materials 19 (2005)

reflection pulse. This process is continued until the residual signal reaches a predefined threshold chosen based on the original signal noise.

The iterative decomposition technique was chosen for the current Western Belfast Bypass project as the process is easier to understand and hence the results easier to check than the power cepstrum technique.

Coupling pulse

The recorded radar signal includes an initial pulse due to the direct signal travelling from the GPR horn's transmitter to its receiver; this is referred to as the "coupling pulse" (see Figure 62).

The coupling pulse is useful as it defines a fixed point in time and can be used to calculate the height of the GPR horn above the surface; however, the coupling pulse can interfere with the subsequent reflection pulses and must be subtracted from the recorded radar signal before attempting to detect the reflection pulses.

The coupling signal can be found by aiming the GPR horn upwards (towards the sky) and taking a recording. The recorded radar signal will contain the clean coupling pulse (without any surface or sub-surface layer reflections).

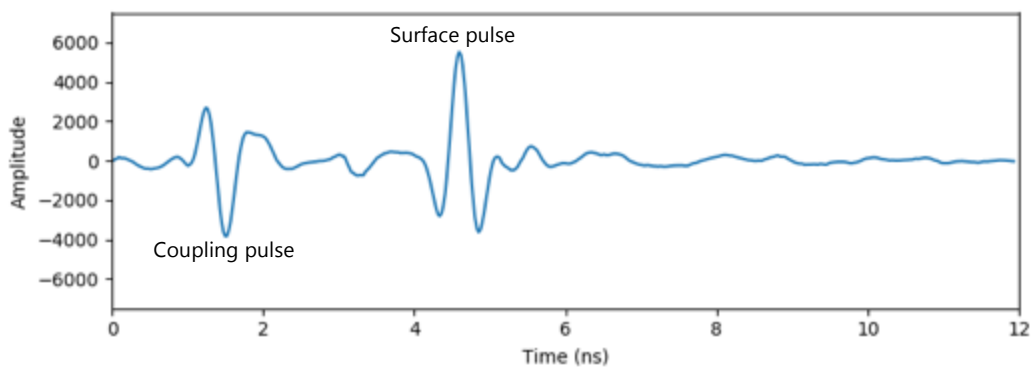


Figure 62 Typical recorded radar signal

Metal plate calibration

In order to calculate the dielectric constant the amplitude of the radar pulse incident on the surface must be found. This is achieved by placing a large metal plate (assumed to be a perfect reflector) on the ground and taking a recording. The peak amplitude of the metal plate reflection is used as the A_{inc} term when calculating the dielectric constant of the first layer.

Fulton Hogan 2GHz GPR system

The Fulton Hogan GPR system is a GSSI SIR20 system with a 2.0 GHz horn. The system is designed to be fitted to a vehicle and driven at road speeds along the survey section (see Figure 63). The system records a "GPR scan" every 0.25 metres along the road resulting in 4,000 scans per 1 km of road surveyed. Each scan is GPS referenced. The measurements are distance-triggered using a wheel encoder attached to one of the rear wheels of the survey vehicle.



Figure 63 Fulton Hogan GSSI SIR20 GPR system with 2 GHz horn fitted to the survey vehicle.

D.2 Surface dielectric constant to air void content relationship

Core samples were taken at nine locations (3 cores per location) in the left-hand shoulder of the Western Belfast Bypass (EPA7, 40 mm target thickness) in October 2019. The air void content for each core sample as determined by the Fulton Hogan laboratory (Christchurch) is included in Table 33 along with the corresponding contemporaneous surface dielectric constant measurement.

The results are plotted in Figure 64 and shows no clear relationship between surface dielectric constant and air void content based on the current measurements.

Table 33 Laboratory air void content for Western Belfast Bypass core samples.

Location ID	Rs/Rp	Laboratory air void content (%)				Surface dielectric constant
		Core #1	Core #2	Core #3	Average	
1	01S-0327/04.950-D	19.8	20.5	21.5	20.6	4.35
2	01S-0327/04.630-D	21.9	22.8	23.0	22.6	4.57
3	01S-0327/04.390-D	20.9	20.4	20.7	20.7	4.56
4	01S-0327/03.790-D	20.5	20.2	20.0	20.2	4.57
5	01S-0327/03.610-I	20.1	20.5	19.0	19.9	4.68
6	01S-0327/05.330-I	22.5	21.7	20.9	21.7	4.42
7	01S-0327/05.250-D	21.3	22.1	21.0	21.5	4.64
8	01S-0327/03.390-D	20.2	19.3	20.6	20.0	4.65
9	01S-0327/04.650-I	23.4	21.2	22.1	22.2	4.39

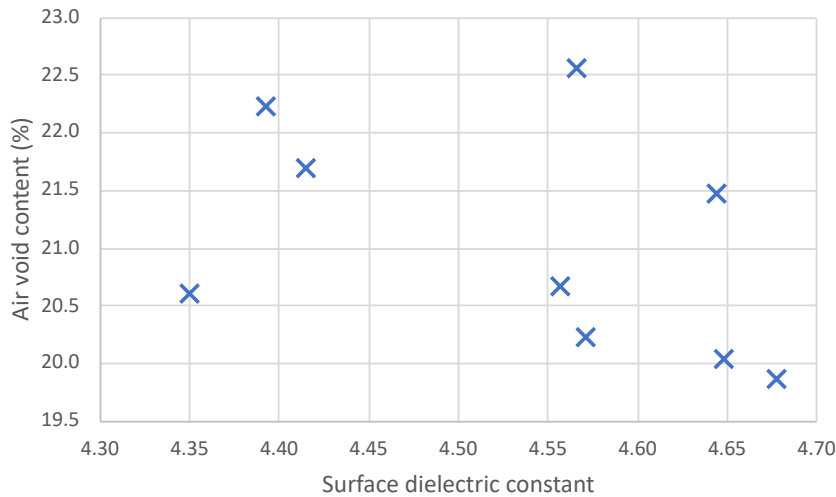


Figure 64 Surface dielectric constant vs laboratory air void content

D.3 Raw data processing methods and problems

Coupling pulse removal

The coupling pulse removal process was performed as follows:

1. The clean coupling pulse is found by aiming the GPR horn upwards and taking a recording.
2. The cross-correlation of the clean coupling pulse signal and the recorded ground reflection signal is calculated and the sample offset is calculated.
3. The clean coupling pulse is then zero-padded to match the coupling pulse in the recorded ground reflection signal. This results in the clean coupling pulse being aligned with the recorded ground reflection signal to within one sample point.

4. The clean coupling pulse is then repeatedly shifted by $1/50^{\text{th}}$ of a sample to find the sub-sample shift required to give the best correlation coefficient (see BS EN 1793-5⁶ for a description of the sub-sample shift process).
5. The sub-sample-shifted coupling pulse is then subtracted from the recorded ground reflection signal.

Figure 65 and Figure 66 show the coupling pulse removal process.

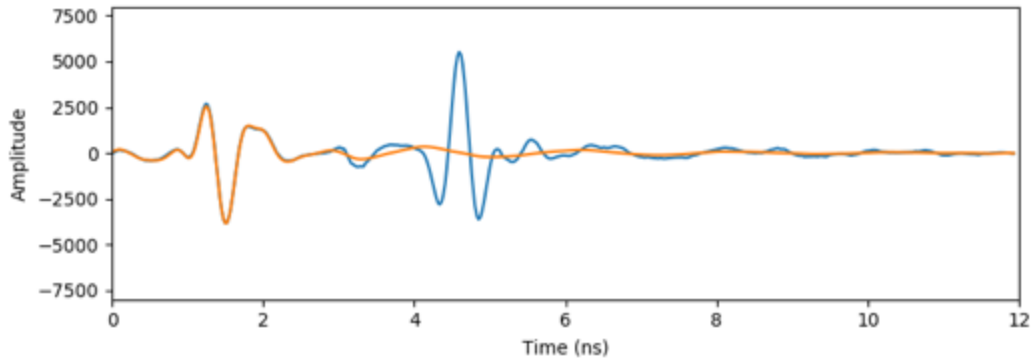


Figure 65 Raw trace with aligned coupling pulse.

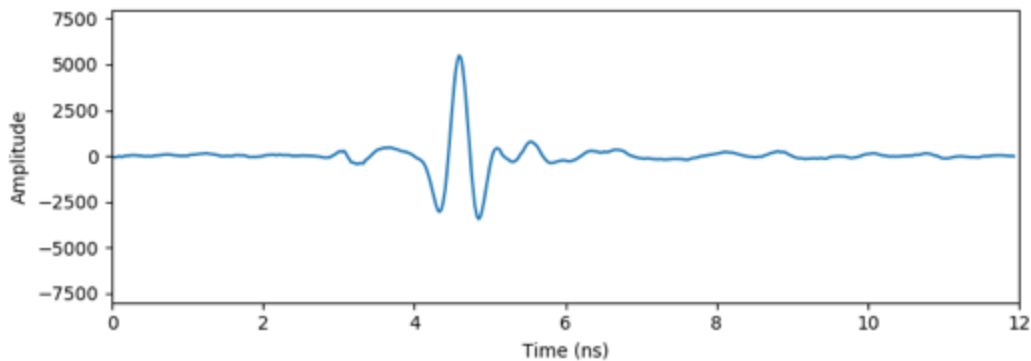


Figure 66 Raw trace with coupling pulse removed, leaving surface and sub-surface reflections.

Incident pulse amplitude

The incident pulse peak amplitude (A_{inc}) is required for determination of the surface layer dielectric constant. The metal plate calibration process provides this value by assuming that the metal plate represents a perfect reflector.

While taking the metal plate calibration measurement it was noted that the metal plate reflection amplitude varied with the height of the GPR horn, suggesting non-trivial attenuation of the radar wave as it travelled through the air. A recording was taken while bouncing the rear of survey vehicle to represent the bumps in the road that would be present during a survey. The results showed a 10% variation in the peak amplitude and that the amplitude was negatively correlated to the sample delay between the coupling pulse and metal plate reflection (GPR horn height) (see Figure 67).

⁶ BS EN 1793-5:2016. Road traffic noise reducing devices – Test method for determining the acoustic performance – Intrinsic characteristics – In situ values of sound reflection under direct sound field conditions.

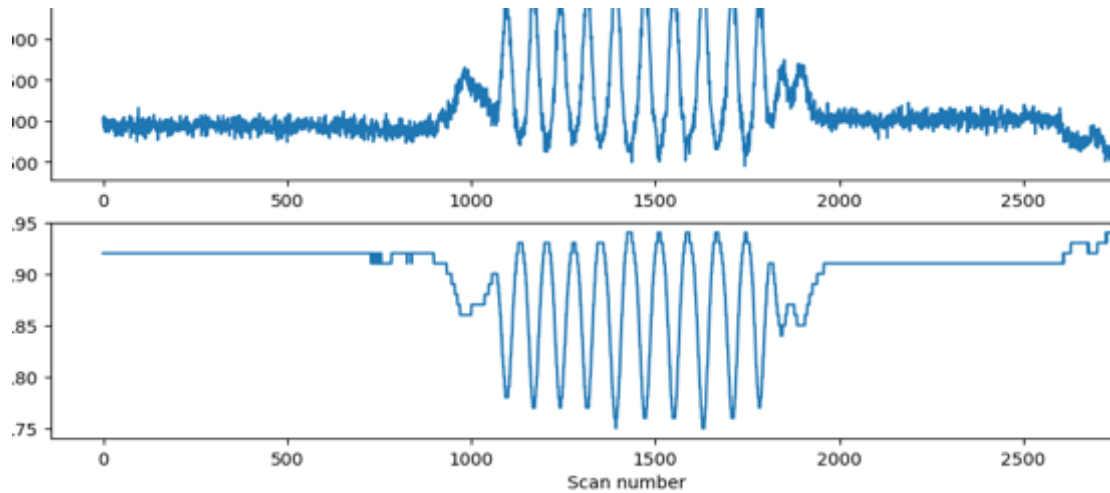


Figure 67 Metal plate peak amplitude (top) and sample delay (bottom) during a bounce test.

Rather than using a constant incident pulse peak amplitude, as is common practice, the decision was made to calculate the effective incident pulse peak amplitude for each GPR trace. Figure 68 shows the linear regression of the metal plate peak amplitude to surface pulse two-way travel time (Δt). The resulting relationship is included below.

$$A_{inc} = -4.4209 \times 10^{12} \Delta t + 32986$$

For the GPR measurements taken on Western Belfast Bypass the effective incident pulse peak amplitude was calculated for each GPR scan using the two-way travel time between the coupling pulse and the surface reflection.

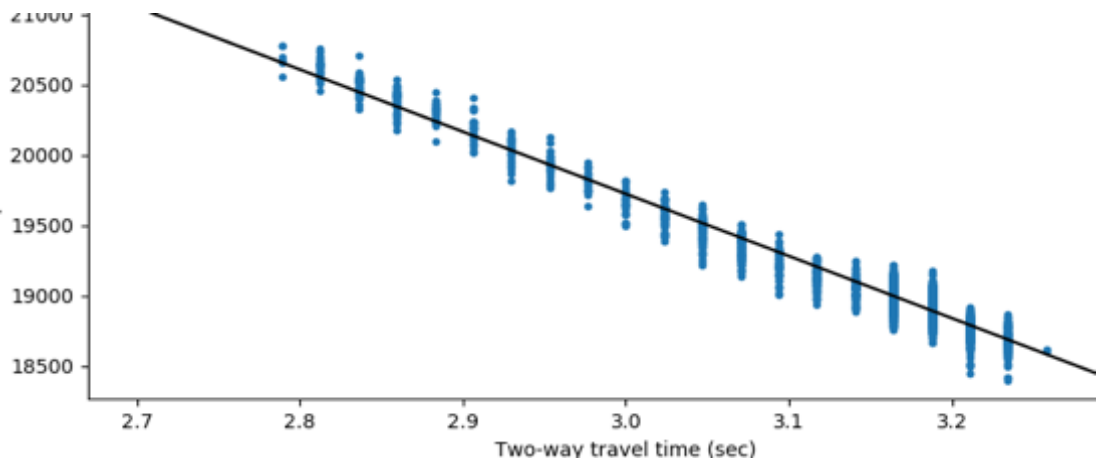


Figure 68 Metal plate amplitude versus coupling pulse to surface reflection two-way travel time.

Subsequent interface reflections and ringing

Interfaces below the asphalt-base interface, such as the base-subgrade interface or an interface between two lifts in the base layer, can obscure the asphalt-base interface in the same way that the surface reflection obscures subsequent interface reflections (i.e. due to the long radar pulse width). A similar problem exists when there is a ringing reflection, which occurs when the radar pulse repeatedly reflects between two layer interfaces. This is a major issue where there are metal objects buried in the ground, but may also cause problems for weaker reflecting interfaces such as the asphalt-base layer interface.

In order to detect the desired asphalt-base interface reflection all nearby interface and ringing reflections must be accounted for. Failure to account for these additional reflection pulses will lead to a poor detection of the asphalt-base interface location.

Iterative decomposition

The iterative decomposition was performed as follows for each "GPR scan":

1. Chose a threshold level based on the noise in the raw signal. The iterative decomposition process will stop when the peak amplitude in the residual signal drops below the threshold value.
2. Remove the coupling pulse using the procedure described in the coupling pulse removal section above.
3. Use the cross-correlation and sub-sample shift process (described in the coupling pulse removal section) to synthesise the surface reflection pulse. An inverted version of the coupling pulse is used as the reference pulse. See Figure 69.
4. Remove the synthesised surface pulse from the signal.
5. Use the cross-correlation and sub-sample shift process to synthesis the next most significant reflection pulse (either a ringing reflection or lift-interface within the base layer).
6. Remove the synthesised pulse from the signal.
7. Repeat steps 4 to 6 until the peak amplitude in the residual signal drops below the threshold set in step 1.

Improve each synthesised pulse. For each synthesised pulse:

8. Subtract the other synthesised pulses and coupling pulse from the raw signal.
9. Use the sub-sample shift process to find a new synthesised pulse that better matched the target reflection pulse.

The peak amplitude of the synthesised surface reflection pulse is used to calculate the surface layer dielectric constant. The first synthesised pulse following the surface reflection is assumed to be the asphalt-base interface. The time delay between the surface reflection and the asphalt-base interface reflection is used to calculate the asphalt layer depth.

Figure 70 compares the raw signal (with coupling pulse removed) to a signal comprising of the combination of all synthesised pulses.

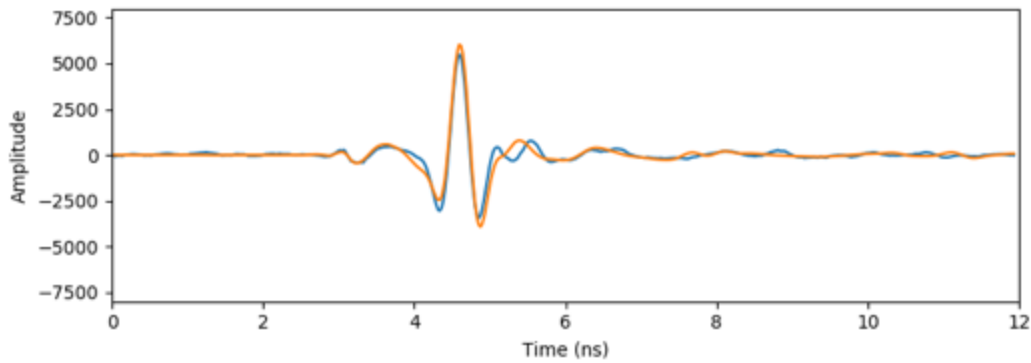


Figure 69 Raw signal with coupling pulse removed (blue) and synthesised surface reflection pulse (orange).

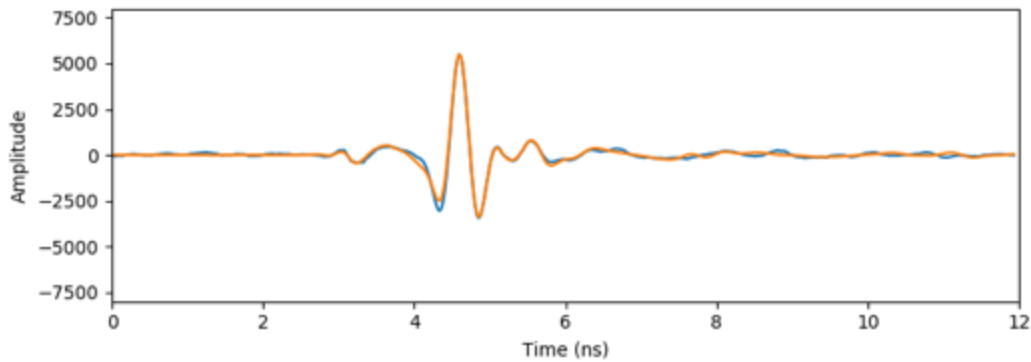


Figure 70 Raw signal with coupling pulse removed (blue) and combination of all synthesised pulses (orange).

While the iterative decomposition technique worked well in removing the surface pulse, problems with ringing reflections meant that the asphalt-base interface could generally not be reliably detected.

It appears that some distortion of the transmitted pulse occurs meaning that the reference pulse, used in the decomposition process, was not a good representation of the target pulse being detected. Subtraction of the synthesised pulse from the target pulse leaves a residual component with a similar shape to the reference pulse. The iterative decomposition process then attempts to synthesise a new pulse representative of the residual pulse, thus effectively splitting the target pulse in two (Figure 71). The problem does not consistently result in a splitting of the asphalt-base interface reflection pulse in to two synthesised pulses.

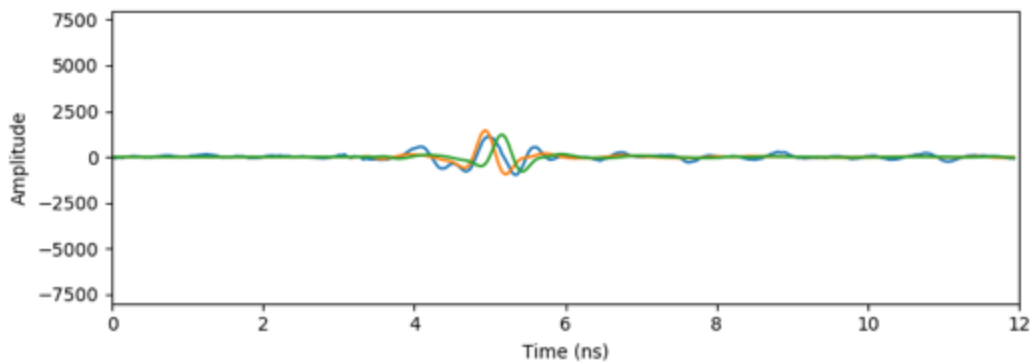


Figure 71 Residual signal after removal of the surface pulse (blue), asphalt-base interface pulse split in to two pulses (orange and green) due to the reference pulse being a poor representation of the target pulse.

D.4 Conclusions and recommendations

Asphalt layer thickness

The use of a ground penetrating radar for asphalt layer thickness measurements has failed to yield reliable results. The main issue being that the surface reflection pulse obscures the reflection pulse of the asphalt-base interface due to the width of the incident radar pulse, which generally limits the minimum resolvable depth to ~75 mm for porous asphalt surfaces.

An iterative decomposition technique was used to remove the surface reflection pulse. While this technique worked well in removing the surface pulse, additional problems with ringing reflections and potential transmitted pulse distortions meant that the asphalt-base interface could not be reliably found.

Further development and testing of the processing algorithm would be required to yield reliable asphalt thickness values. Specifically:

- Investigate the power cepstrum technique to see if it better deals with the ringing reflections and transmitted pulse distortions.
- Modify the reference pulse used at each stage of the iterative decomposition process to account for the transmitted pulse distortions.

Asphalt layer dielectric constant

The relationship between asphalt surface dielectric constant and air void content was investigated using core samples from nine locations on an EPA7 (40 mm thick) surface. No clear relationship was found.

Appendix E Temperature and position loggers

E.1 Background

The temperature and position logger specifications were as follows:

- 1-4 input channels for 4-20mA infrared temperature sensor.
- GPS positioning, synchronised with temperature readings.
- 1 Hz minimum sample rate.
- Stand-alone unit with on-board power supply and SD storage.
- Rugged case.
- Simple mounting arrangement.

No off-the-shelf system was available to perform the temperature and position monitoring at a reasonable cost that would allow three pieces of construction equipment to be equipped; therefore, the decision was made to develop a bespoke system.

Two base options were considered:

DataTaker – Commercial data logging platform

Advantages	Disadvantages
20mA analog input available	No wireless comms on base model.
128MB storage	No built-in GPS receiver.
6A 1.2Ah internal battery	1.5 kg
	High power usage (1.35W or 113mA@12V for 1Hz sampling) probably requiring an additional battery (adding weight).
	Unfamiliar software.

Particle Asset Tracker – Commercial Internet of Things (IoT) platform

Advantages	Disadvantages
Built-in GPS receiver and low-cost accelerometer.	No on-board storage
Built-in 3G modem.	No built-in 20mA sensor input
Small and light.	Requires external battery (but free to choose).
Familiar software and large support network.	

The Particle Asset Tracker was chosen as it provided more flexibility and familiar software, while having a good support network to assist with implementation of the on-board SD storage and 20mA sensor input. The 3G modem also provided a means of verifying correct logger operation during the paving shifts, something that could not be easily done with the DataTaker platform.

Five 4-20mA infrared temperature sensors were purchased and 3D printed plastic clamps were designed to hold each sensor (Figure 72). Magnetic mounts were used to secure the logger enclosure and temperature probes to the construction equipment (Figure 73).

The final bill of materials for the logger units was as follows.

Item
Particle Asset Tracker
20mA sensor circuit board
SD storage circuit board
SD card
Printed circuit board (custom design with power management and signal routing circuitry)
Active GPS antenna
Plastic enclosure
12V lead acid battery

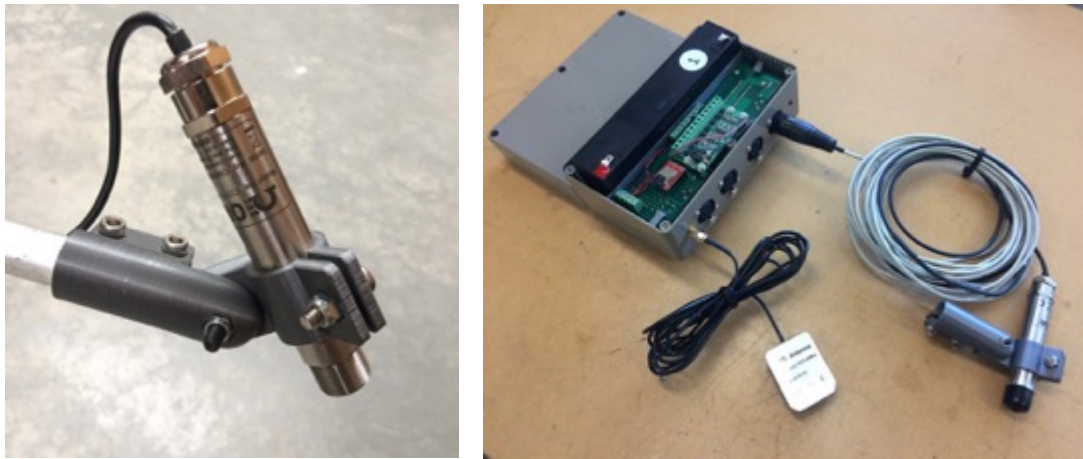


Figure 72 Infrared temperature probes and 3D printed mounts (left), logger unit with GPS antenna and temperature probes connected (right).

E.2 Paver monitoring

E.2.1 Logger and sensor mounting

The logger unit was fixed to the horizontal crossbar that forms part of the pavers roof. The temperature probe signal cables ran along the horizontal crossbar to each vertical roof support where the temperature probes were fixed. The GPS antenna was secured to the roof of the paver. All equipment was removed at the end of each paving shift.

Figure 73 shows the position of the logger unit and temperature probes on the paver.

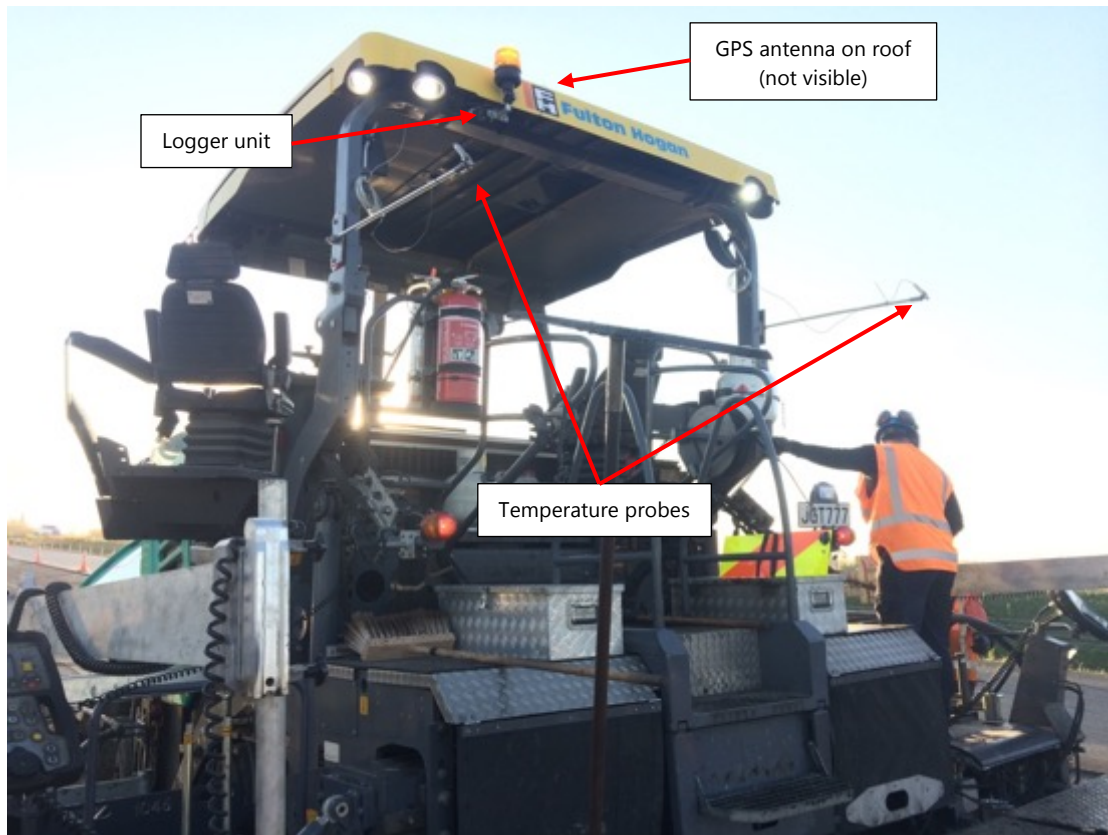


Figure 73 Temperature logger positioning on paver

E.2.2 Data collection and processing

The temperature and position data was collected during eight construction shifts. At least two temperature sensors (aimed at the left and right wheel paths) were used during all shifts. A third temperature sensor was added for shifts 5-8 and this was aimed in the middle of the lane.

The data was processed using the following procedure:

1. The start and end reading number for each continuously paved section of road was found by manually inspecting the data. The start and end reading numbers were stored in the SQL database. E.g. the first continuous run during shift 1 started at the northern extent of the project and ended at the northern edge of Dickies Rd bridge.
2. The GPS coordinates associated with each temperature reading was converted to Rs/Rp positions and the field added to each temperature reading.
3. Two datasets were then created from the base dataset:
 - Screed dataset – screed positions and start/stop points within each continuous paved section. The displacement values were adjusted based on the offset displacement of the GPS antenna from the screed (2 metres in front, see Figure 74). The speed and distance between readings was used to determine where paving was temporarily halted and an "is_stopped" field was added to each temperature reading.

- Temperature dataset – temperature readings. The displacement values were adjusted based on the offset displacement of the GPS antenna from the temperature sensors (4 metres in front, see Figure 74).
4. A uniform 1 metre grid of start and end displacements was then built and the minimum, maximum, mean and standard deviations of temperature readings within each 1 metre segment were calculated.
 5. Since the temperature sensors are aimed behind the screed, when the paver stops there is a section of asphalt between the screed and temperature sensors that starts to cool. The temperatures of this cooled section will be read when the paver starts to move again, however, these later values are invalid as the asphalt has been cooling for a variable period of time. An additional field was added to note whether each 1 metre road segment held valid data.
 6. In some cases a person or object obscured the sensor's view of the asphalt mat and resulted in low readings. The validity field was updated to remove any readings below 80°C and any readings where the channel 1 (left wheel path) and channel 2 (right wheel path) data differed by more than 10°C.

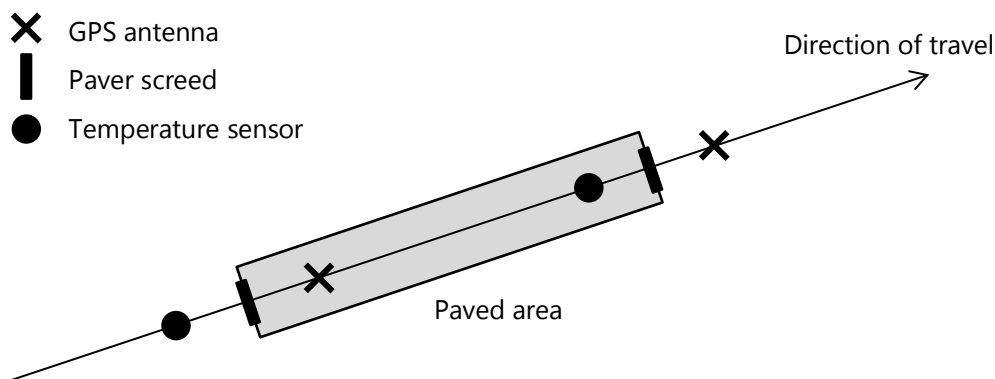


Figure 74 Diagram showing the position of GPS antenna, paver screed and temperature sensors during paver monitoring.

E.3 Roller monitoring

E.3.1 Logger and sensor mounting

The logger unit was installed inside the cab of each roller. The temperature probe signal cable and GPS antenna cable ran out the driver's door. The temperature probes were fixed to the front of each roller and the GPS antenna was secured to the roof. The logger units were removed at the end of each paving shift. The temperature probes and GPS antenna were left attached to the rollers between shifts (each temperature probe was covered with a plastic bag to protect it from rain).

Figure 75 shows the position of the logger unit and temperature probes on one of the rollers.



Figure 75 Temperature logger positioning on roller

E.3.2 Data collection and processing

The temperature and position data was collected during the eight construction shifts. No measurements were recorded for the secondary roller during shifts 1 (due to mechanical breakdown) and shift 6 (due to a faulty logger unit).

The data was processed using the following methodology:

1. The data was ordered by shift and time, and each shift was processed separately.
2. The GPS coordinates associated with each reading was converted to Rs/Rp positions and the field added to each reading.

Temperature dataset

3. A uniform 20 metre grid of start and end displacements was built. The readings were then grouped into their corresponding 20 metre segment based on the Rs/Rp positions.

4. The maximum, minimum, mean, median and standard deviations were calculated for each 20 metres segment.

Roller pass dataset

5. Direction changes were determined by analysing the Rs/Rp position between adjacent readings and this was used to group sets of readings into individual continuous roller passes.
6. A uniform 20 metre grid of start and end displacements was built and the number of roller passes crossing each 20 metre segment were counted. The following scaling procedure was then applied:
 - The total count was divided by two (to set the definition of one pass to include a forward and backward movement).
 - The resulting count was multiplied by the roller width of (1.68 metres) and the divided by the average paved width for the shift (from the construction tracesheets).

Appendix F 3D Lidar Scan Data

Lidar data was provided for the chipseal and asphalt surfaces as separate "las" files. The data was processed using the following procedure:

1. The "las" files were processed into "tiff" files with 0.2 metre resolution and loaded into QGIS.
2. The 2018 HSD survey lane centrelines were used as the reference centrelines. The reference centreline provided the mid-lane position.
3. The mid-lane position was offset by 0.8 metres to the left, to give the left wheel path line.
4. Cross-sections of each surface were taken using the left wheel path lines for each lane. The resulting cross-section was a set of points where the polyline crosses a surface triangulation line (i.e. it is an interpolated version of the original "tiff" surface).
5. By using the same polyline as the basis for the cross-section on both the chipseal and asphalt surfaces, the height points were taken at identical positions. The thickness was calculated by subtracting the chipseal surface height from the asphalt surface height.
6. The GPS coordinates for each point were then converted to Rs/Rp positions.
7. A uniform 1 metre grid of start and end displacements was then built and the minimum, maximum, mean and standard deviations of the thickness readings within each 1 metre segment were calculated.

Appendix G 1 metre Mean Profile Depth Data

The 1 metre mean profile depth (MPD) readings were provided by WDM for the northbound carriageway and the final ~400 metres of the southbound carriageway. The files also covered the remainder of Rs 01S-0333, however, these areas were not required as part of this study.

The data was provided as displacement – mean profile depth pairs. The relationship between the displacement and the Rs/Rp reference system was determined by manually inspecting the mean profile depth trace and identifying surface transitions. The following tables provide details of the alignment; the highlighted rows were used as the datum point and “rubber-banding” was performed using the calculated scaling factor. The mean profile depth values were then mapped (interpolated) back on to a 1 metre grid.

Table 34 Northbound

		Northbound, left lane	Northbound, right lane
	Measurement name	S1D034419_S10_190126163127	S1D034419_S10_190126163127
Start	Surface transition	WBB southern extent (SMA10 to EPA7)	WBB southern extent (SMA10 to EPA7)
	MPD displacement	10,385 metres	10,413 metres
	Rp displacement	316 metres (road_id: 3656)	316 metres (road_id: 3656)
End	Surface transition	WBB northern extent (EPA7 to SMA10)	WBB northern extent (EPA7 to SMA10)
	MPD displacement	13,990 metres	14,021 metres
	Rp displacement	2,404 metres (road_id: 1715*)	2,404 metres (road_id: 1715*)
	MPD distance	3,605metres	3,608 metres
	Rp distance	3,590 metres	3,590 metres
	Difference	15 metres	18 metres
	Scaling factor	0.9958	0.9950

* Road id 1715 ends at Rp displacement 5,678 metres.

Table 35 Southbound

		Southbound, left lane	Southbound, right lane
	Measurement name	S11033319_S10_190127080316	S11033319_S10_190127091130
Start	Surface transition	Groynes bridge (EPA7 to SMA10)	Groynes bridge (EPA7 to SMA10)
	MPD displacement	40 metres	40 metres
	Rp displacement	5,750 metres (road_id: 1716*)	5,750 metres (road_id: 1716*)
End	Surface transition	WBB southern extent, after ramp SMA (SMA10 to EPA10)	WBB southern extent, after ramp SMA (SMA10 to EPA10)
	MPD displacement	884 metres	879 metres
	Rp displacement	830 metres (road_id: 3650)	830 metres (road_id: 3650)
	MPD distance	844 metres	839 metres
	Rp distance	849 metres	849 metres
	Difference	5 metres	10 metres
	Scaling factor	0.9941	0.9882

* Road id 1716 ends at Rp displacement 5,769 metres.

Appendix H Permeability Testing

H.1 Existing methods

H.1.1 TNZ P/23:2005 – Field permeability of OGPA

Measurement procedure

The method uses a 150 mm diameter ring that is sealed to the OGPA matt with a suitable silicon product.

300mL of water is added to the inside of the ring to saturate the OGPA matt. Once the level of this water has dropped flush with the top of the matt, a further 150mL of water is added to the ring in one quick pour and the time for the water to drain flush with the matt surface again is recorded.

The process is repeated with two or more 150mL portions, added separately. The period between adding 150mL portions of water to the ring should be kept to a minimum with the only delay being to record the drainage times.

The average of the three reading should be no more than 12 seconds at the time of laying.

Suitability for permeability study

The method is intended as a simple field check (pass/fail) to determine whether a newly constructed OGPA surface meets a minimum permeability standard. The 150mL volume is considered too small to provide sufficient precision when attempting to compare permeability (drain times) between sites.

H.1.2 TNZ T/11:2003 – Permeability of hot mix asphalt

Measurement procedure

The method uses the standpipe permeameter to assess permeability of hot mix asphalt pavement surfacings by measuring the rate of ingress of water into the surface. A well compacted dense grade mix should be impermeable and any water that flows into the material indicates that the desired impermeable state has not been achieved.

The testing apparatus includes a 150 mm diameter non-corroding metal base (chamber) with a 540 mm tall vertical stand pipe. The chamber is sealed to the asphalt surface and filled to the 440 mm mark. The rate of fall (mm/sec) is determined from the change in water level after a set time has elapsed (nominally 30 seconds).

Suitability for permeability study

The method causes non-trivial water pressure inside the chamber. When applied to a porous surface there is a risk that the high pressure will force water through pores directly beneath the seal. Once outside the chamber, the water can rise back out of the surface layer and flow freely across the surface of the asphalt layer. For this reason a high pressure (high head) technique is considered inappropriate for a thin porous surface layer.

H.1.3 ASTM C1701

Measurement procedure

The method uses a 300 mm diameter ring that is sealed to the surface using a sealant material. The surface is pre-wet by pouring 3.6L of water into the ring but maintaining a head of 10-15 mm. The measurement is then taken by repeating the process with a 3.6L of water and recording the time for the water to drain down flush with the pervious surface.

Suitability for permeability study

During initial testing the 10-15 mm head was generally found to be suitable to prevent water rising back to back to the surface and flow freely away. The pre-wetting technique was found

to give varying results (see below) and the requirement for a sealant putty at each site proved impractical for quick measurements in the field.

H.2 Chosen method

The ASTM C1701 method showed the most promise; however, the decision was made to use a 150 mm diameter ring to maintain consistency with the existing TNZ methods and reduce the sealing length. Figure 76 shows a photograph of the final test rig.

Automatic filling

An automatic water level valve was developed using the “self-filling water bowl” concept to maintain a set water level inside the ring, thus removing the need for an operator to continually pour water into the ring during testing. A bucket provided a water reservoir, which was topped up after each measurement. The automatic water level valve worked most successfully with a 5-15 mm head.

A sight tube was installed on the side of the bucket to allow the operator to determine when 3.6L of water had drained from the bucket.

Sealing

Due to the impracticality of applying a sealant putty at each location a 15 mm thick closed cell foam was used to provide a sealing surface. Testing showed that a 50 kg weight was required to achieve a suitable seal between the foam ring and asphalt surface.

Pre-wetting

The system was tested on an EPA7 30 mm surface at the CAPTIF Road Research facility to check the effect of pre-wetting.

Several consecutive tests were performed (keeping the time between tests to a minimum) at specific locations to investigate the effect of prewetting. Table 36 presents the results for a trafficked and untrafficked section of the CAPTIF surface and show that the drain times are affected by an accumulation of water in the surface layer. A steady state is reached once a sufficient volume of water has entered the surface layer.

In order to maintain consistency and limit the duration of each measurement no pre-wetting will be used during the field measurements.

Table 36 Effect of prewetting

Test no.	Time to drain 3.6L of water	
	Station “0”, 1 metre right of wheel path (untrafficked)	Station “0”, in wheel path (trafficked)
1	75 sec	161 sec
2	95 sec	229 sec
3	107 sec	255 sec
4	115 sec	279 sec
5	120 sec	
6	122 sec	
7	123 sec	



Figure 76 Permeability test rig